基于表面等离激元的量子光学量子信息

古 英

人工微结构和介观物理国家重点实验室 &
北京大学物理学院

FIO下载：http://www.phy.pku.edu.cn/~lypeng/fio.htm

*email: ygu@pku.edu.cn

Mar. 19, 2012

http://www.phy.pku.edu.cn/~guying/index.html

Outline:

一、表面等离激元光学简介

二、表面等离激元相关的几个工作

三、介观量子交叉领域的发展现状及前景

四、交叉领域相关的几个工作

五、总结

一、表面等离激元光学简介

Plasmonics 表面等离激元光学

研究： 金属和介质表面以及纳米金属颗粒的光学性质。

解读： Surface plasmon polariton （SPP)

Surface: 金属和介质的界面

Plasmon: 金属界面自由电子的集体振荡，借用等离子的概念

Polariton: 元激发，模式

属于： Plasmonics, Mesoscopic optics, nano optics, nano photonics, near field optics

金和银的介电常数值

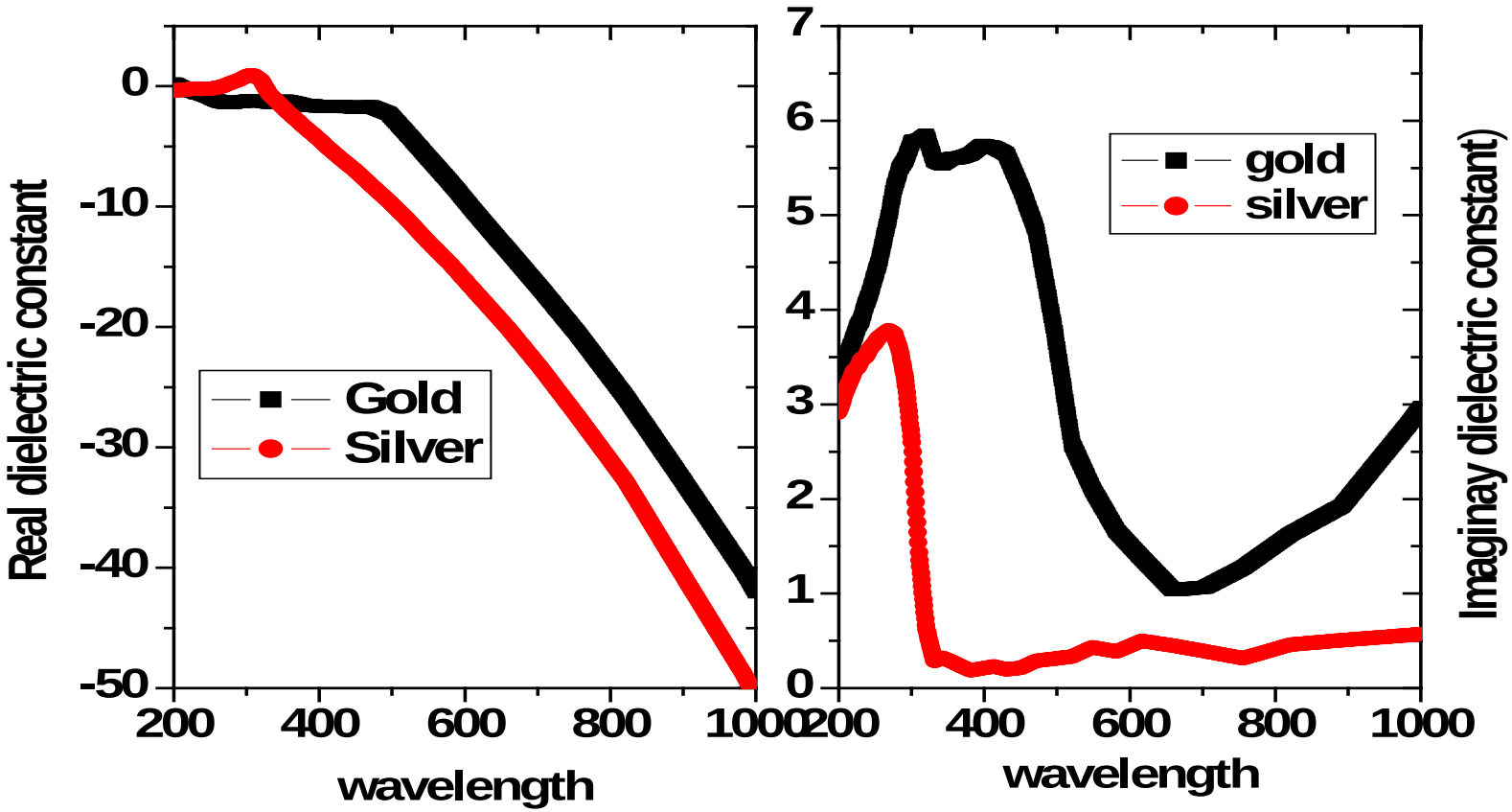

Optical Constants of the Noble Metals

P. B. Johnson and R. W. Christy

PRB, 6, 4370 (1972).

表面等离激元（SPPs）

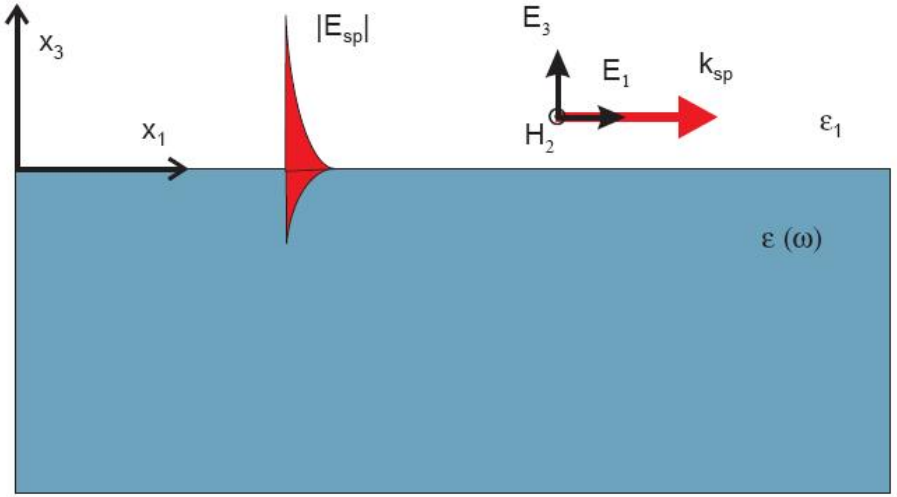

表面等离激元：在金属和介质交界面，由于表面电荷密度的振荡，束缚在界面的电磁波模式。

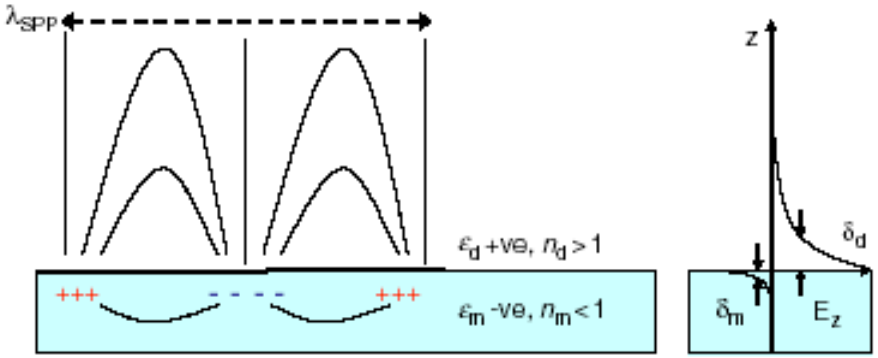

$$k_x = \omega\sqrt{\frac{\varepsilon_1\varepsilon_2}{\varepsilon_1+\varepsilon_2}} \quad \geq \quad \omega\sqrt{\varepsilon_1} > k_0$$

$$E = E_0 \exp(ik_x x - k_z z)\exp(-i\omega t)$$

A. V. Zayatsa, et al, Phys Rep. 2005, 408:131–314
B. W. L. Barnes et al,. J Opt A: Pure Appl Opt. 2006, 8:S87–S93

表面等离激元的特点

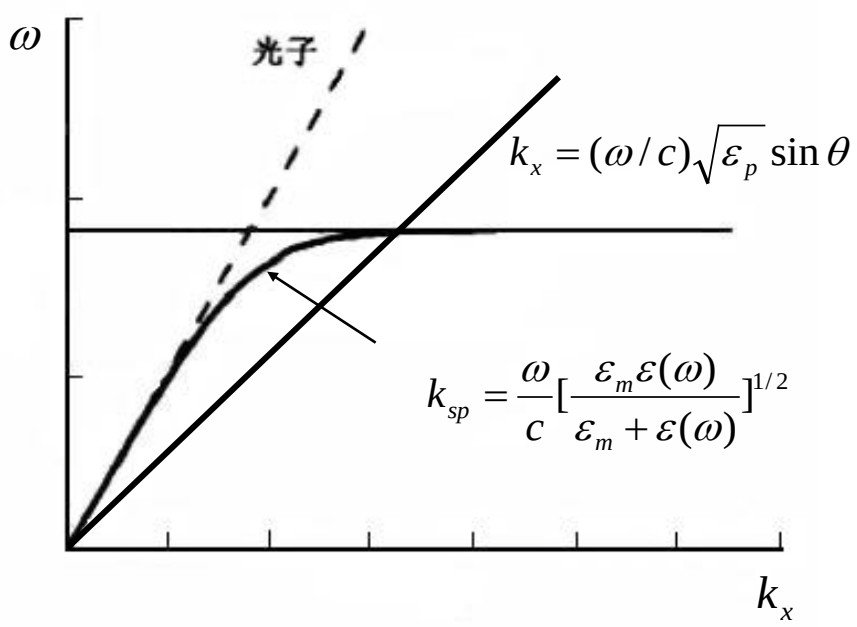

1. 波矢比同频率的光要大。
2. 在介质和金属两侧都是倏逝场，随着离界面距离的增加，电磁场强度指数衰减（电磁场能量局域在界面附近）。

表面等离激元色散曲线

表面等离激元中的一些尺度概念

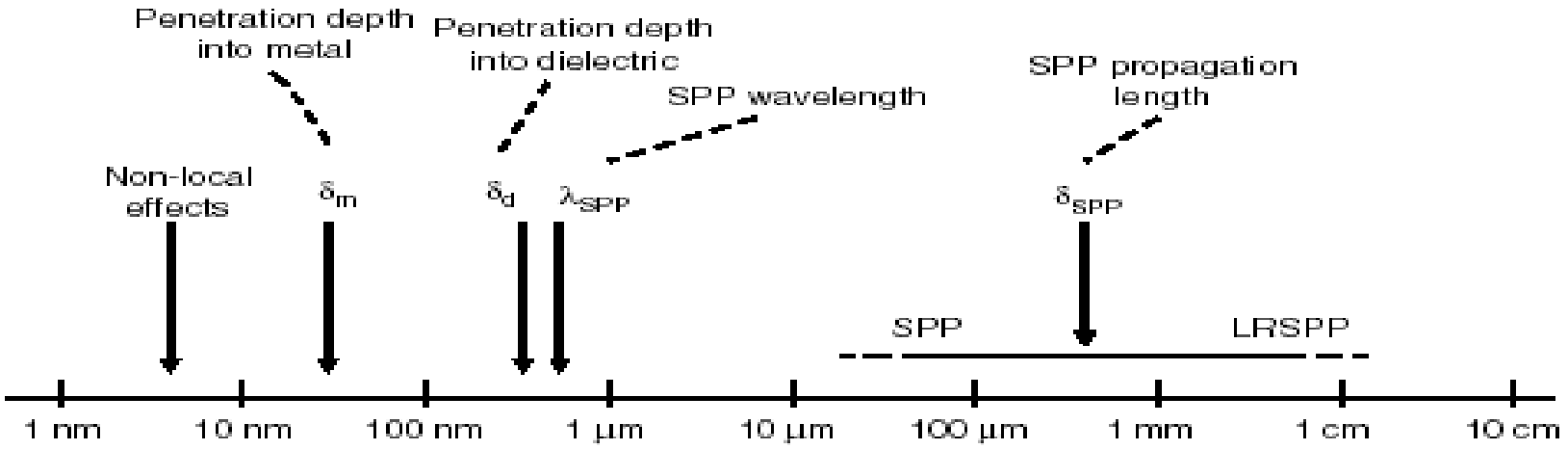

（局域）表面等离激元共振（LSPR或者SPR）

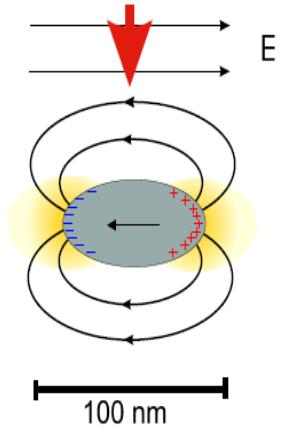

Figure 1.3: Particle plasmon

局域表面等离激元共振：局域在纳米金属颗粒或纳米结构上的电荷密度振荡。

1. 共振波长由纳米结构的形状、尺寸、材料、周围介质决定。
2. 共振时有局域场增强

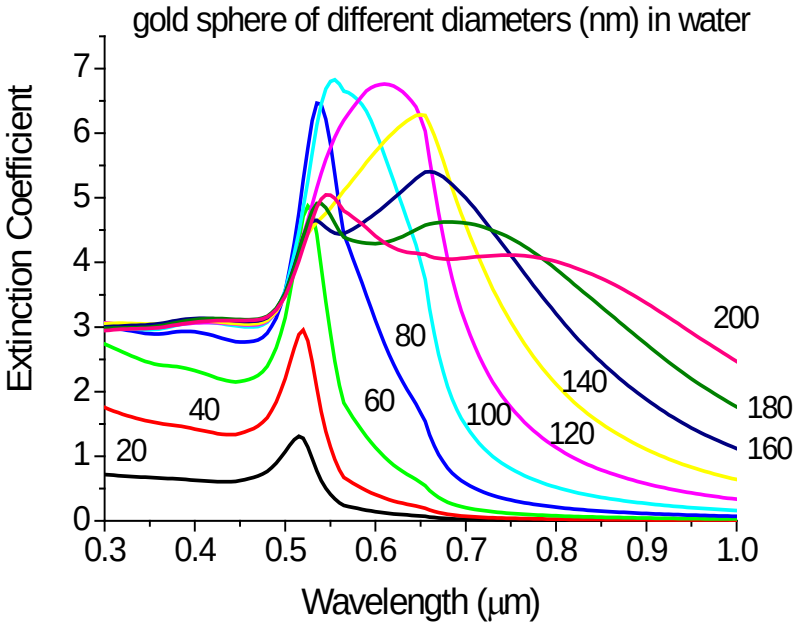

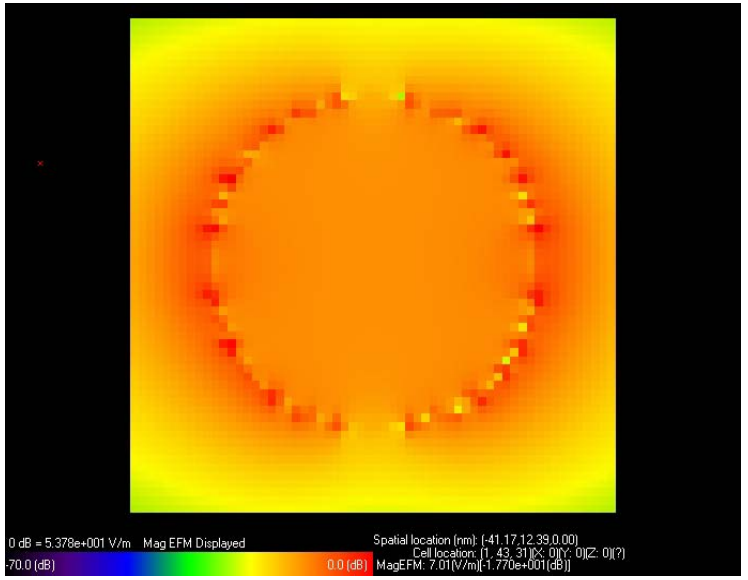

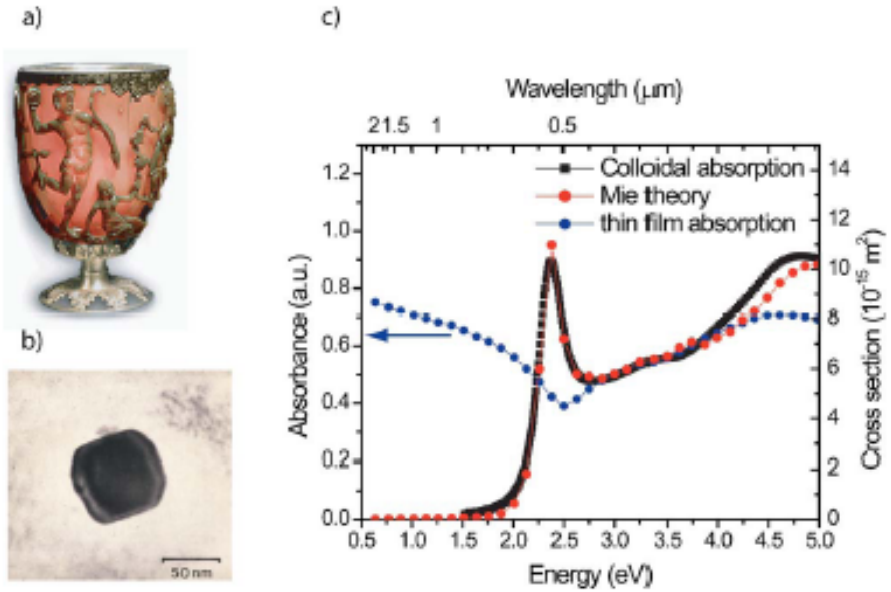

Fig. 1(a) by example of the Lycurgus cup (Byzantine empire, 4th century A. D.). The glass cup, on display in the British Museum, shows a striking red color when viewed in transmitted light, while appearing green in reflection. This peculiar behavior is due to small Au nanoparticles embedded in the glass [Fig. 1(b)], which show a strong optical absorption of light in the green part of the visible spectrum [Fig. 1(c)].

Plasmonics: Localization and guiding of electromagnetic energy in metal/dielectric

Stefan A. Maier and Harry A. Atwater, JOURNAL OF APPLIED PHYSICS 98, 011101 2005

Wood's anomalies，1902

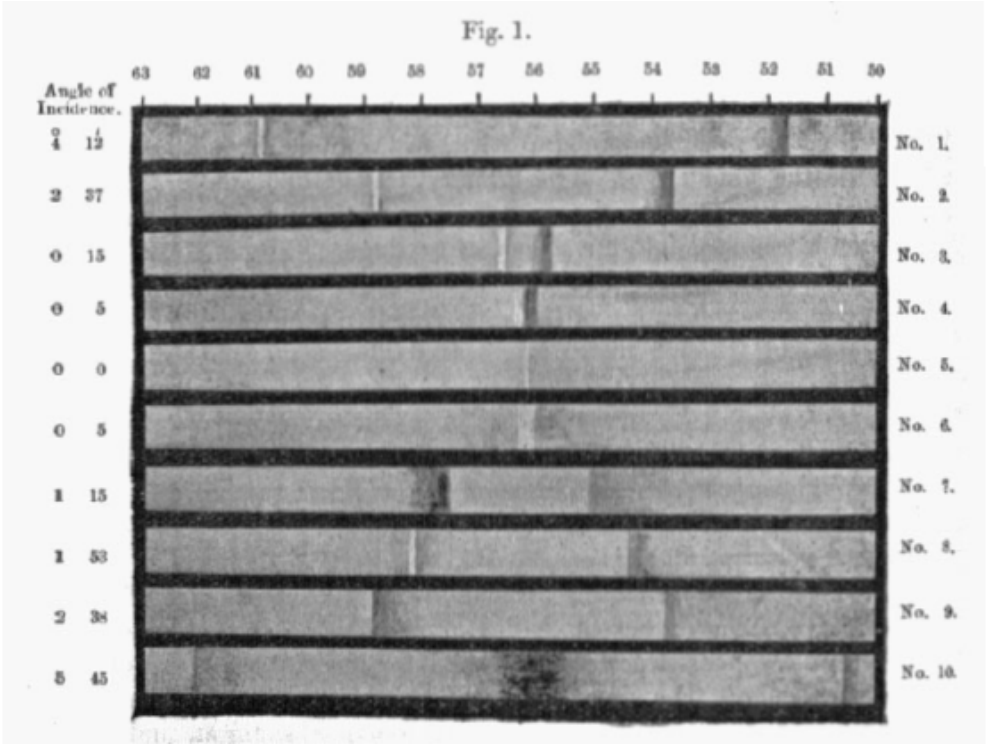

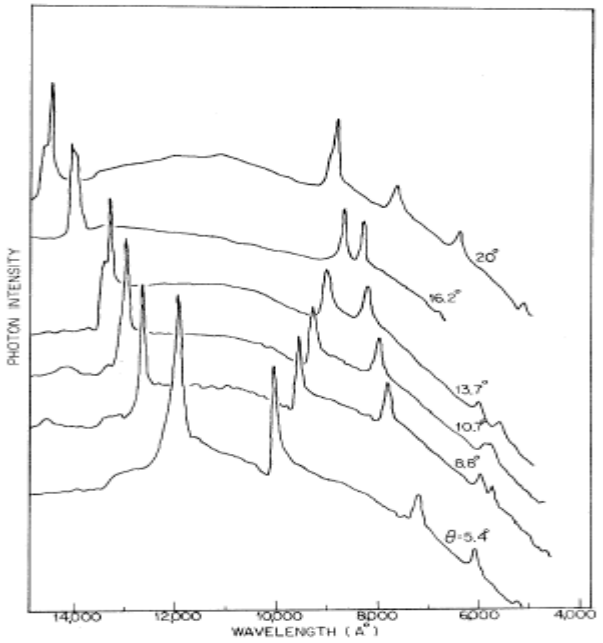

On a Remarkable Case of Uneven Distribution of Light in a Diffraction Grating Spectrum

R W Wood 1902 *Proc. Phys. Soc. London* 18 269

SURFACE-PLASMON RESONANCE EFFECT IN GRATING DIFFRACTION

RITCHIE RH, ARAKAWA ET, COWAN JJ, et al （1968） PRL, 21 , 1530.

Mie theory , 1908

Exact solution of sphere, spherical symmetry structure
Absorption, scattering, and extinction

Zenneck (1907) & Sommerfeld (1909)

Demonstrated (theoretically) that radio frequency surface EM waves occur at the boundary of two media when one medium is either a "lossy" dielectric, or a metal, and the other is a loss-free medium.

They also suggested that it is the "lossy" (imaginary) part of the dielectric function that is responsible for binding the EM wave to the interface.

Theory

Ritchie (1957)

Demonstrated theoretically the existence of Surface plasma excitations (surface plasmons) at a metal surface.

Stern (1958)

Showed (theoretically) that surface EM waves at a metallic surface involved EM radiation coupled to surface plasmons.

Derived, for the first time, the dispersion relations for surface EM waves at metal surfaces.

Experiment

Powell & Swan (1960)

Observed the excitation of **surface plasmons** at metal interfaces using electrons.

Otto (1968)

Devised the ATR (prism coupling) method for the coupling of bulk EM waves (optical) to surface EM waves.

Kretschmann (1971)

Modified the Otto geometry is now the most widely used device geometry.

Knoll (1989)

Introduced the technique of Surface Plasmon Microscopy

Extraordinary optical transmission
T.W.Ebbesen group , 1998

Start point of SPP

Bottleneck: low light transmittivity of apertures smaller than the wavelength of incident photon

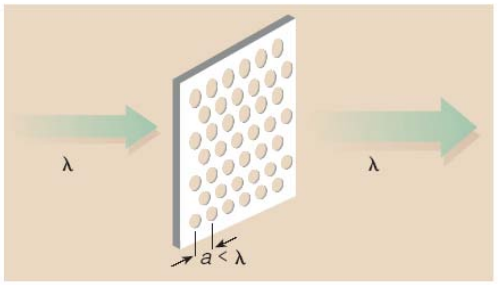

Hole arrays in silver film:
metal film thickness t
Periodicity of holes a_0
Scale of holes d

Results:
Extraordinary transmission
Maximum at $\lambda/d \sim 10$
Influence of t (in APL)

Explanation:
Coupling of light and plasmons

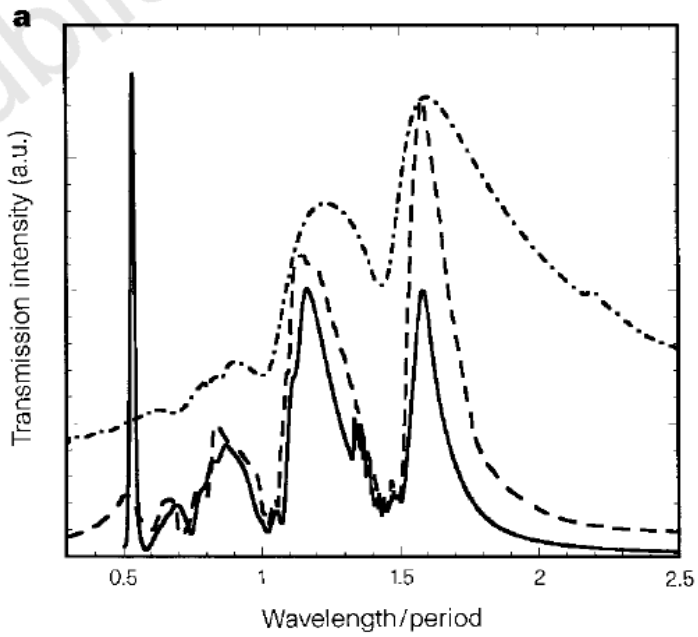

Extraordinary optical transmission through subwavelength holes
T.W. Ebbesen et al, NATURE |VOL 391 | 12 FEBRUARY 1998

Beaming light from a bull's eyes structure
T.W.Ebbesen group , 2002

Progress work

To solve: light diffracts in all directions when an aperture is small.

Bull's eye of Ag film:
thickness 300nm
Groove periodicity 500nm
And depth 60nm
Hole diamter 250nm

Results:
Beaming light

Explanation:
Coupling of light and plasmons

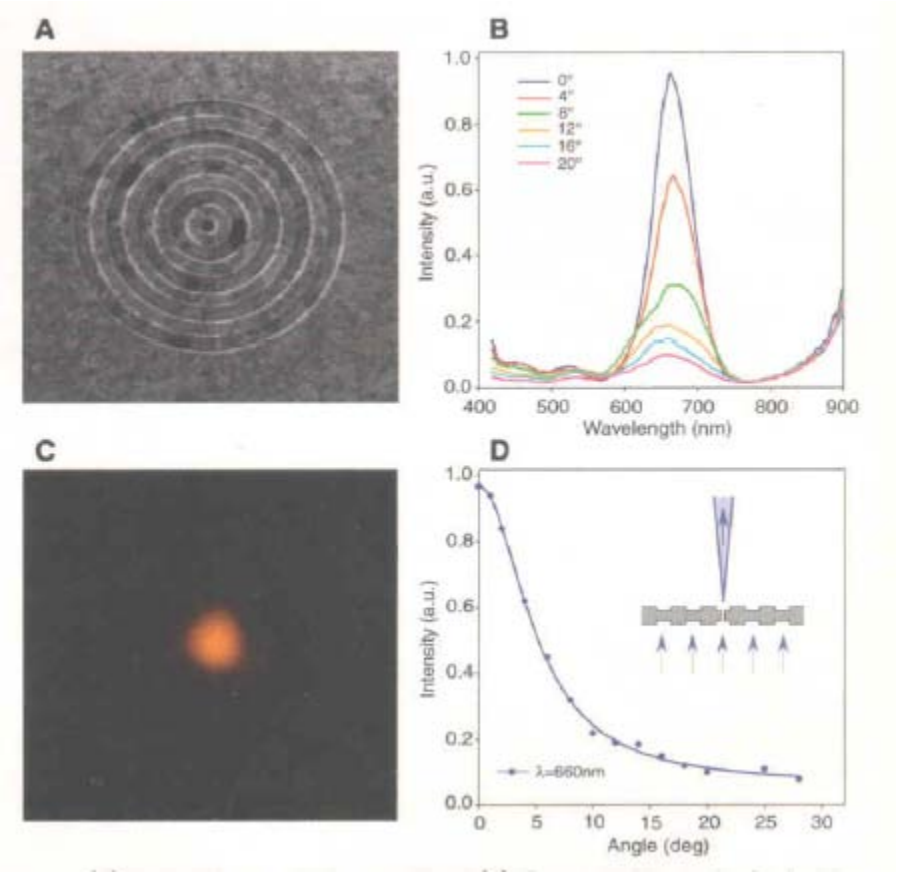

Beaming light from a subwavelength hole, T.W. Ebbesen et al, Science,297,820(2002)

Synthesis of Ag and Au nanocubes
Xia YN el al, 2002

Progress work

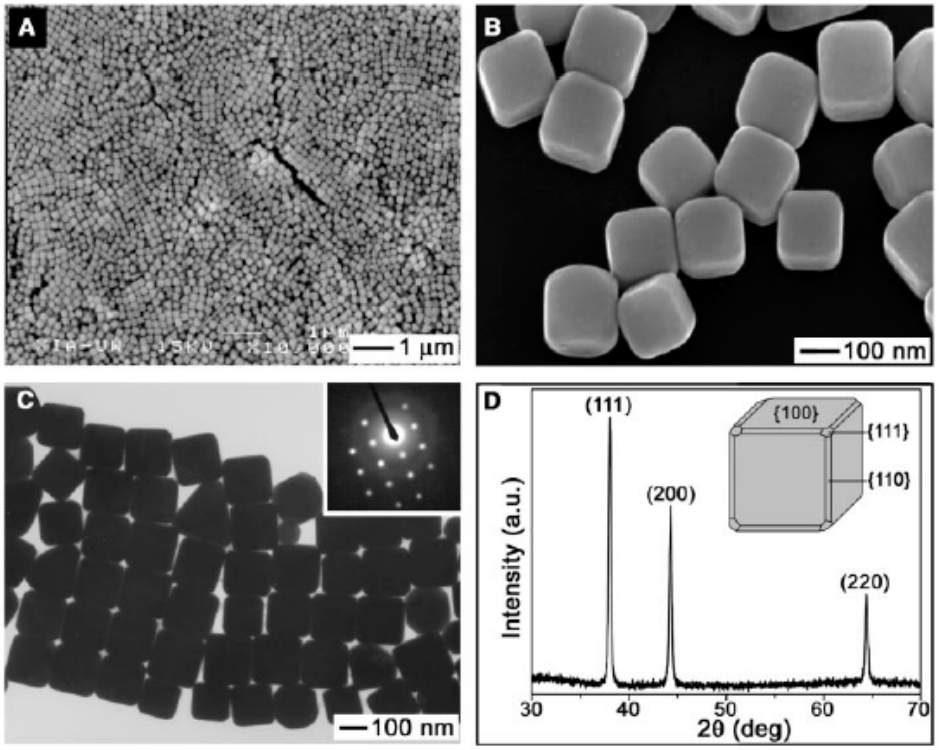

Significience:

Controlling the size, shape, and structure of metal nanoparticles is technologically important to tailor the plasmonic properties.

Shape-Controlled Synthesis of Gold and Silver Nanoparticles
Yugang Sun and Younan Xia, science, 76 (2002); 298 Science

各种形状金属颗粒SPR的共振范围

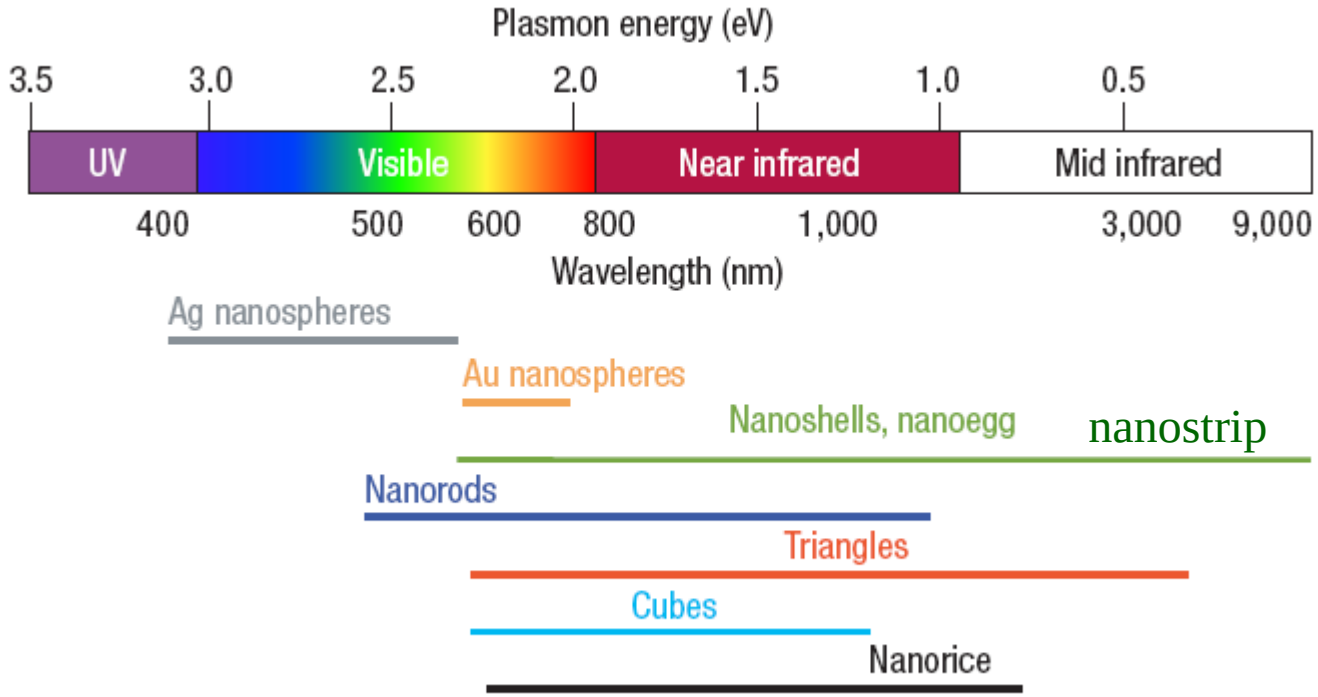

结论：通过调节纳米金属颗粒的形状，SPR可发生在可见光、红外和中红外波段。

实际上：在太赫兹和微波波段，SPR的研究也很广泛。

Nano-optics from sensing to waveguiding, N.J. Halas, nature photonics | VOL 1 |641| 2007

A hybridization model for plasmon response
N J Halas el al, 2003

Progress work

To solve: surface plasmon resonances in nanoshells

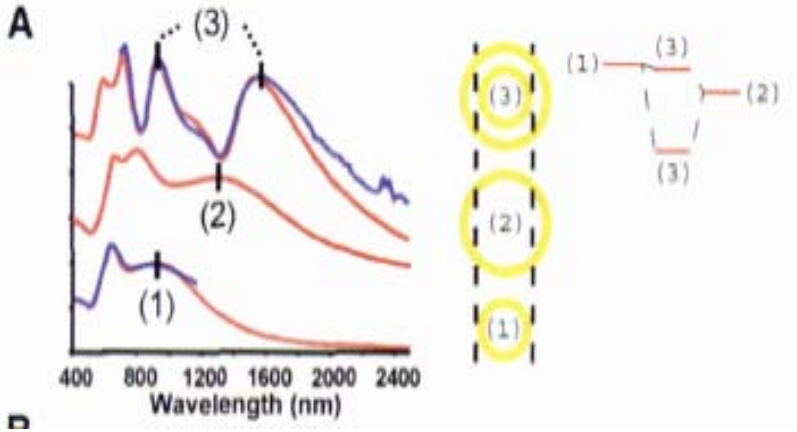

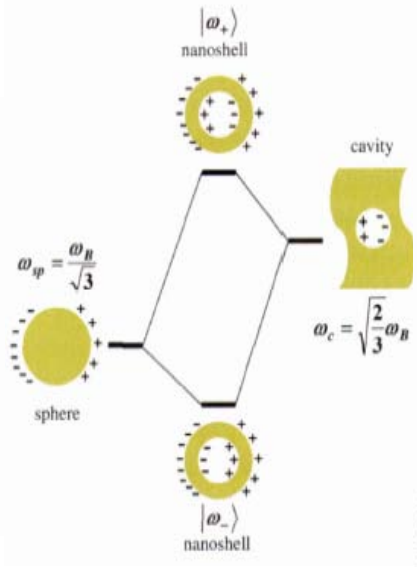

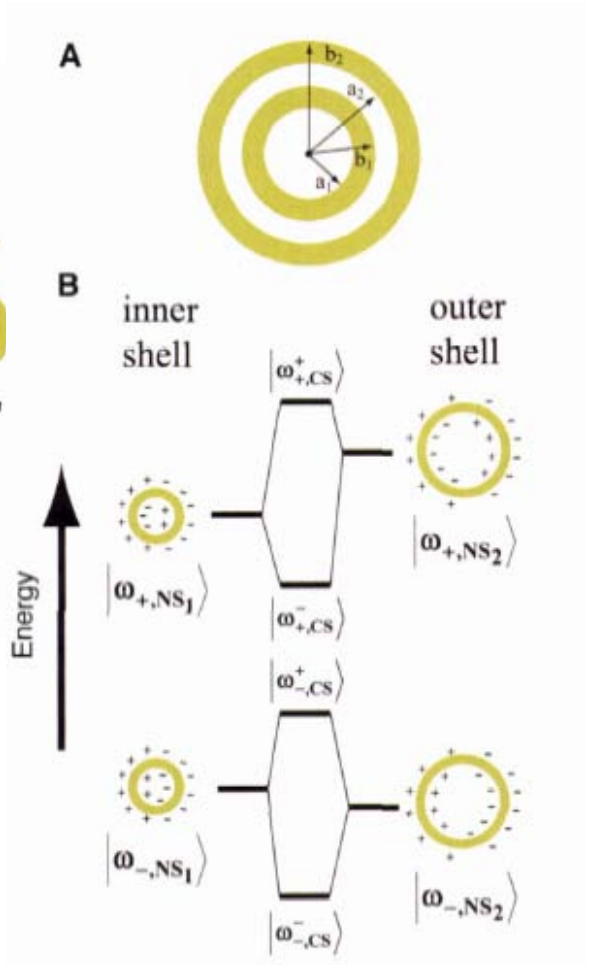

A hybridization of sphere and cavity

A hybridization of inner and outer shells

Results:

Several response peaks

A hybridization model for the plasmon response of complex nanostructures

E Prodan; C Radloff; N J Halas; P Nordlander,Science, 302,419, 2003.

Surface plasmon subwavelength optics

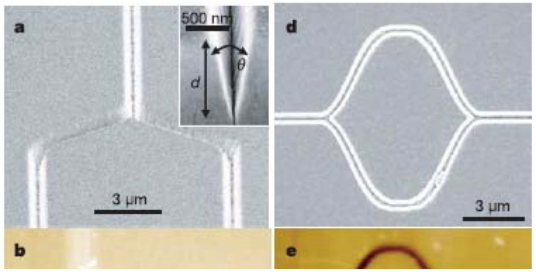

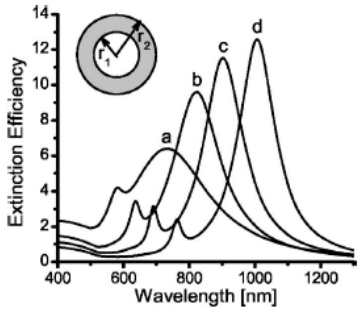

FIG. 1. Plasmon resonances of silica/Au nanoshell structures in water with r_1=60 nm and r_2 = (a) 80 nm, (b) 70 nm, (c) 67 nm, and (d) 65 nm, respectively.

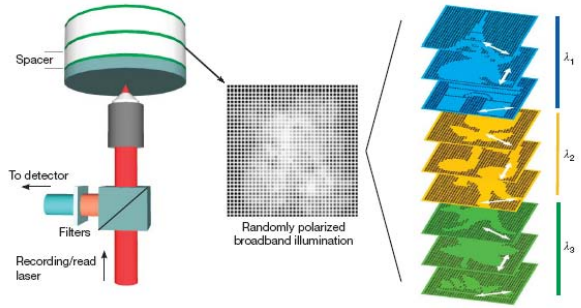

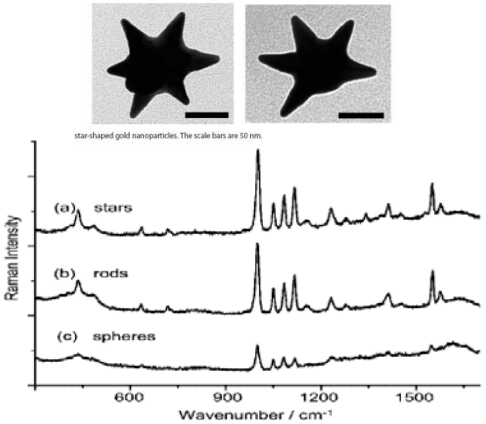

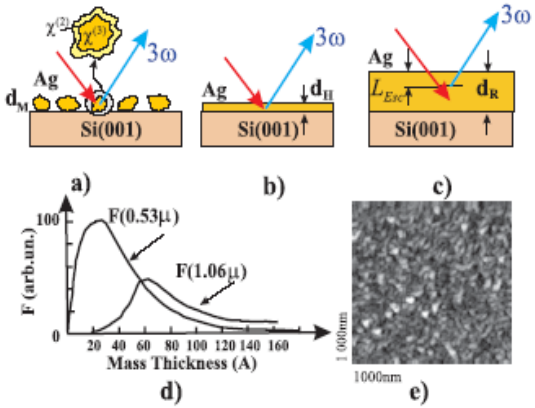

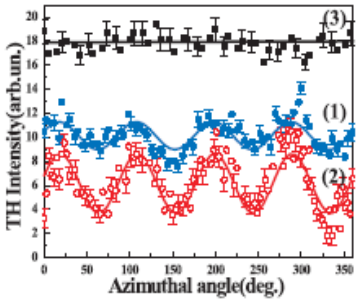

表面等离激元光学是纳米尺度上光子学和电子学的结合，在光子回路，数据存储，光谱学，生物光子学，太阳能及非线性光学方面都有应用。

William L. Barnes, Alain Dereux & Thomas W. Ebbesen, nature, 424, 824 (2003)

Plasmon-assisted transmission of entangled photons E. Altewischer el al, 2002

Application work

Aim to: Investigate the effects of nanostructured metal on entangled photons.

Results:
Such arrays convert photons into surface-plasmon —optically excited compressive charge density waves — which tunnel through the holes before reradiating as photons.

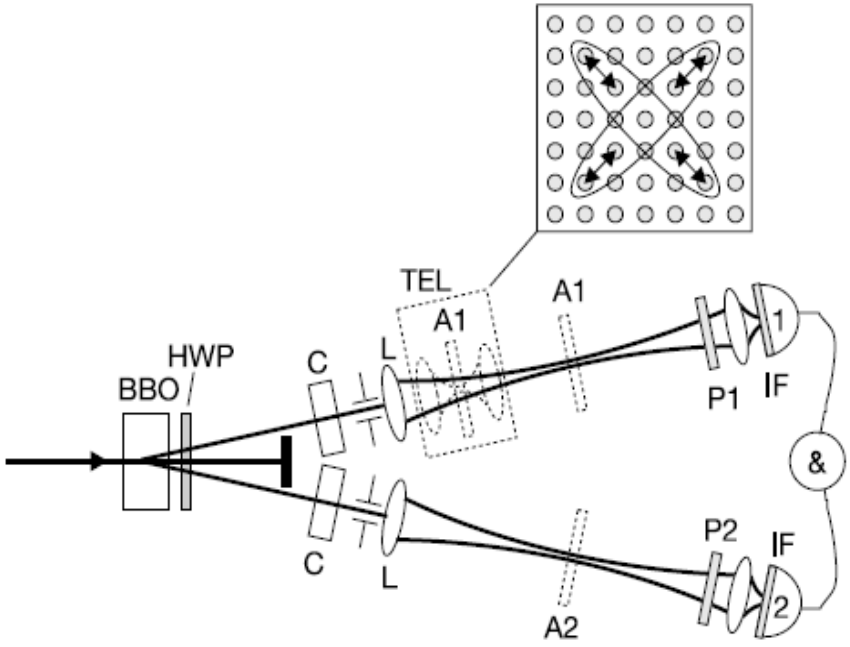

Explanation:
Conversion between photons and plasmons, quantum feature of SPP

Plasmon-assisted transmission of entangled photons,
E. Altewischer, M. P. van Exter & J. P. Woerdman, NATURE |VOL 418 | 304| 2002 |

Forster Energy Transfer Across a Metal Film
W. L. Barnes et al, 2004

Application work
Molecular plasmonics

Aim to: realize the Forster energy transfer between donor and acceptor across silver film

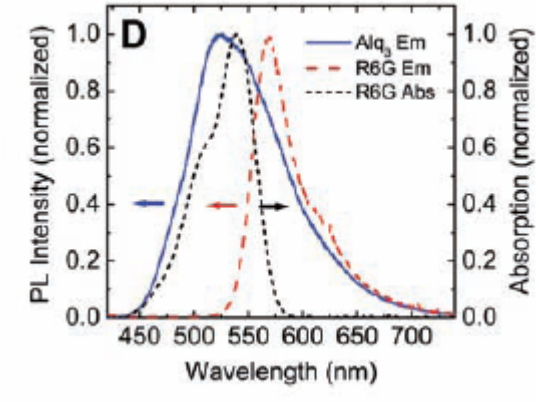

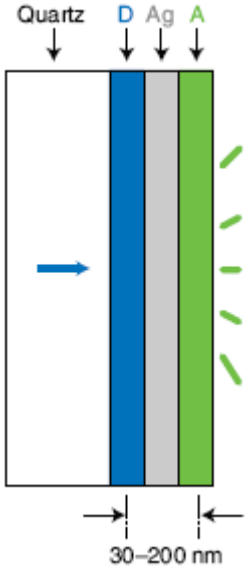

Significance:
toward the realization of an active plasmonic device by combining thin polymer films with thin silver films

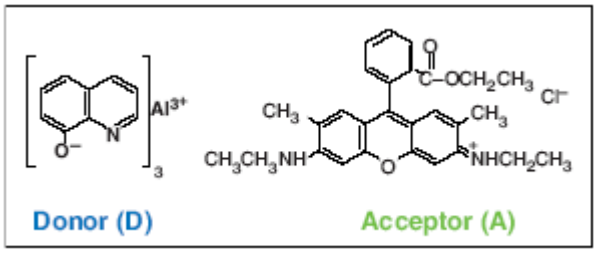

Energy Transfer Across a Metal Film Mediated by Surface Plasmon Polaritons
P. Andrew and W. L. Barnes,science,306,1002(2004).

Generation of single optical plasmons in metallic nanowires coupled to quantum dots
M. D. Lukin et al, 2007

Crossing work

Aim to: efficient coupling between quantum dots and SPP, single photon switch and transistor, long range quantum bits.

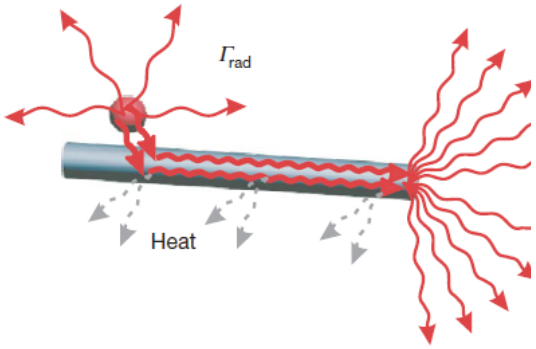

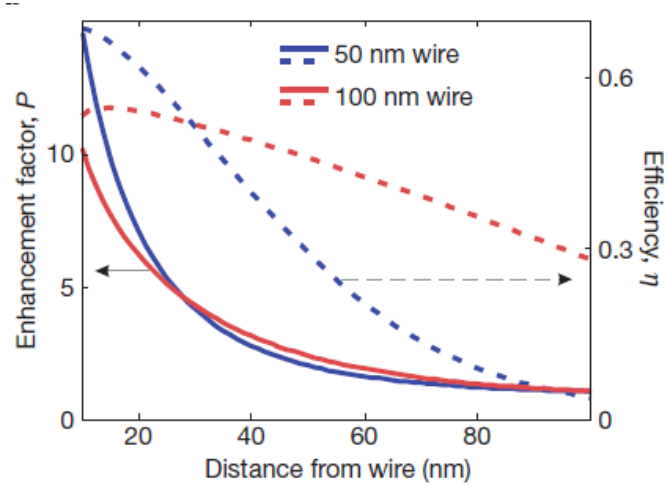

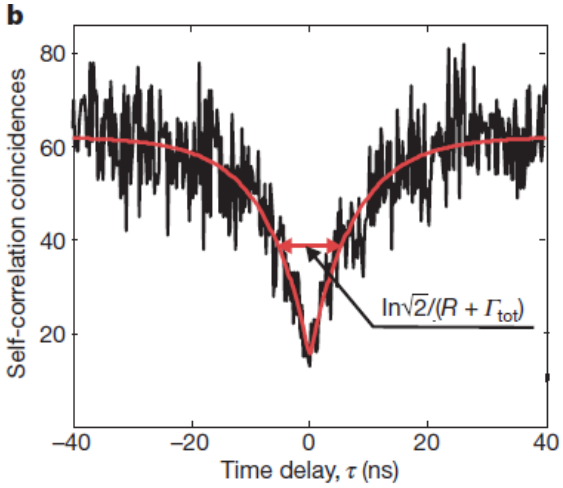

Results:

Realizing single quanta of surface plasmon.

Generation of single optical plasmons in metallic nanowires coupled to quantum dots
A. V. Akimov et al, NATURE|Vol 450|402| 2007

Quantum light switch: A single-photon transistor using nanoscale surface plasmons
M. D. Lukin et al, 2007

Crossing work

在未来的计算机中光子能够代替电子吗？光子回路体积小，易于集成，损耗小，传的快，但是光子间没有相互作用，实现量子操控比较困难。光子与表面等离激元间的交换弥补了这一不足，下面是量子发射体和表面等离激元强耦合的单光子晶体管。

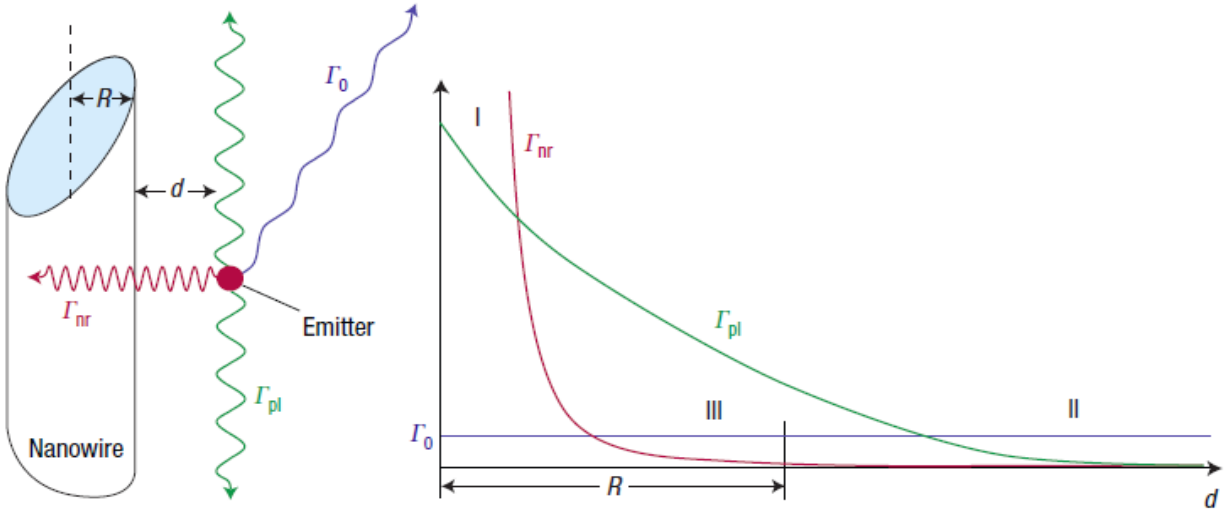

A single-photon transistor using nanoscale surface plasmons,M. D. Lukin et al, NATURE PHYSICS|Vol 3|807| 2007; Quantum light, switch,M.Orrit, NATURE PHYSICS|Vol 3|755| 2007

Core-shell nanostructure spaser
M. A. Noginov et al, 2009

Progress work

Aim to: realize a ‘spaser’ generating stimulated emission of surface plasmons in resonating metallic nanostructures adjacent to a gain medium.

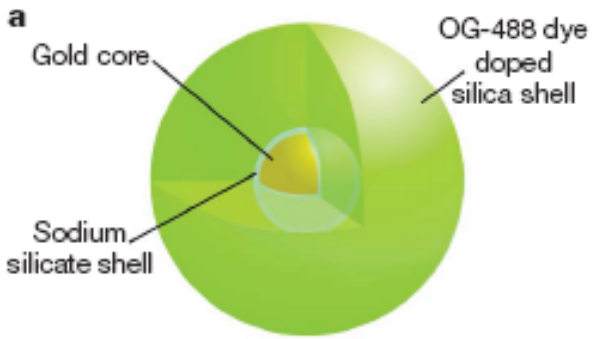

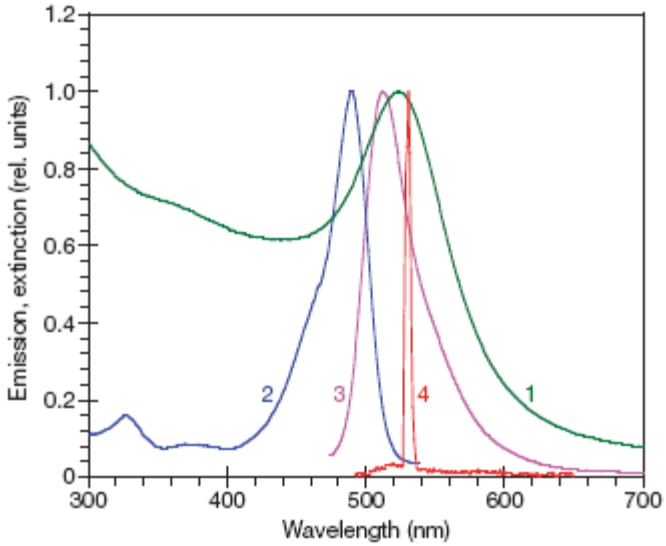

Parameters:
gold core : 14 nm
Shell: 44 nm
Wavelength: 525 nm

Significance:
the smallest nanolaser
the first operating at visible wavelengths.

Demonstration of a spaser-based nanolaser, M. A. Noginov et al, NATURE| Vol 460|1110| 2009

Nano-spaser based on hybrid waveguide
X. Zhang et al, 2009

Progress work

Challenge to: realize ultracompact lasers generating coherent optical fields at a nanoscale, far beyond the diffraction limit

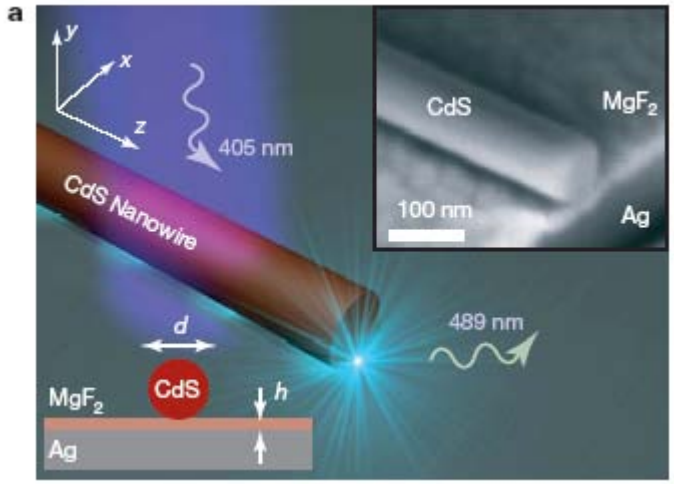

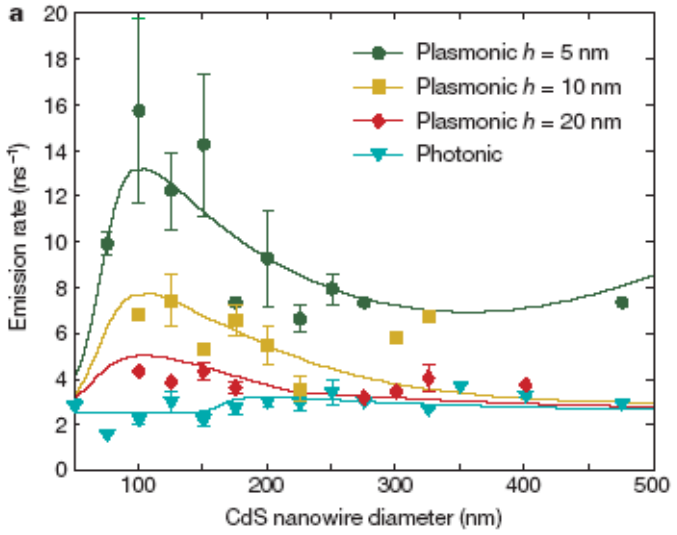

Significance:

Plasmonic modes have no cutoff, downscaling of the lateral dimensions of both the device and the optical mode is demonstrated.

Plasmon lasers at deep subwavelength scale, X.Zhang et al, NATURE|Vol 461|629| 2009

modified plasmon–matter interaction with mesoscopic quantum emitters
Mads Lykke Andersen, et al. 2010

Progress work

Aim to: experimentally demonstrate various decay channels with considering the size of quantum emitters.

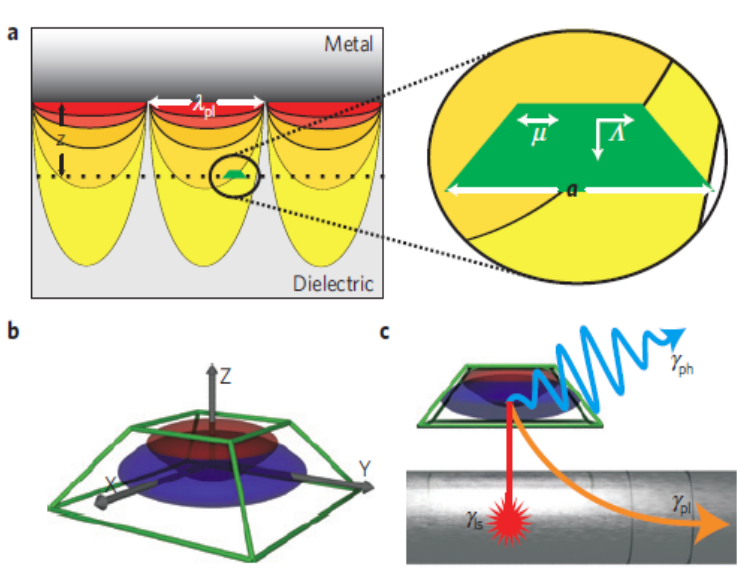

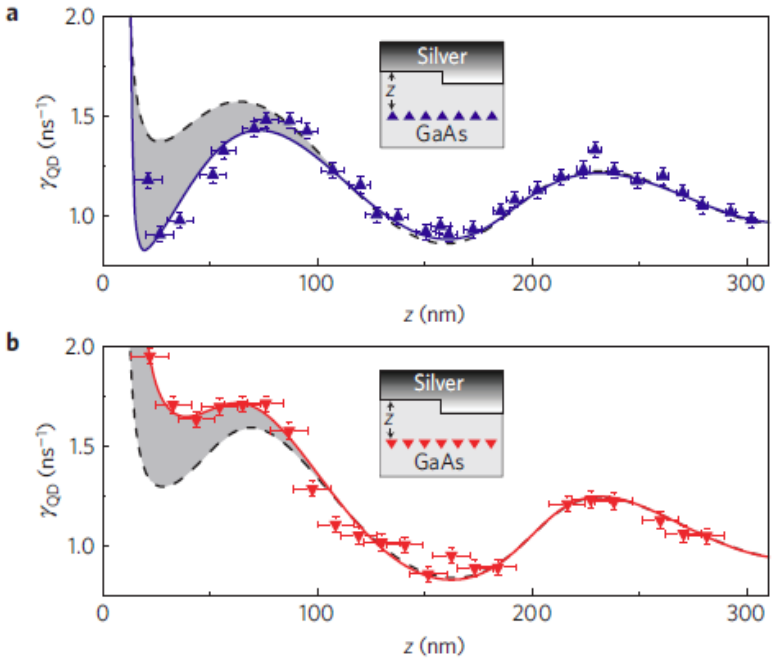

Significance: the effect of the size of nanoscale quantum dot on the coupling between SPP and quantum emitter.

Strongly modified plasmon–matter interaction with mesoscopic quantum emitters

Mads Lykke Andersen, et al. nature physics, DOI: 10.1038/NPHYS1870, 2010

APPLIED PHYSICS: The Case for Plasmonics

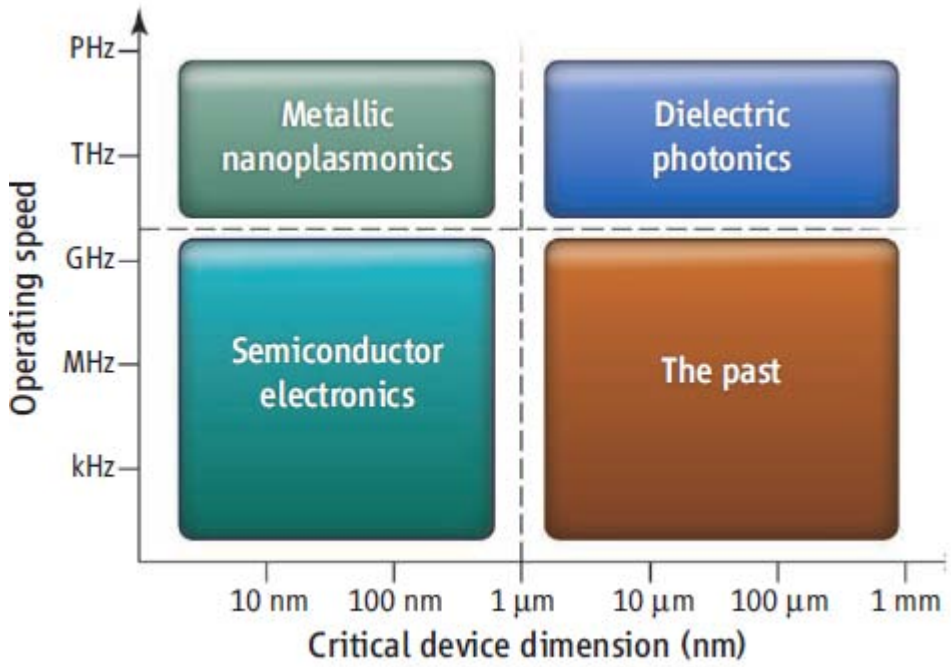

By squeezing light into nanoscale volumes, plasmonic elements allow for fundamental studies of light-matter interactions at length scales that were otherwise inaccessible

The Case for Plasmonics
Mark L. Brongersma, et al,science, VOL 328,440 (2010).

二、表面等离激元相关的几个工作

2.1 解决表面等离激元共振的格林函数方法 应用

2.2 纳米金属颗粒阵列中几何共振的调制

2.3 基于表面等离激元的杂化波导结构

由于介观体系的细微结构可以和波长相比拟，甚至比波长小得多，在处理此类问题时，边界尤为复杂，可解析求解的几类特例已不能满足许多实际问题的需要。

所以，目前发展出多种数值方法和理论方法，如：

纯数值计算：有限时域差分 FDTD,有限元算法，FEM

电偶极近似的算法：离散偶极近似 DDA

耦合偶极子近似 CDA

周期性结构中常用算法：多重散射MMS

平面波展开PWE

处理不规则纳米结构：格林函数方法 GFM，

转移矩阵方法TMM

各种方法的比较

Mie理论：只能针对球形及其球对称的拓扑结构。

离散偶极近似和耦合偶极近似：可处理任意形状纳米结构问题，受到计算大型矩阵难题的限制。但计算较小颗粒阵列时快速、准确。

FDTD：直接从麦克斯韦方程出发，在时域上作了差分抽样计算，这就将计算大矩阵的问题转化为耗时的代价来解决，可处理任意纳米结构。

格林张量法：不规则形状，近场可以用入射波长，几何形状、介电常数明确表示出来。

格林矩阵法：在给定入射波长和几何结构下，在介电常数的空间中给出所有可能共振的模式。表现系统的本征性质。

常用软件：FDTD，Comsol, solution

2.1 解决表面等离激元共振的格林函数方法 应用

格林函数方法

格林并失方法

通过引入格林并失，解决不规则亚波长结构中的近场问题，除了格林并失对角元项中的奇点问题，没有任何近似。因为考虑了多极散射，计算精度较高。计算电磁场后，给出吸收、散射和消光峰等。

An incident light $E_0(r)e^{i\omega t}$ impinges on the following system, the scattering field E(r) is a solution of the wave equation:

$$-\nabla \times \nabla \times \mathbf{E}(\mathbf{r}) + k^2 \varepsilon_r(\omega)\mathbf{E}(\mathbf{r}) + k^2 \varepsilon_s(\mathbf{r},\omega)\mathbf{E}(\mathbf{r}) = \mathbf{0}, \quad (1)$$

With $\varepsilon(\mathbf{r},\omega) = \varepsilon_r(\omega) + \varepsilon_s(\mathbf{r},\omega)$

In the scattering: $\varepsilon(r,\omega)$

out the scattering: εr

In E(r), $e^{i\omega t}$ is cancelled.

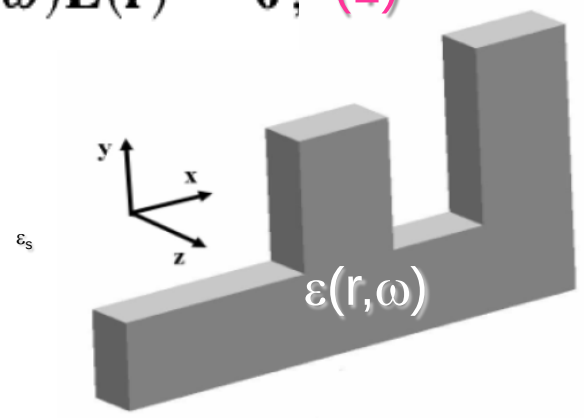

Generalized field propagator for electromagnetic scattering and light confinement , Olivier J. F. Martin et al, Phys. Rev. Lett. 74, 526 (1995)

Introducing the operators

$$L = -\nabla \times \nabla \times \qquad e_r = k^2 \varepsilon_r(\omega) \qquad e_s = k^2 \varepsilon_s(\omega)$$

Eq.(1) can be rewritten as

$$(\mathbf{L} + \mathbf{e}_r + \mathbf{e}_s)\mathbf{E} = \mathbf{0} \qquad (2)$$

and $E^0(r)$ satisfies $(\mathbf{L} + \mathbf{e}_r)\mathbf{E}^0 = \mathbf{0}$ (3)

The Green's tensor G^0 associated with the reference is

$$(\mathbf{L} + \mathbf{e}_r)\mathbf{G}^0 = \mathbf{1} \qquad (4)$$

$$\rightarrow \quad G^0 = (L + e_r)^{-1}$$

The Green's tensor G^0 associated with the complete system is $(\mathbf{L} + \mathbf{e}_r + \mathbf{e}_s)\mathbf{G} = \mathbf{1}$ (5)

$$\rightarrow \quad G = (L + e_r + e_s)^{-1}$$

Generalized field propagator for electromagnetic scattering and light confinement,
Olivier J. F. Martin et al, Phys. Rev. Lett. 74, 526 (1995)

If (2) = (3) , then

$$(L+e_r+e_s)E=(L+e_r)E^0$$
$$\Rightarrow G^{-1}E=(G^o)^{-1}E^0$$
$$\Rightarrow GG^{-1}E=G(G^o)^{-1}E^0$$
$$\Rightarrow E=G(L+e_r+e_s-e_s)E^0$$
$$\Rightarrow E=(I-Ge_s)E^0$$

In the r-representation

$$\mathbf{E}(\mathbf{r})=\int d\mathbf{r}'[\delta(\mathbf{r}-\mathbf{r}')-k^2\mathbf{G}(\mathbf{r},\mathbf{r}',\omega)\cdot\varepsilon_s(\mathbf{r}',\omega)]\cdot\mathbf{E}^0(\mathbf{r}') \quad (6)$$

Finally, we get Lippmann-Schwinger equation

$$\mathbf{E}(\mathbf{r})=\mathbf{E}^0(\mathbf{r})-k^2\int d\mathbf{r}'\,\mathbf{G}^0(\mathbf{r},\mathbf{r}',\omega)\varepsilon_s(\mathbf{r}',\omega)\cdot\mathbf{E}(\mathbf{r}')\,. \quad (7)$$

This is the main results of Green's tensor method

Generalized field propagator for electromagnetic scattering and light confinement,
Olivier J. F. Martin et al, Phys. Rev. Lett. 74, 526 (1995)

几点说明或解释：

$$\mathbf{E}(\mathbf{r}) = \mathbf{E}^0(\mathbf{r}) - k^2 \int d\mathbf{r}' \mathbf{G}^0(\mathbf{r}, \mathbf{r}', \omega)\varepsilon_s(\mathbf{r}', \omega) \cdot \mathbf{E}(\mathbf{r}') . \qquad (7)$$

（1）从上式可以看出，散射体内或散射体外任何一点的电场可以用散射体内格林并失和散射体内电场求积后的叠加来表示，大大简化了纳米散射体中电磁散射的复杂边界问题。

（2）通常的解法是先自洽解出散射体内的电场，然后代入上式得到空间任何一点的电场，包括近场和远场。这里可以是金属或介质。

（3）原则上说，知道电场后可以计算消光、吸收和散射。但在实际纳米金属结构应用中，通常只给出散射体内吸收峰或者散射峰去代表表面等离激元共振（SPR）。

关于G和G^0的说明：

这里G^0是3D系统的Green’s tensor ： $\mathbf{G} = \mathbf{G}^0 - \mathbf{G}^0 \mathbf{e}_s \mathbf{G}$

$$\mathbf{G}^0(\mathbf{r}, \mathbf{r}', \omega) = -\left(\mathbf{1} - \frac{1 - ik_r R}{k_r^2 R^2}\mathbf{1} - \frac{-3 + 3ik_r R + k_r^2 R^2}{k_r^2 R^4}\mathbf{R}\,\mathbf{R}\right)\frac{\exp[ik_r R]}{4\pi R}, \quad (8)$$

where $R = |\mathbf{R}| = |\mathbf{r} - \mathbf{r}'|$ and $k_r^2 = \varepsilon_r(\omega)k^2$.

（1）可以看到，G0包含了电多极的成分，比偶极近似精确。

（2）在r=r’时，G0存在奇点问题。通常的处理方法是在一个R=0小区域内用积分，直接给出积分值即可。具体可参考以下文献。

（3）需要指出的是，这里奇点的存在是格林并失方法中唯一的近似。

Yaghjian A. D., Proc. IEEE, 68 (1980) 248.

格林矩阵方法 (Green's matrix method or GMM)

在格林并失的方法基础上发展出的新方法，解决不规则金属亚波长结构中的表面等离激元共振问题。其特点是通过求解纳米散射体中格林矩阵的本征值和本征矢，以及定义共振容量的概念，直接给出体系的共振信息及近场信息。

优点：解决了任意纳米结构的表面等离激元共振及近场这一类问题，一方面可更深入揭示SPR的物理，另一方面将对金属纳微结构的裁剪、共振控制及混合型纳米器件的设计提供指导。

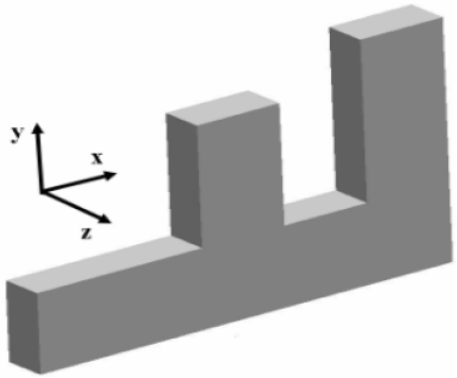

Resonance capacity of surface plasmon on subwavelength metallic structures ,Y.Gu et al, EPL, 83 (2008) 27004

Starting from Lippmann-Schwinger equation

$$\mathbf{E}(\mathbf{r}) = \mathbf{E}^0(\mathbf{r}) - k^2 \int d\mathbf{r}' \mathbf{G}^0(\mathbf{r}, \mathbf{r}', \omega)\varepsilon_s(\mathbf{r}', \omega) \cdot \mathbf{E}(\mathbf{r}') .$$

If the clusters subspace V is divided into N pieces with the volume δV (with $\delta V \ll V$), eq. (3) becomes

线性问题转化为矩阵的本征问题

$$\sum_{\mathrm{r}' \in V} [\epsilon_s(\mathrm{r}, \omega)\widetilde{G^0}(\mathrm{r}, \mathrm{r}', \omega) - \delta_{\mathrm{r},\mathrm{r}'}]\widetilde{E}(\mathrm{r}) = -\widetilde{E^0}(\mathrm{r}) \qquad (4)$$

ε_s

with $\widetilde{G^0}(\mathrm{r}, \mathrm{r}', \omega) = \delta V k^2 G^0(\mathrm{r}, \mathrm{r}', \omega)$. Let us rewrite it in the form

$$\sum_{\mathrm{r}' \in V} [\widetilde{G^0}(r, r', \omega) - sI]\widetilde{E}(r) = \frac{-\widetilde{E^0}(\mathrm{r})}{\epsilon_s(\mathrm{r}, \omega)}, \qquad (5)$$

where $s = \frac{1}{\epsilon(\mathrm{r},\omega) - \epsilon_0(\omega)}$. $\widetilde{G^0}$, a $3N * 3N$ matrix, is called Green's matrix.

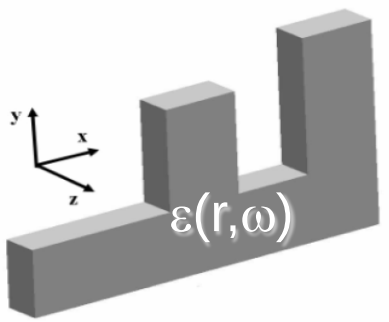

Resonance capacity of surface plasmon on subwavelength metallic structures , Y.Gu et al, EPL, 83 (2008) 27004

本征值直接和材料参数对应：

$$s = \frac{1}{\epsilon(\mathrm{r},\omega) - \epsilon_0(\omega)}$$

可直接用本征矢表示电磁场，包括近场和远场。

Electric fields in the nanostructures：

$$\tilde{E}(\mathrm{r}) = \sum_{n=1}^{3N} \frac{sL_n \cdot \widetilde{E^0}(\mathrm{r})}{(s - s_n)} . R_n .$$

Electric fields outside the nanostructures

$$E(\mathrm{r}) = E^0(\mathrm{r}) + k^2 \sum_{n=1}^{3N} \frac{L_n \cdot \widetilde{E^0}(\mathrm{r})}{(s - s_n)} . [\sum_{\mathrm{r}' \in C} G^0(\mathrm{r}, \mathrm{r}', \omega) \cdot R_n] .$$

Resonance capacity of surface plasmon on subwavelength metallic structures , Y.Gu et al, EPL, 83 (2008) 27004

Resonance Capacity (RC)

Definition in view of the inside electric field energy of the nanostructures

$$C_n = \frac{\int_V d\mathbf{r}' |\epsilon_n| . [res|E(\mathbf{r}')|]_n^2}{\int_V d\mathbf{r}' |\epsilon_0(\omega)| . |E^0(\mathbf{r}')|^2}$$

$$[res|E(\mathbf{r}')|]_n = |\frac{L_n . E^0(\mathbf{r}')}{\epsilon_n(\mathbf{r},\omega)} . R_n|$$

where

$$\epsilon_n = \frac{1}{s_n} + \epsilon_0(\omega).$$

$$(\epsilon_d E_{d\perp} = \epsilon_m E_{m\perp}),$$

Resonance capacity of surface plasmon on subwavelength metallic structures , Y.Gu et al, EPL, 83 (2008) 27004

Physics meaning:

（1）RC quantitatively expresses the ability to gather the electromagnetic energy from the environment for free electrons in metals.

（2）the larger RC means the larger value of $\varepsilon_m E_m$, so the more enhanced near field Ed

（3）by RC distribution, we can select those SPRs with the strong near fields in the subwavelength metallic structures

（4）the extinction peaks of far field should correspond to those SPRs with the high values of RC

Resonance capacity of surface plasmon on subwavelength metallic structures ,
Y.Gu et al, EPL, 83 (2008) 27004

Comparison with the nanoantena experiment

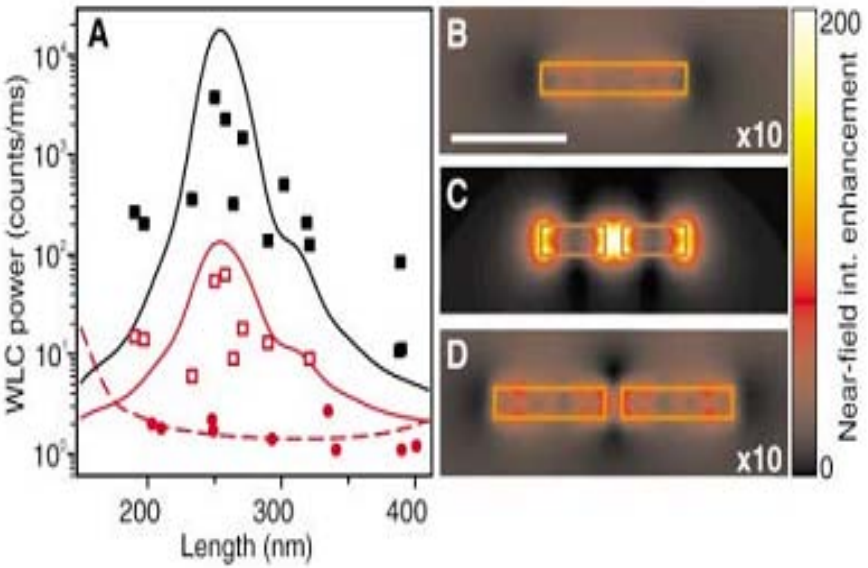

Science, 308, 1607 (2005)

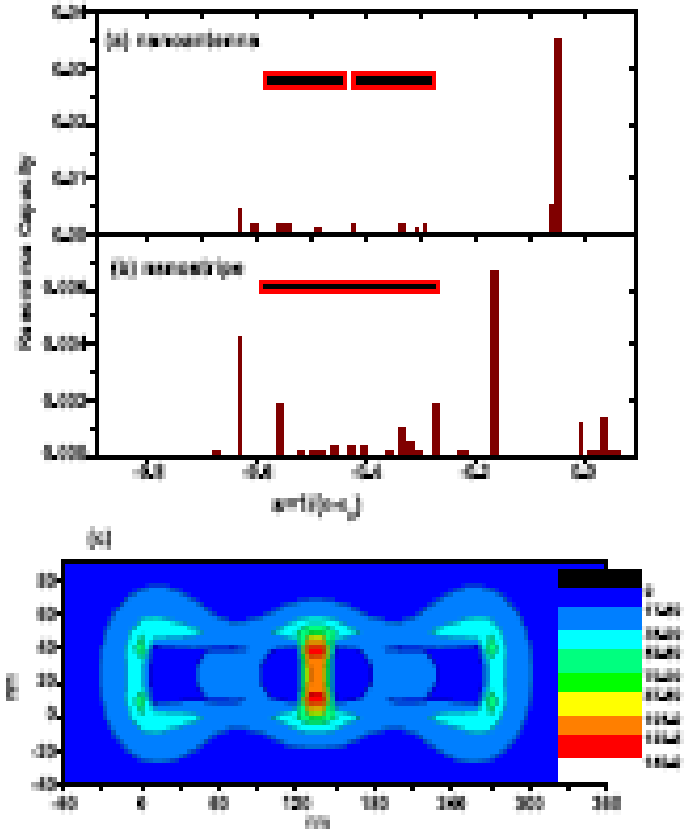

GMM results

Nanoantena effects ：at the wavelength 830nm, a nanostrip 260×40×45nm3 has no SPR, while with a gap, SPR happens.

Resonance capacity of surface plasmon on subwavelength metallic structures , Y.Gu et al, EPL, 83 (2008) 27004

Resonance capacity distribution of rectangular nanostrips

λ = 632nm

结果发现：
扁平的纳米金属条能够在光波段发生共振

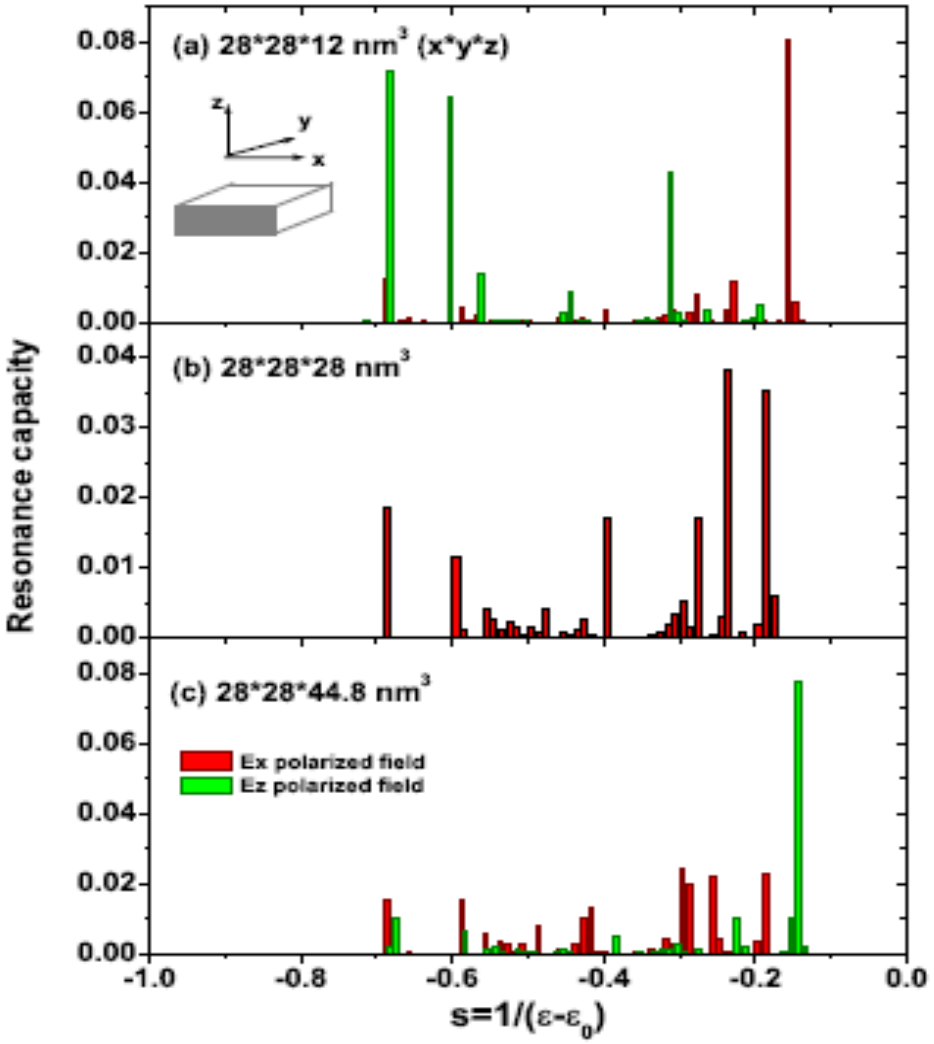

Resonance capacity of surface plasmon on subwavelength metallic structures , Y.Gu et al, EPL, 83 (2008) 27004

On the other hand:

RC distribution has a little modification with increasing the wavelength for an example

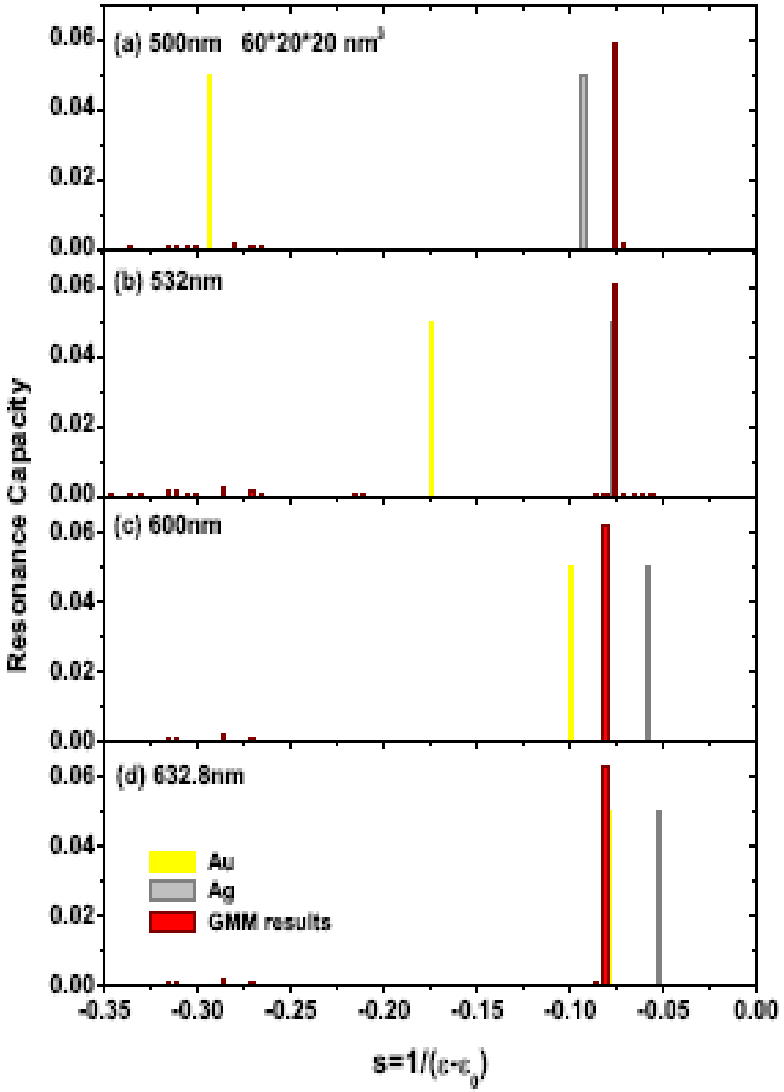

GMM的缺点：

由于格林矩阵对称，只能得到实的介电常数值，而金属中有虚部，会带来计算的不准确。

但是：

由于金属介电常数的虚部和实部比值很小，略去虚部的考虑不会影响其SPR性质。

Resonance capacity of surface plasmon on subwavelength metallic structures , Y.Gu et al, EPL, 83 (2008) 27004

从可见到红外的纳米金属条等离激元共振设计

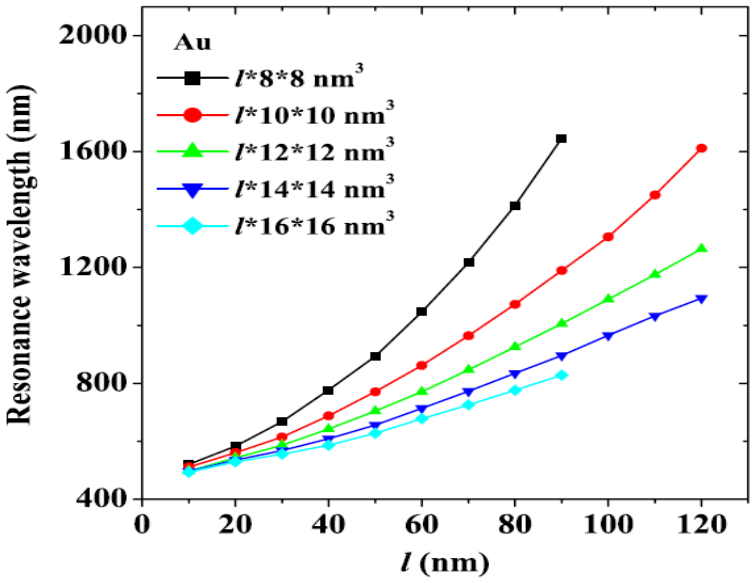

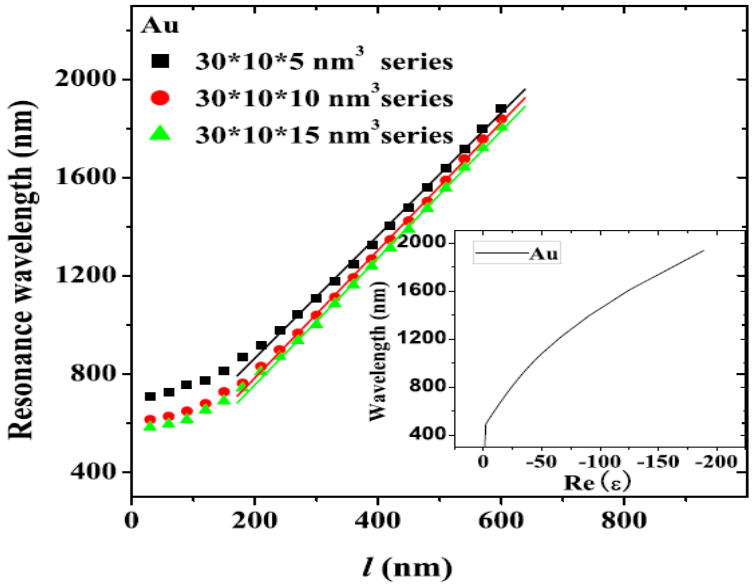

固定横截面后，增加纳米金条的长度，SPR可从可见调到红外；横截面越小，可调性越好。

在波长900 nm后，固定金条长宽高比例的各个系列，共振和尺度间存在线性关系：长度每增加一个纳米，共振红移2.6nm。

J.Li et al, Journal of Modern Optics（2009）56，1396–1402

二元纳米金属结构中表面等离激元共振的相互作用

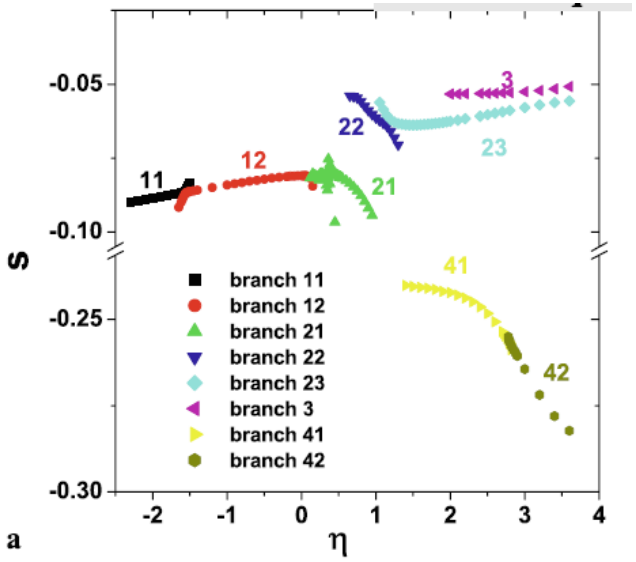

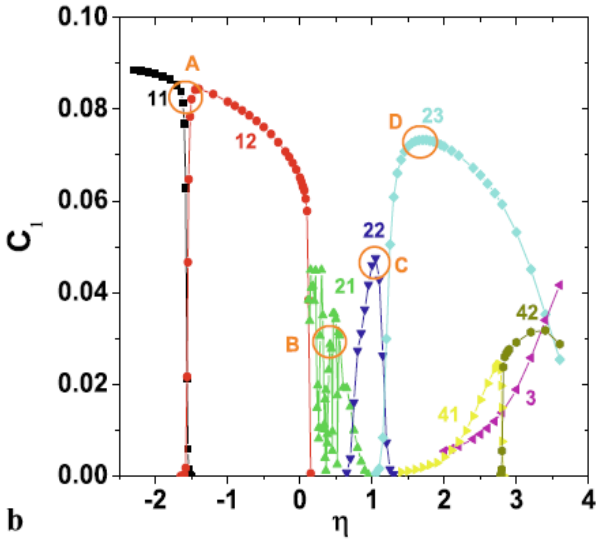

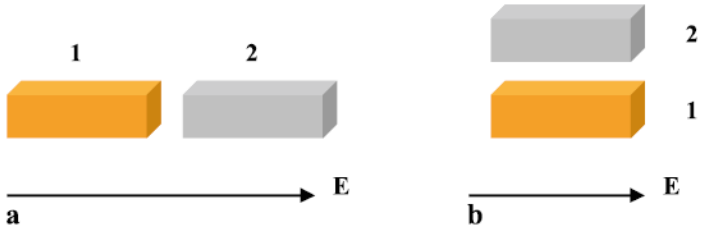

随着两块金属介电常数的变化，固定入射波长下，出现以下共振区域：

介电影响区

共振混乱区

联合共振区

共振高原区

新共振枝出现区

Y. Gu et al., Appl Phys B (2010) 98: 353–363

利用二元纳米金属结构控制表面等离激元共振

利用不同共振区性质的不同来控制共振的波长和强度。通常来说，两种金属的介电常数相当时，比较容易得到共振波长的调节；而介电常数相差比较大时，可得到巨大的近场增益。

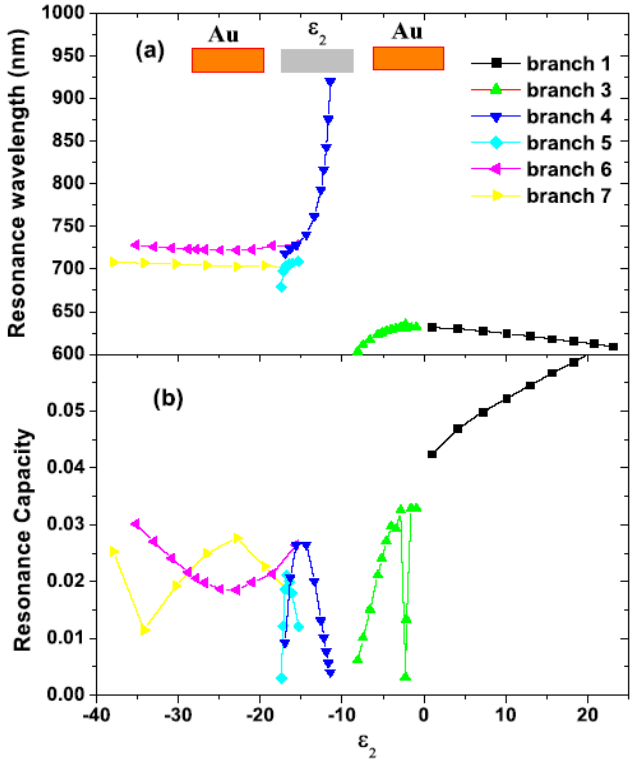

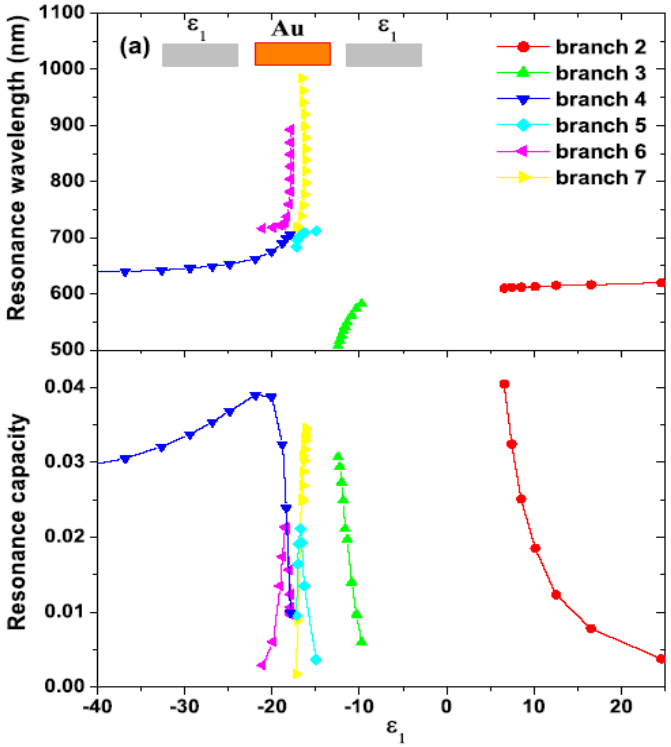

Y. Gu et al., JOURNAL OF APPLIED PHYSICS（2010）107, 114313

2.2 纳米金属颗粒阵列中表面等离激元共振的调制

几何共振（Geometric resonances）

几何共振：在周期性金属结构中，衍射级与局域表面等离激元共振互相激励，互相增强，形成一种特殊的表面等离激元共振–几何共振

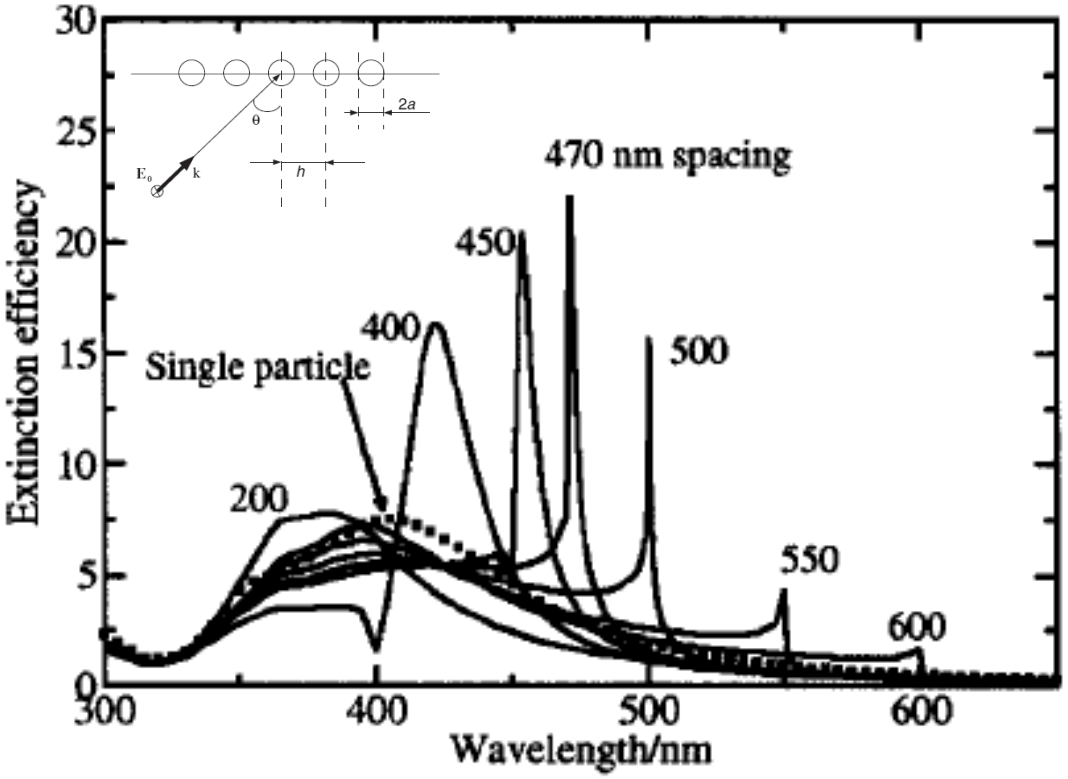

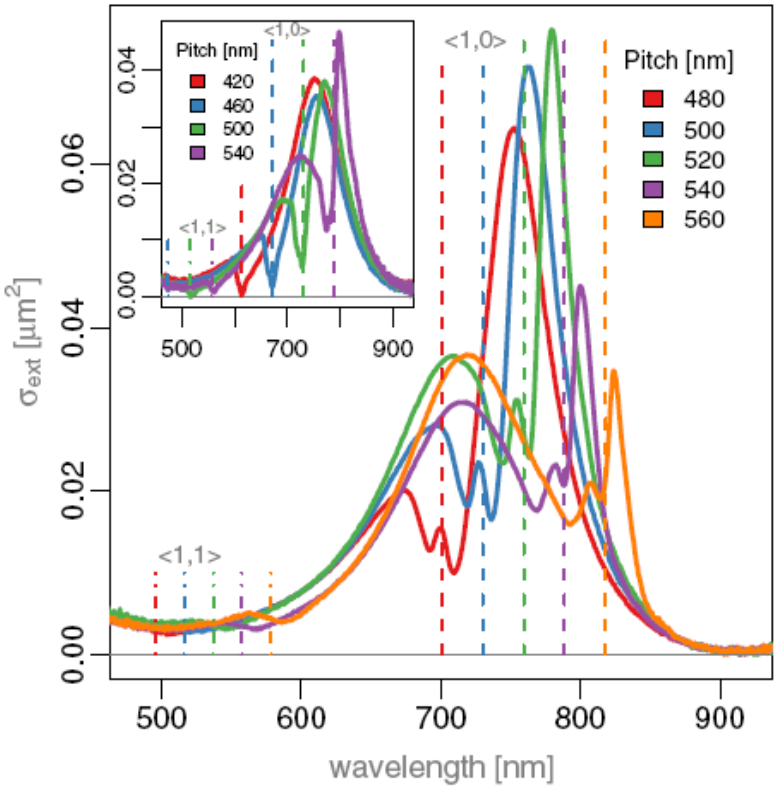

理论计算：一维银纳米小球链

实验：二维金的椭球阵列

1.Zou, Janel, and Schatz， J. Chem. Phys., 120, 10871 (2004)

2. Baptiste Auguie´* and William L. Barnes. PRL 101, 143902 (2008)

几何共振的特点

- 共振线宽很窄，一般为几个纳米。
- 强度大，相应局域场增强也大。
- 对于颗粒随机偏离周期位置，不敏感。对制作精度要求不高
- 各种几何形状颗粒的周期性阵列都能产生几何共振。

耦合偶极子近似

当颗粒尺度比入射波长小得多时，颗粒主要是偶极被激发。系统对电磁辐射的响应是由自洽的电偶极极化P_i。假设一个体系有N个颗粒，第i个颗粒的极化率α_i，那么r_i处的极化强度为

$$\mathbf{P}_i = \alpha_i \mathbf{E}_{\mathrm{loc},i}$$

这里的局域场包含入射场和其它颗粒的散射场之和

$$\mathbf{E}_{\mathrm{loc},i} = \mathbf{E}_{\mathrm{inc},i} + \mathbf{E}_{\mathrm{dipole},i} = \mathbf{E}_0 \exp(\mathrm{i}\mathbf{k}\cdot\mathbf{r}_i) - \sum_{j=1,j\neq i}^{N} \mathbf{A}_{ij}\cdot\mathbf{P}_j, \quad i = 1,2,\ldots,N,$$

上面即是一个**3N维线型方程组**，求解及得到各个颗粒的极化强度，再根据光学原理即可计算系统的消光截面等光学量

$$C_{\mathrm{ext}} = \frac{4\pi k}{|\mathbf{E}_0|^2} \sum_{j=1}^{N} \mathrm{Im}(\mathbf{E}^*_{\mathrm{inc},j}\cdot\mathbf{P}_j).$$

特别适合计算较小纳米颗粒组成的阵列。**速度快、精度高**

我们在纳米金属颗粒阵列中几何共振的调制研究中的三个工作：

- 金/银纳米颗粒阵列中几何共振的调节
- 液晶中纳米金属颗粒阵列几何共振的调节
- 基于二维纳米金属颗粒阵列多重几何共振的可调谐波分复用

二元金属纳米颗粒阵列

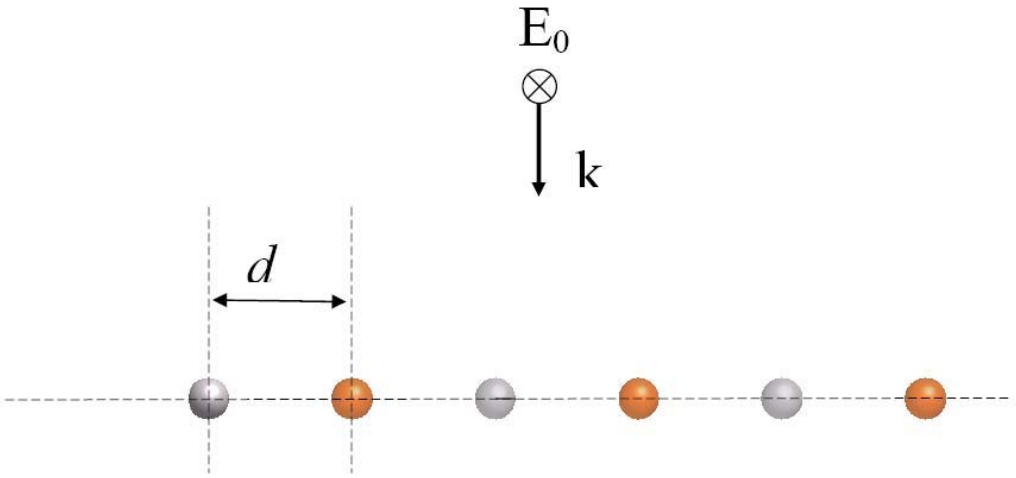

结构：由银/金纳米小球构成的二元阵列。

主要优点：

1. 在较宽的频谱范围得到窄的强的几何共振
2. 有优异的可调性

Jia Li, Ying Gu and Qihuang Gong, Opt. Express 18, 17684 (2010).

我们推广了半解析的计算方法

S_{odd}和S_{even}分别计算来自距离为颗粒间距奇数倍和偶数倍处所有颗粒的偶极耦合效果

$$S_{even} = \ldots + A_{i,i-3} + A_{i,i-1} + A_{i,i+1} + A_{i,i+3} + \ldots$$

$$S_{odd} = \ldots + A_{i,i-4} + A_{i,i-2} + A_{i,i+2} + A_{i,i+4} + \ldots$$

$$\mathbf{P}_1 = \frac{\frac{1}{\alpha_2} - (S_{even} - S_{odd})}{(\frac{1}{\alpha_2} - S_{even})(\frac{1}{\alpha_1} - S_{even}) - S_{odd}^2}\mathbf{E_0} \qquad \mathbf{P}_2 = \frac{\frac{1}{\alpha_1} - (S_{even} - S_{odd})}{(\frac{1}{\alpha_2} - S_{even})(\frac{1}{\alpha_1} - S_{even}) - S_{odd}^2}\mathbf{E_0}$$

$$C_{ext} = 2\pi kN\,\mathrm{Im}\left(\frac{(\frac{1}{\alpha_1} + \frac{1}{\alpha_2}) - 2(S_{even} - S_{odd})}{(\frac{1}{\alpha_2} - S_{even})(\frac{1}{\alpha_1} - S_{even}) - S_{odd}^2}\right)$$

高效，精确地计算阵列整体，及组成部分的消光，吸收，散射截面等物理量

Jia Li, Ying Gu and Qihuang Gong, Opt. Express 18, 17684 (2010).

二元阵列的几何共振及其特点

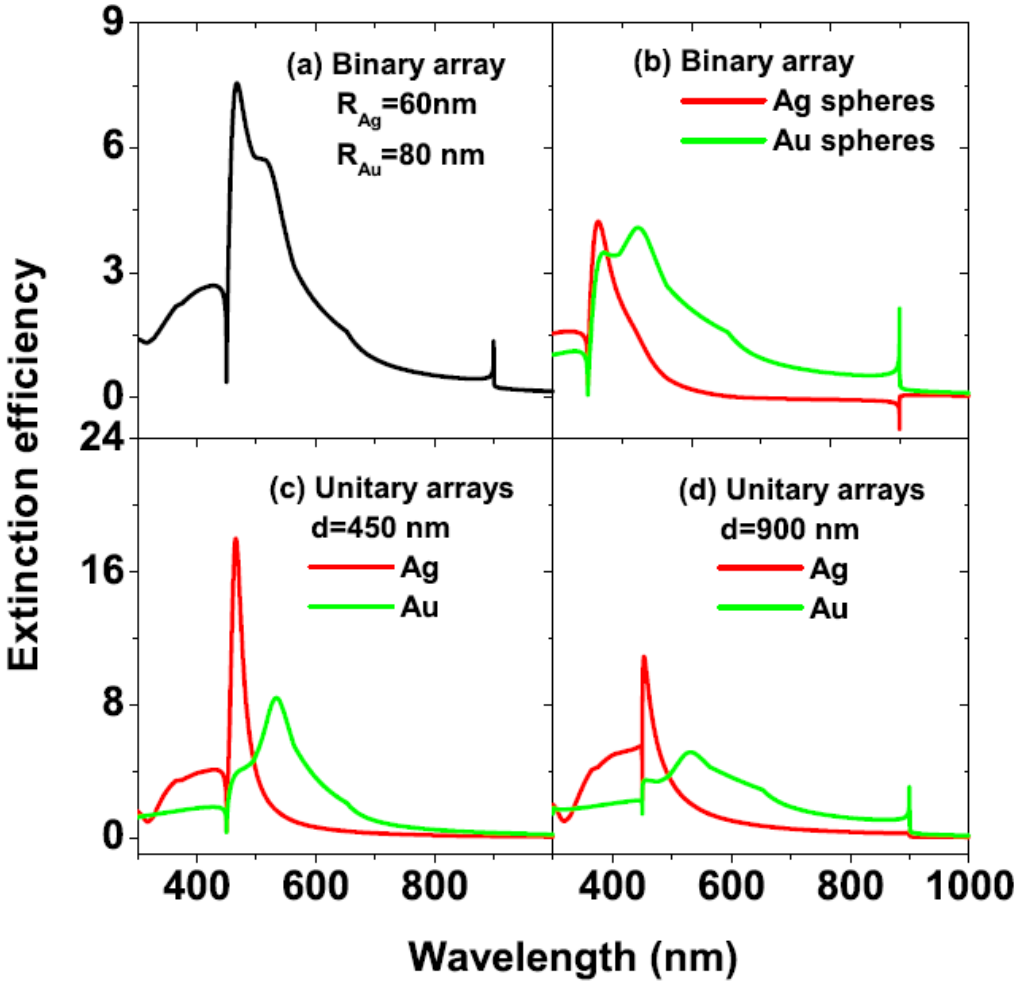

1.450 nm 处的共振，一元和二元阵列都有

2.相对于最小间距同为**450 nm**的一元阵列，二元阵列在**900 nm** 附近出现“新”的共振峰。金银小球的散射光是相位是相反的，也即金和银对共振的贡献相反。

Jia Li, Ying Gu and Qihuang Gong, Opt. Express 18, 17684 (2010).

几何共振的强度和宽度的调节

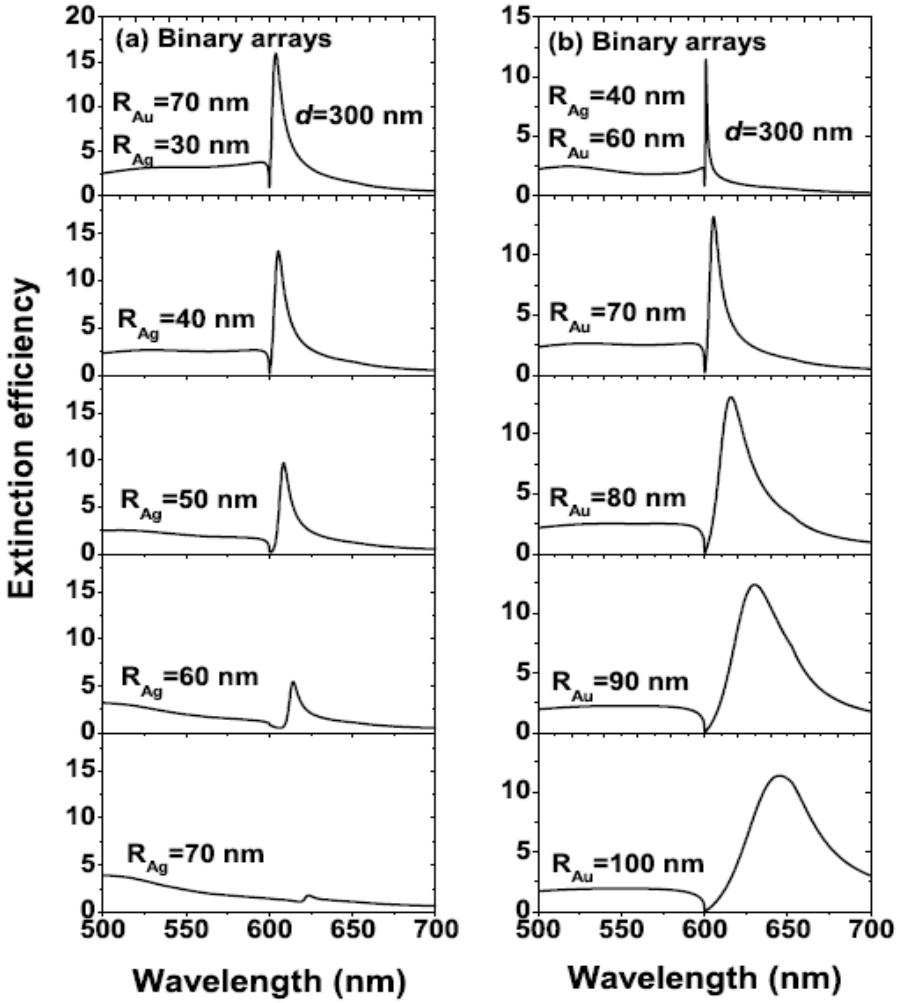

“新”几何共振的波长约为最小间距的2倍，金银小球散射光在入射方向上有一约π的相位差。

1.利用它们的干涉相消，通过调整银颗粒的尺寸，实现对共振强度的有效调节。

2.另一个方面，金颗粒的散射强度大于银颗粒，金颗粒支配共振，通过改变它的尺寸调谐共振宽度。

液晶中几何共振的调节及控制

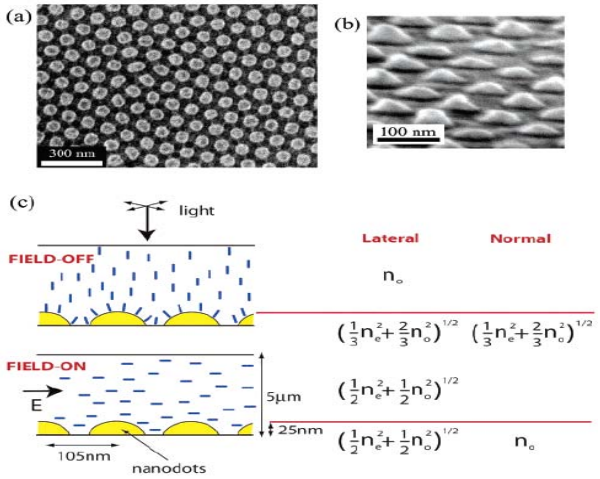

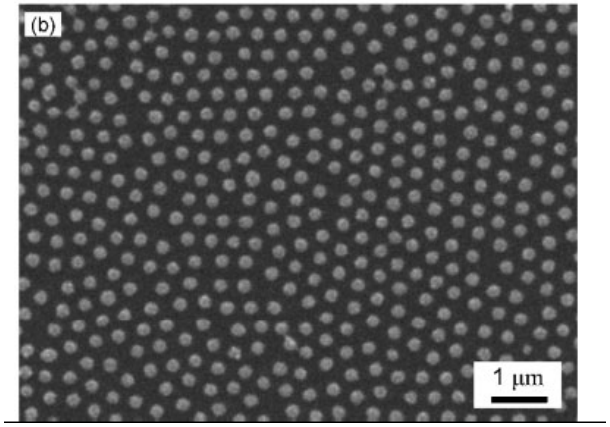

纳米盘+LC，调节范围～30 nm

纳米颗粒+LC，调节范围<10 nm

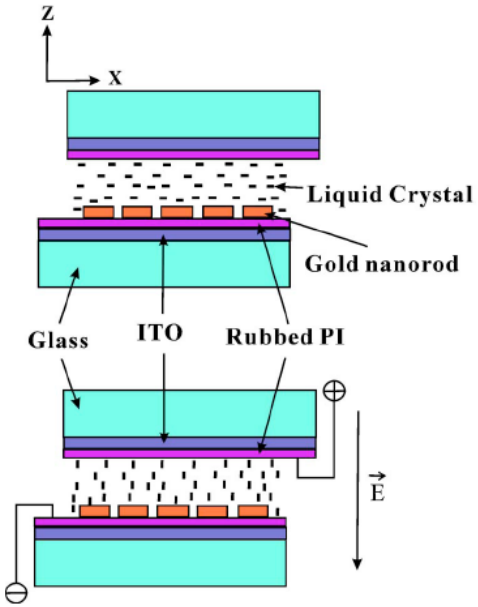

纳米棒+LC，调节范围5-25 nm

在已有的工作中，研究的都是局域表面等离激元的调节（LSPR），调节范围最多不超过40 nm。我们用阵列的几何共振，可以很容易达到100 nm。

P. A. Kossyrev et al, Nano Lett. 5, 1978 (2005).
K. C. Chu et al，Appl. Phys. Lett. 89, 103107 (2006).
V. K. S. Hsiao et al, Adv. Mater. 20, 3528 (2008).

我们的结构

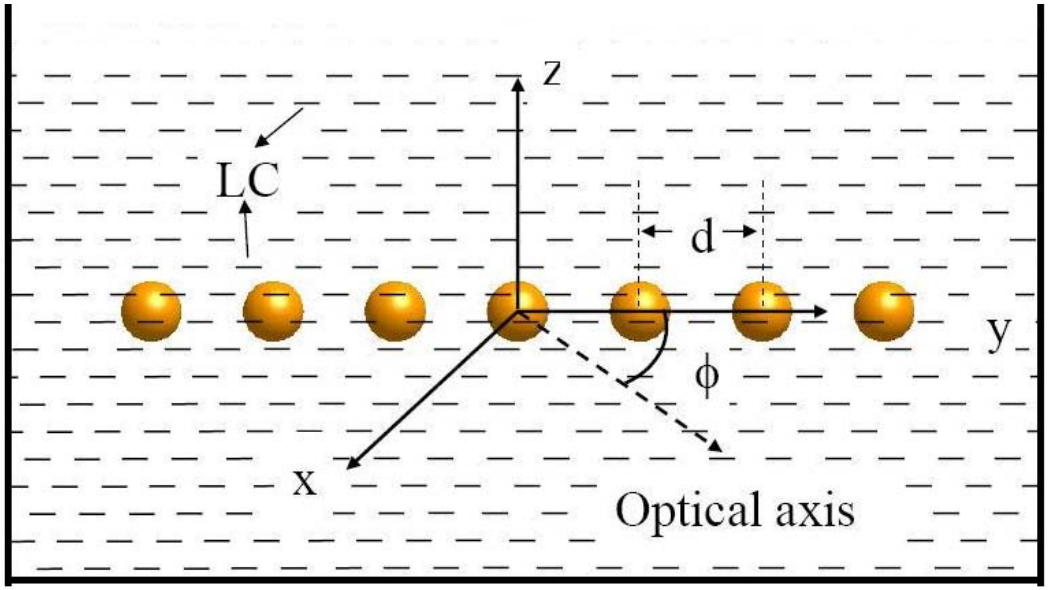

沿着轴向传播的散射光所感受的折射率：

$$n_{GR} = \frac{n_o n_e}{\sqrt{n_e^2 \cos^2\phi + n_o^2 \sin^2\phi}},$$

结构简单：浸在向列型液晶中的金纳米小球一维阵列。

调节原理：几何共振波长大致等于相邻小球之间的轴向光程差，我们通过改变液晶的光轴方向改变阵列轴向折射率，从而调节几何共振。

Jia Li, Yi Ma, Ying Gu, Iam-Choon Khoo and Qihuang Gong, Appl. Phys. Lett. 98, 213101 (2011).

调节范围与阵列周期成正比

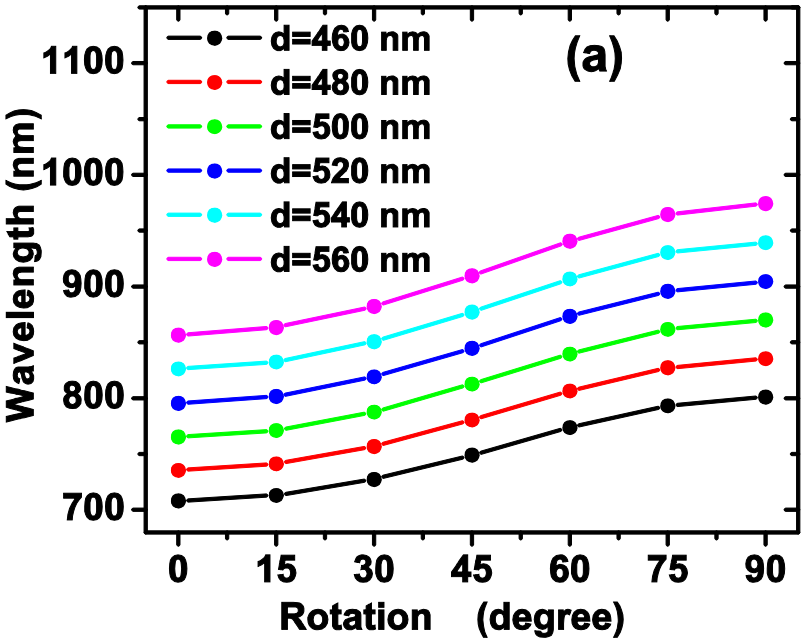

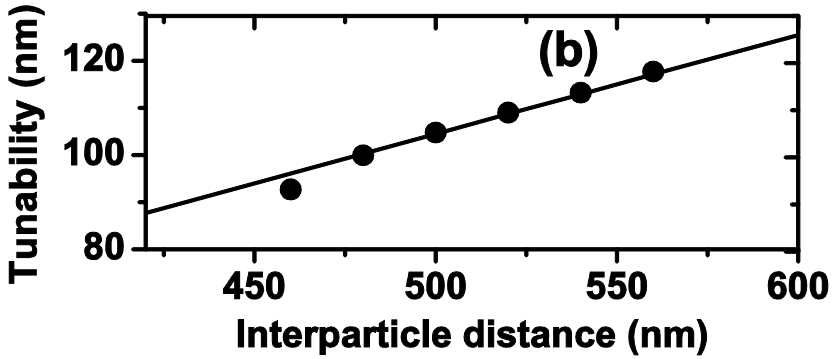

调节范围与阵列周期成正比：

$$\Delta\lambda = \Delta n \cdot d,$$

阵列的周期为**460-560 nm**范围内时，调节范围为**92.7-111.7 nm**。

另外：我们还可以选用双折射较大的液晶实现更大的调节范围。

Jia Li, Yi Ma, Ying Gu, Iam-Choon Khoo and Qihuang Gong, Appl. Phys. Lett. 98, 213101 (2011).

基于二维金属纳米颗粒阵列多重几何共振的可调谐波分复用结构

几种常见波分复用结构

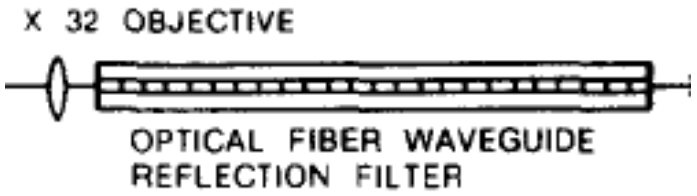

波导光栅，长约**1m**

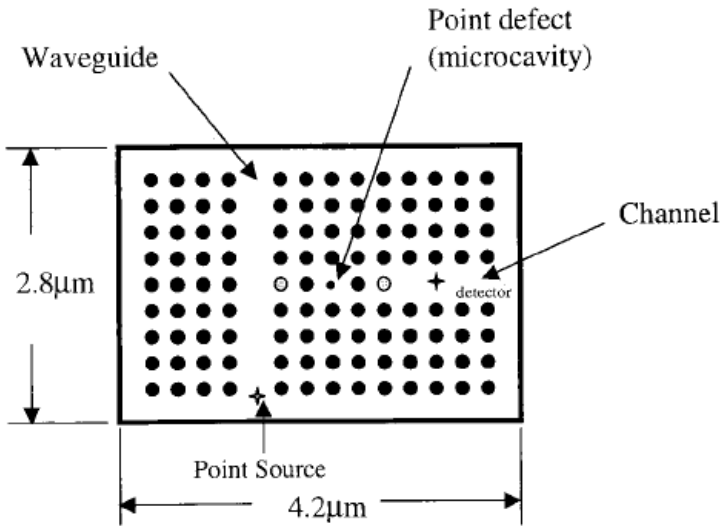

基于光子晶体的波分复用结构，微米量级

阵列波导光栅、光纤布拉格光栅：**cm**甚至**m**的量级
基于光子晶体的波分复用结构：几十个微米。
一般波分复用结构比较复杂，尺度大，对制备技术要求很高。

1. C. Dragone, Lightwave Technol. 1989,7:479–489
2. S. Shi A. Sharkawy, D. W. Prather, Appl Opt. 2001, 40:2247–2252

我们提出的可调谐波分复用结构

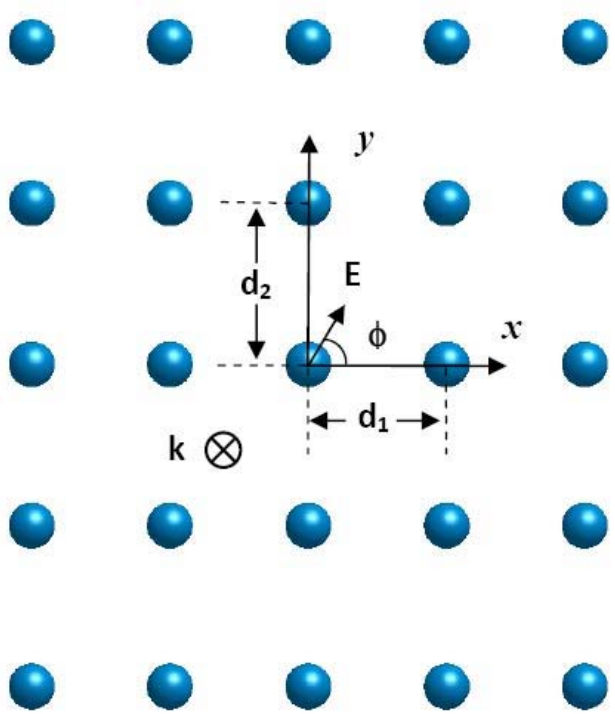

结构：二维银纳米小球构成的阵列。R=80 ～200 nm。

1.结构简单、易于制备。
2.尺度很小，且易于与其它结构集成。
3.具有优良的可调性。

Jia Li, Xiaoyong Hu, Ying Gu and Qihuang Gong, Opt. Lett. 35, 4051 (2010).

阵列的多重几何共振

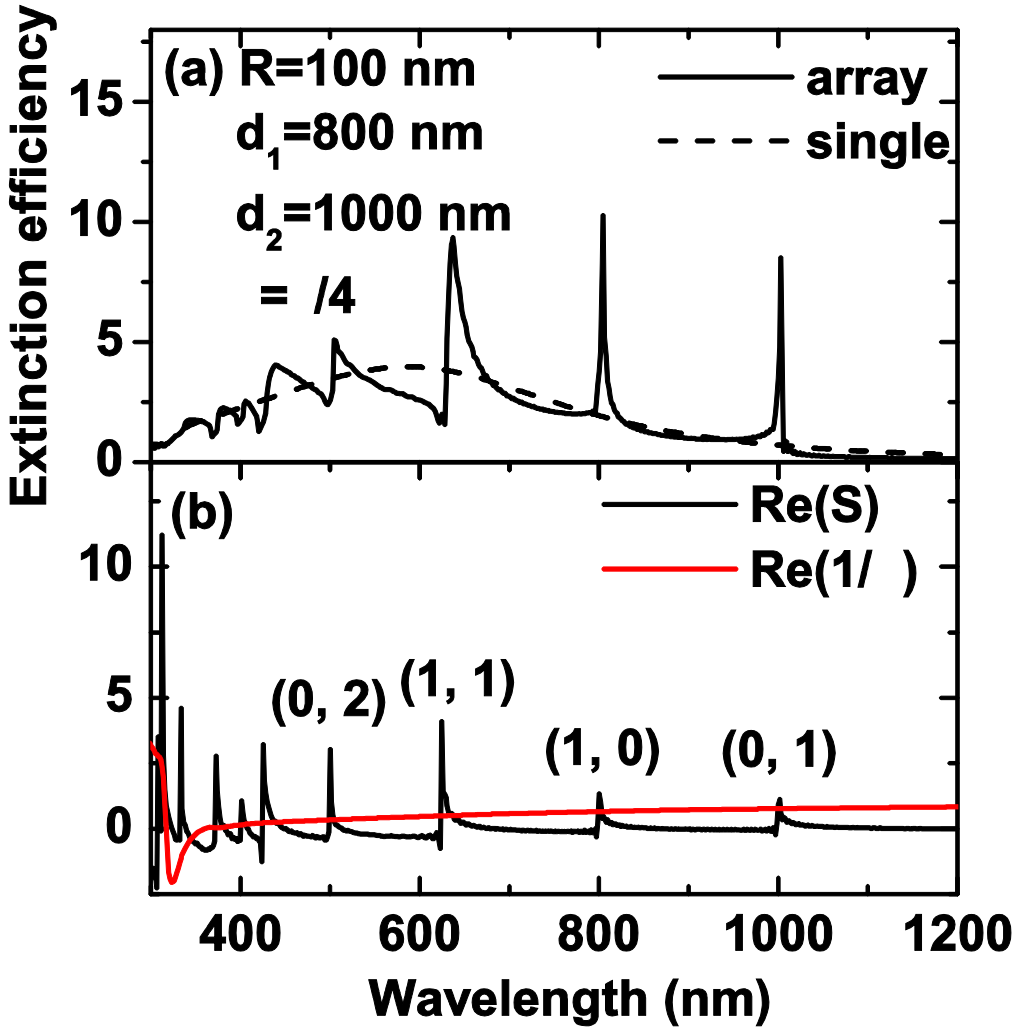

各个衍射极，如果落在SPR的光谱范围之内，均能激发出较强的几何共振。

多重几何共振特点：

强度较大：大于SPR

线宽很窄：一般为几个纳米

Jia Li, Xiaoyong Hu, Ying Gu and Qihuang Gong, Opt. Lett. 35, 4051 (2010).

信道的激活及压制、信道所在波段的可调性

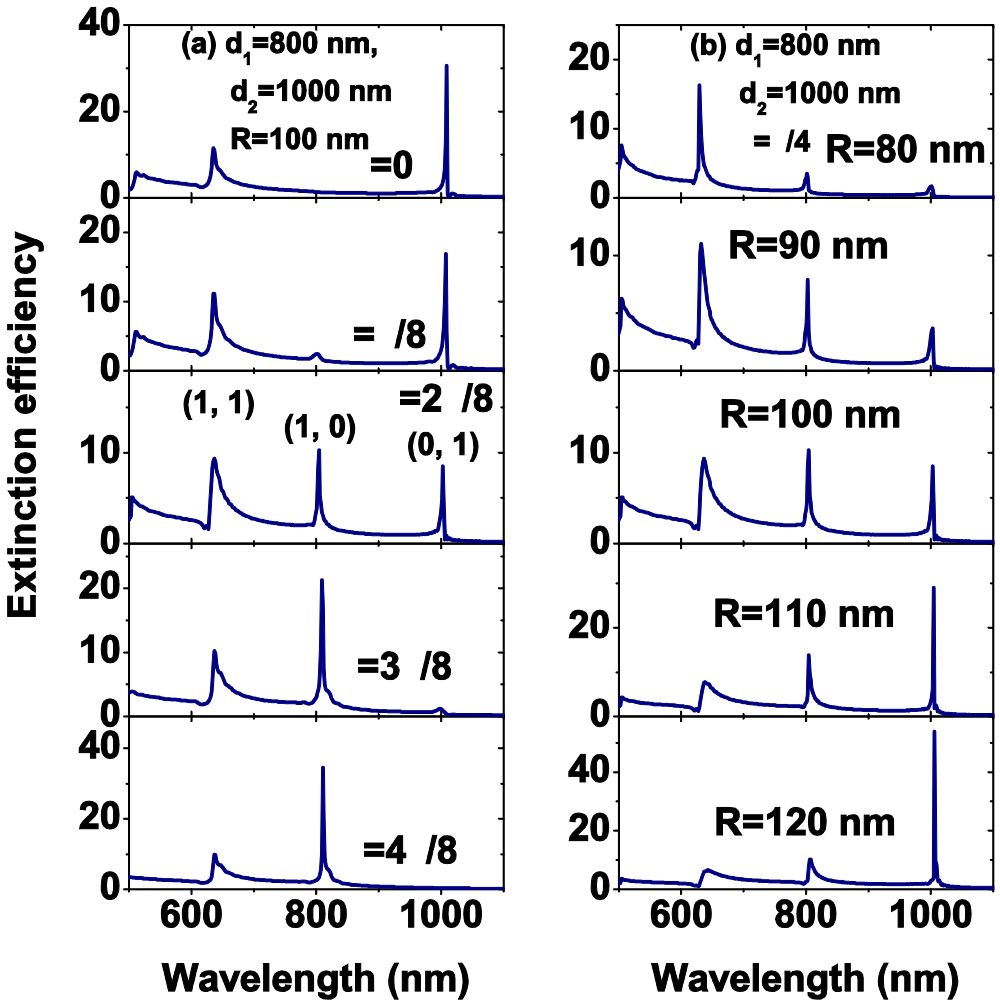

由于偶极耦合的特点，垂直于入射光偏振的方向上才能有效耦合。所以通过改变入射光偏振，激活某个信道或完全压制某个信道。

在SPR的频谱范围内，几何共振才能有比较大的强度，通过改变颗粒的尺寸，调节较强共振的位置。

Jia Li, Xiaoyong Hu, Ying Gu and Qihuang Gong, Opt. Lett. 35, 4051 (2010).

2.3 基于表面等离激元的杂化波导结构

Various surface plasmon polariton (SPP) waveguides

Planar waveguide, Groove waveguide, Cylindrical SPP waveguide, nanoparticle chain, Bend metallic waveguide, hybrid(or dielectric-loaded) waveguide

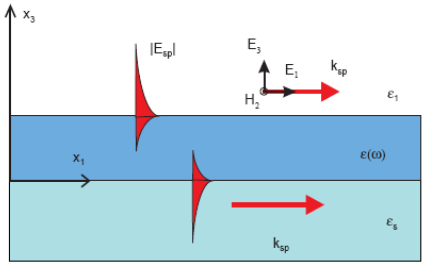

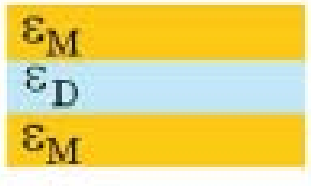

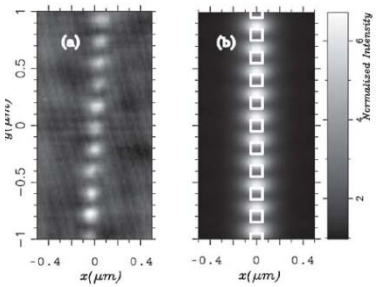

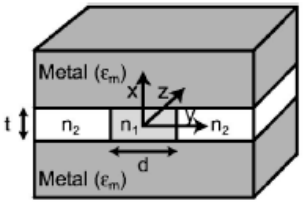

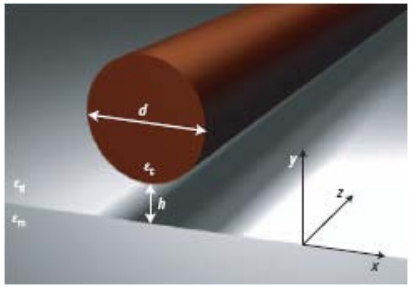

Advantage:

Light confinement in a subwavelength scale

Disadvantage:

Short propagation length due to the loss

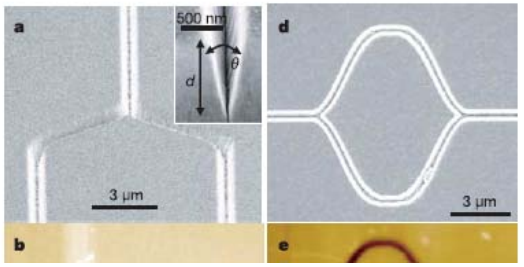

Fuminori Kusunokia et al, APPLIED PHYSICS LETTERS 86, 211101 (2005); Oulton, et al, Nature Photon. 2 (2008) 496; T.W. Ebbesen et al, NATURE|Vol 440|508| 2006; E. Feigenbaum, M. Orenstein, J. Lightwave Tech. 25 (2007) 2547; A.V. Zayats et al, Physics Reports 408 (2005) 131–314.

Hybrid SPP waveguide

Sub-wavelength confinement and long-range propagation

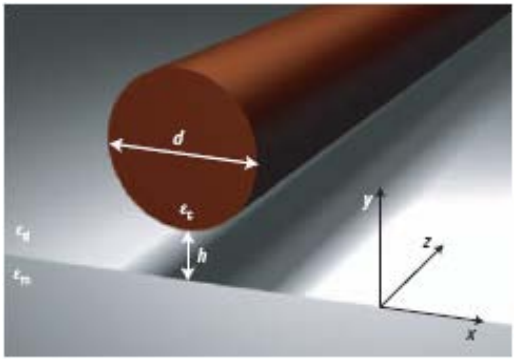

dielectric cylindrical nanowire
ε_c =12.25, d, λ=1550nm
dielectric gap n_c=2.25, h
metallic half-space Ag

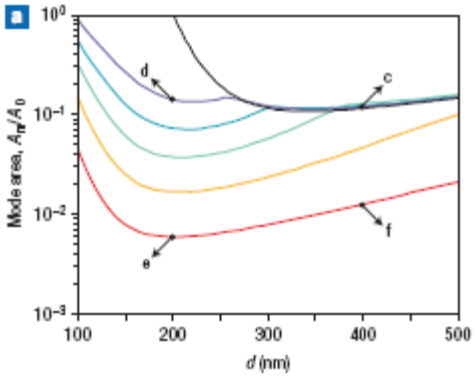

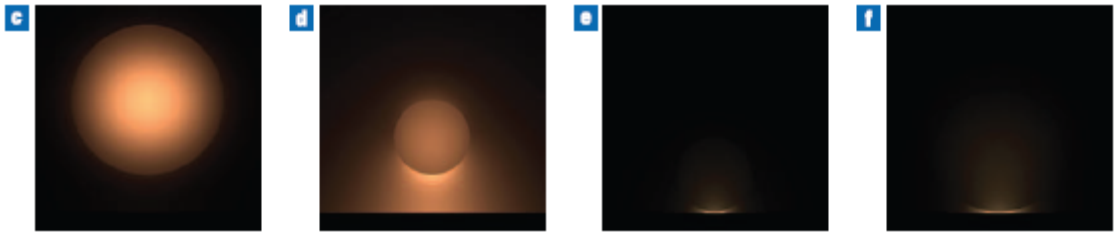

Results:
tightly confined field in the vicinity of the gap,low-loss light transport

Explanation:
Hybridization of the fundamental mode of a dielectric cylinder with the SPP of a dielectric-metal interface.

A hybrid plasmonic waveguide for subwavelength confinement and long-range propagation,
R. F. Oulton, et al, Nature Photon. 2 (2008) 496

Maxwell equations in cylindrical coordinates:

$$
\begin{aligned}
E_r &= \left(\frac{ik_z}{\gamma_j} f_n^{j\,\prime}(\gamma_j r) - \frac{\mu_j \omega n}{\gamma_j^2 r c} g_n^j(\gamma_j r) \right) \cdot S_n, \\
E_\phi &= \left(-\frac{n k_z}{\gamma_j^2 r} f_n^j(\gamma_j r) - \frac{i \mu_j \omega}{\gamma_j c} g_n^{j\,\prime}(\gamma_j r) \right) \cdot S_n, \\
E_z &= f_n^j(\gamma_j r) \cdot S_n, \\
H_r &= \left(\frac{n \epsilon_j \omega}{\gamma_j^2 r c} f_n^j(\gamma_j r) + \frac{ik_z}{\gamma_j} g_n^{j\,\prime}(\gamma_j r) \right) \cdot S_n, \\
H_\phi &= \left(\frac{i \epsilon_j \omega}{\gamma_j c} f_n^{j\,\prime}(\gamma_j r) - \frac{n k_z}{\gamma_j^2 r} g_n^j(\gamma_j r) \right) \cdot S_n,
\end{aligned}
$$

and

$$
H_z = g_n^j(\gamma_j r) \cdot S_n,
$$

柱形金属-介质波导中低损耗亚波长局域的杂化表面等离激元模式

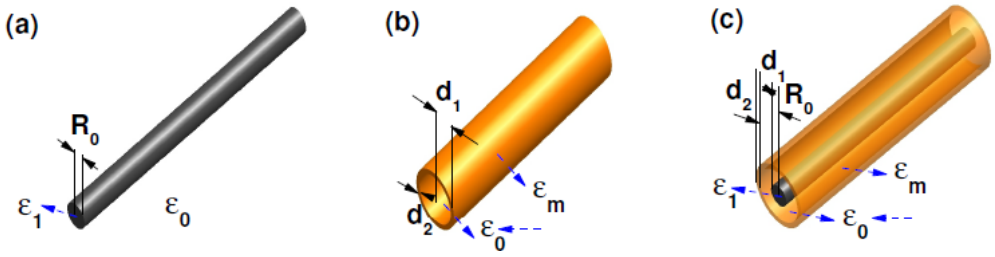

优质杂化表面等离激元模式（传播长度十几微米，金属管内能流分布高于90%）和劣质杂化表面等离激元模式（传播长度几微米，金属管内能流分布低于40%）在相位匹配条件下发生模式转换，传播性质调换。利用锥形介质芯，先激发劣质模式，可以通过模式转换提高优质模式的激发效率。

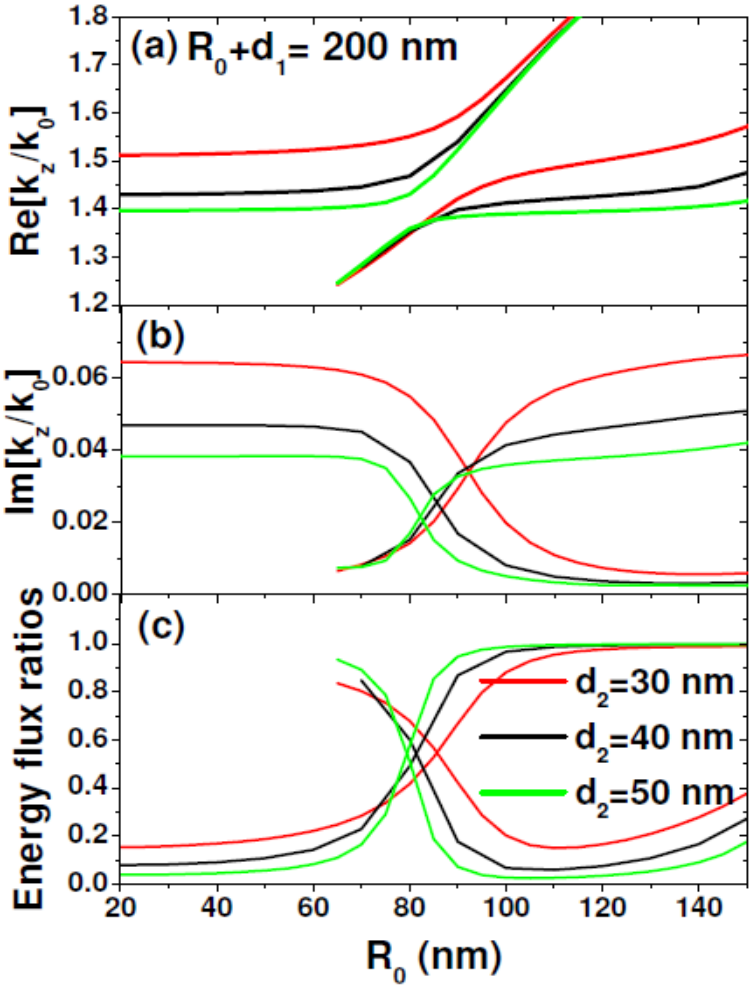

EPL（2011）in press.

柱形金属-介质波导中传播长度和光场限制的相互制约

被SiO_2包裹的金纳米线嵌套在BN纳米管中，构成杂化表面等离激元波导。

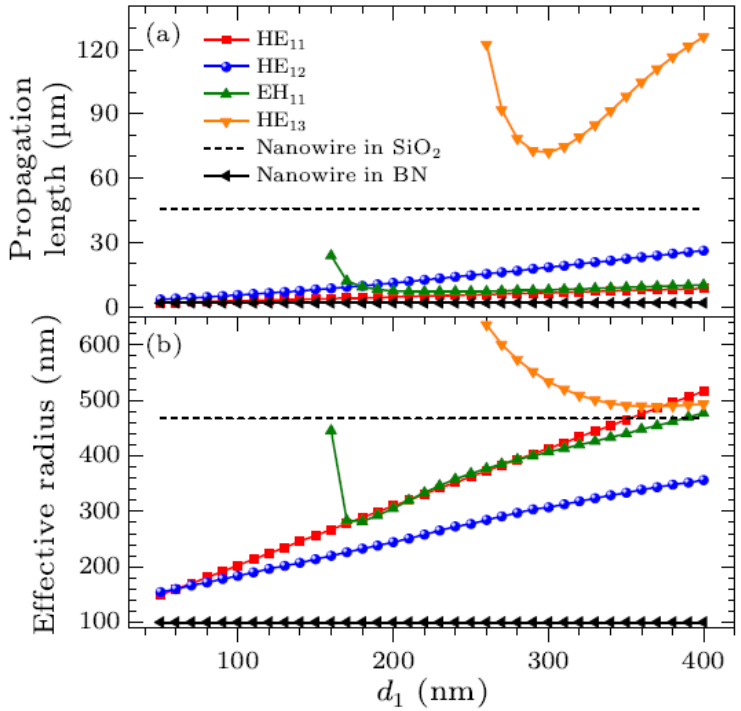

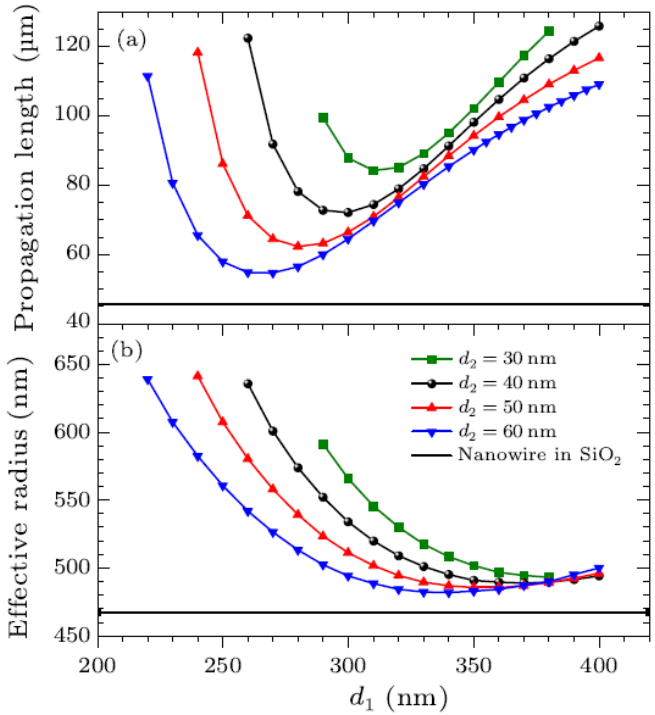

传播性质最好的HE_{13}杂化模式有较多的能量分布在SiO_2层中，具有亚波长的有效半径，传播长度120－200λ，超过金纳米线的两倍。改变介质层厚度以及介电常数，显示出传播长度和有效半径之间的相互制约，可调控杂化模式的传播性质。

CHIN. PHYS. LETT. (2011) 28, 057303

强电场局域在纳米狭缝中的长程表面等离激元模式

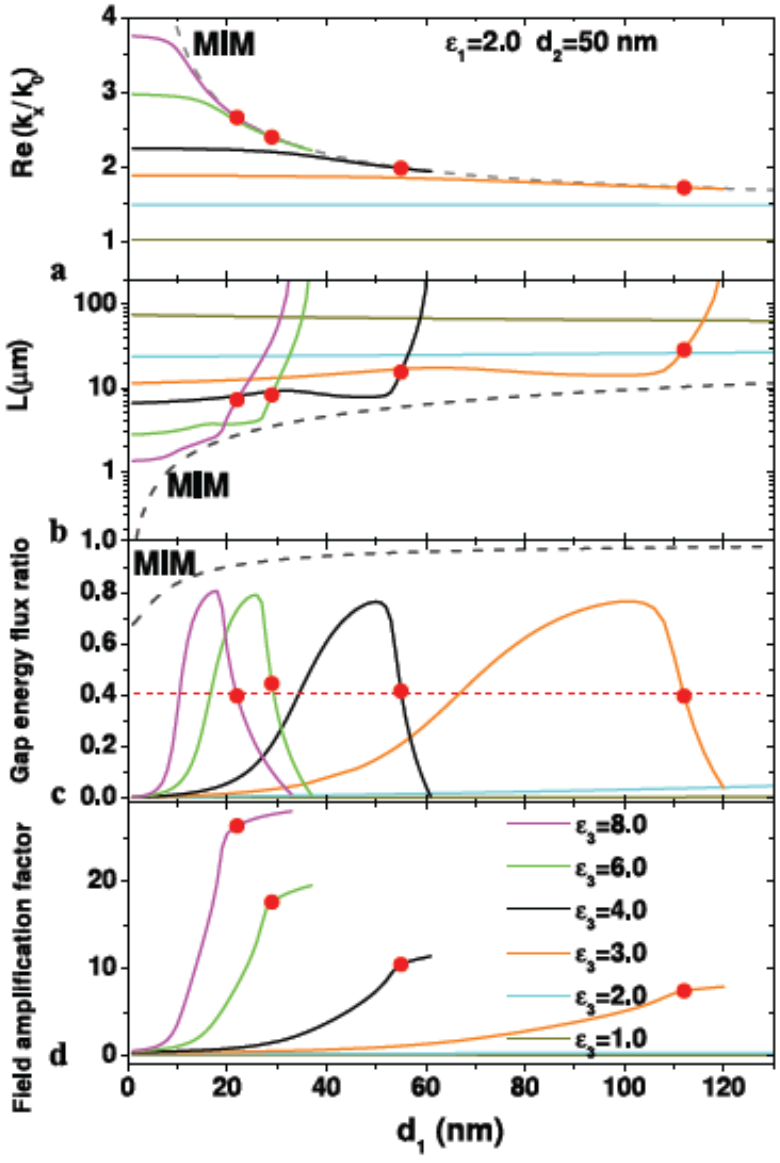

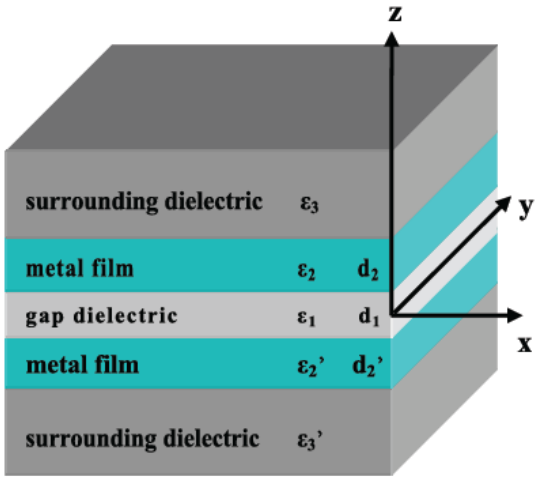

五层对称平板波导由高介电常数介质包覆含有低介电常数狭缝的MIM波导构成。其长程反对称模式在截止狭缝厚度附近传播长度很大，光场限制降低，但在狭缝中有很强的局域电场。增加内外介质的介电常数差或金属层厚度，可以增大隙缝中的电场强度，有益于光场与物质相互作用。

Appl Phys B (2011) 104:919–924

TM 表面模式电磁场形式

$$H_y(x,z,t)=\begin{cases} H_{y3}\exp i(k_x x+k_{z3}z-\omega t), & z\geq d_1/2+d_2 \\ H_{y2}^{+}\exp i(k_x x+k_{z2}z-\omega t)+H_{y2}^{-}\exp i(k_x x-k_{z2}z-\omega t), & d_1/2\leq z<d_1/2+d_2 \\ H_{y1}^{+}\exp i(k_x x+k_{z1}z-\omega t)+H_{y1}^{-}\exp i(k_x x-k_{z1}z-\omega t), & -d_1/2\leq z<d_1/2 \\ H_{y2}^{+'}\exp i(k_x x+k'_{z2}z-\omega t)+H_{y2}^{-'}\exp i(k_x x-k'_{z2}z-\omega t), & d'_1/2+d'_2\leq z<d'_1/2 \\ H'_{y3}\exp i(k_x x-k'_{z3}z-\omega t), & z<d'_1/2+d'_2 \end{cases}$$

由连续性边条件解得色散关系式

$$\begin{aligned} \exp(i2k_{z1}d_1)=&[\exp(ik_{z2}d_2)(\frac{k_{z3}}{\varepsilon_3}-\frac{k_{z2}}{\varepsilon_2})(\frac{k_{z2}}{\varepsilon_2}-\frac{k_{z1}}{\varepsilon_1})+\exp(-ik_{z2}d_2)(\frac{k_{z3}}{\varepsilon_3}+\frac{k_{z2}}{\varepsilon_2})(\frac{k_{z2}}{\varepsilon_2}+\frac{k_{z1}}{\varepsilon_1})] \\ &\times[\exp(ik'_{z2}d'_2)(\frac{k'_{z3}}{\varepsilon'_3}-\frac{k'_{z2}}{\varepsilon'_2})(\frac{k'_{z2}}{\varepsilon'_2}-\frac{k_{z1}}{\varepsilon_1})+\exp(-ik'_{z2}d'_2)(\frac{k'_{z3}}{\varepsilon'_3}+\frac{k'_{z2}}{\varepsilon'_2})(\frac{k'_{z2}}{\varepsilon'_2}+\frac{k_{z1}}{\varepsilon_1})] \\ &\times[\exp(ik_{z2}d_2)(\frac{k_{z3}}{\varepsilon_3}-\frac{k_{z2}}{\varepsilon_2})(\frac{k_{z2}}{\varepsilon_2}+\frac{k_{z1}}{\varepsilon_1})+\exp(-ik_{z2}d_2)(\frac{k_{z3}}{\varepsilon_3}+\frac{k_{z2}}{\varepsilon_2})(\frac{k_{z2}}{\varepsilon_2}-\frac{k_{z1}}{\varepsilon_1})]^{-1} \\ &\times[\exp(ik'_{z2}d'_2)(\frac{k'_{z3}}{\varepsilon'_3}-\frac{k'_{z2}}{\varepsilon'_2})(\frac{k'_{z2}}{\varepsilon'_2}+\frac{k_{z1}}{\varepsilon_1})+\exp(-ik'_{z2}d'_2)(\frac{k'_{z3}}{\varepsilon'_3}+\frac{k'_{z2}}{\varepsilon'_2})(\frac{k'_{z2}}{\varepsilon'_2}-\frac{k_{z1}}{\varepsilon_1})]^{-1} \end{aligned}$$

三、介观量子交叉领域的发展现状及前景

结合了光子学和电子学的优点，通过将光场压缩在纳米尺度，允许在纳米尺度上研究光与物质相互作用。

表面等离激元本质上是电磁波，具有波粒二象性。

在未来的计算机中光子能够代替电子吗？光子回路体积小，易于集成，损耗小，传的快，但是光子间没有相互作用，实现量子操控比较困难。光子与表面等离激元间的交换弥补了这一不足，可在单光子探测，纠缠，可控相位门，量子的非线性效应方面有应用。

表面等离激元如何介入和量子体系的相互作用?

Weak coupling:

1）在表面等离激元结构的近场区域内为偶极跃迁提供了较强的各向异性真空环境

2）激发的表面等离激元是局域的电磁波，可以发生在纳米尺度上定域的与原子系综的相互作用

Strong coupling:

3）量子的表面等离激元与单量子体系的相互作用

Surface plasmon polariton (SPP)

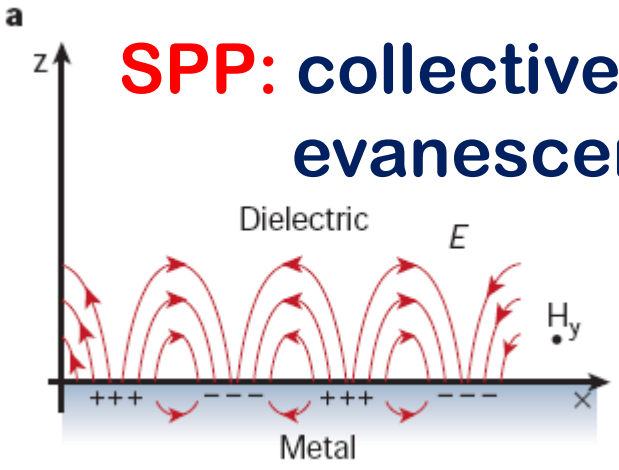

SPP: collective oscillations of free electrons
evanescent EM mode bound to surface

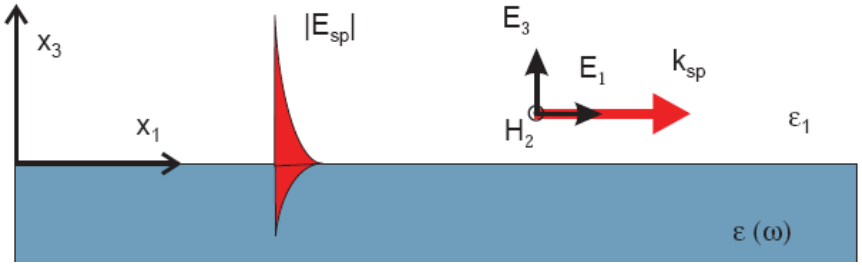

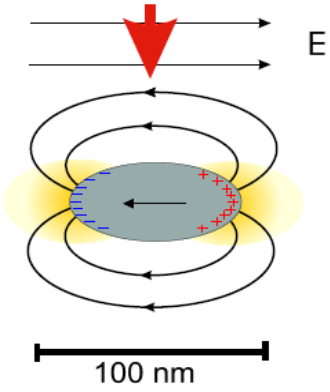

Figure 1.3: Particle plasmon

Localized SP or SPR:
localized oscillation
strong local field

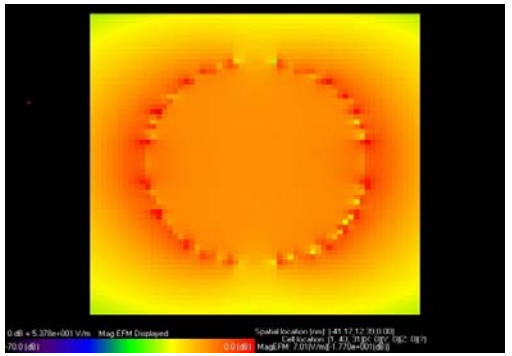

ultrasmall optical mode volume Vm

William L. Barnes, Alain Dereux & Thomas W. Ebbesen, nature, 424, 824 (2003);
V. Zayatsa, et al, Phys Rep. 2005, 408:131–314;

What's new for quantum emitters
with ultrasmall optical mode Vm?

Weak coupling: Purcell factor $F=\gamma/\gamma_0$

anisotropic electric mode density of oscillations

→ anisotropic optical mode density →

anisotropic decay rates → enhanced (F>1)or supressed (F<1) spontaneous emission at subwavelength scale

Strong coupling: Cavity QED

V_m is extremely small → g ($\propto \frac{1}{\sqrt{V_m}}$) is very large

Q is not high due to loss

→ Low-light level nonlinear optics

R. R. Chance, A. Prock, and R. Silbey, J. Chem. Phys.62, 2245 (1975); D. E. Chang et al., Phys. Rev. Lett. 97, 053002 (2006); Edo Waks and Deepak Sridharan, Phys. Rev. A, 82, 043845 (2010)

Main research work in this field:

1. Decay rate modification at subwavelength scale
2. Near field excitation of quantum emitters
3. Strong coupling between plasmonic nanostructures and quantum emitters

Decay rate modification of quantum emitter

$$\Gamma = \frac{2}{\hbar}\,\mathrm{Im}\{\mu_i G_{ij}(0,\omega_A)\mu_j\}$$

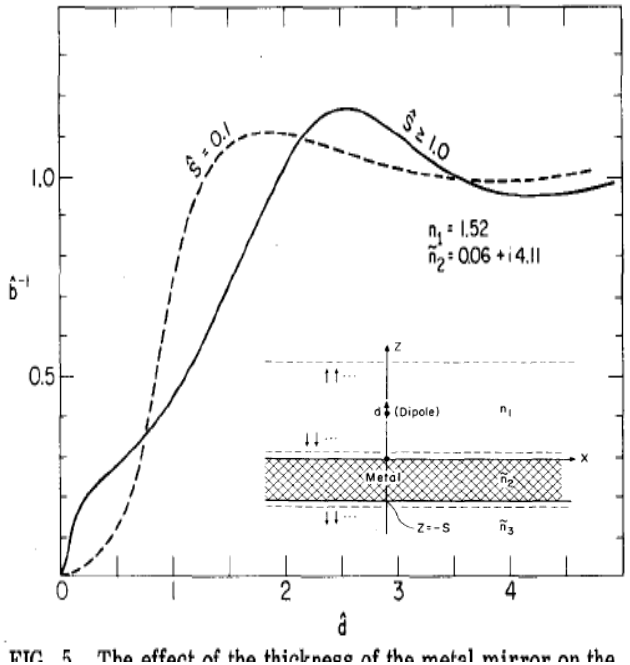

FIG. 5. The effect of the thickness of the metal mirror on the

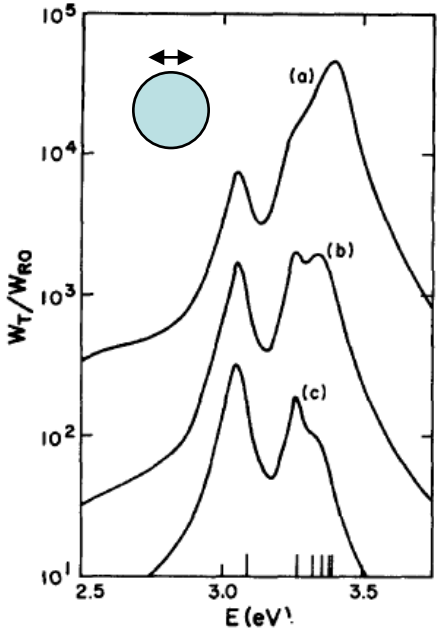

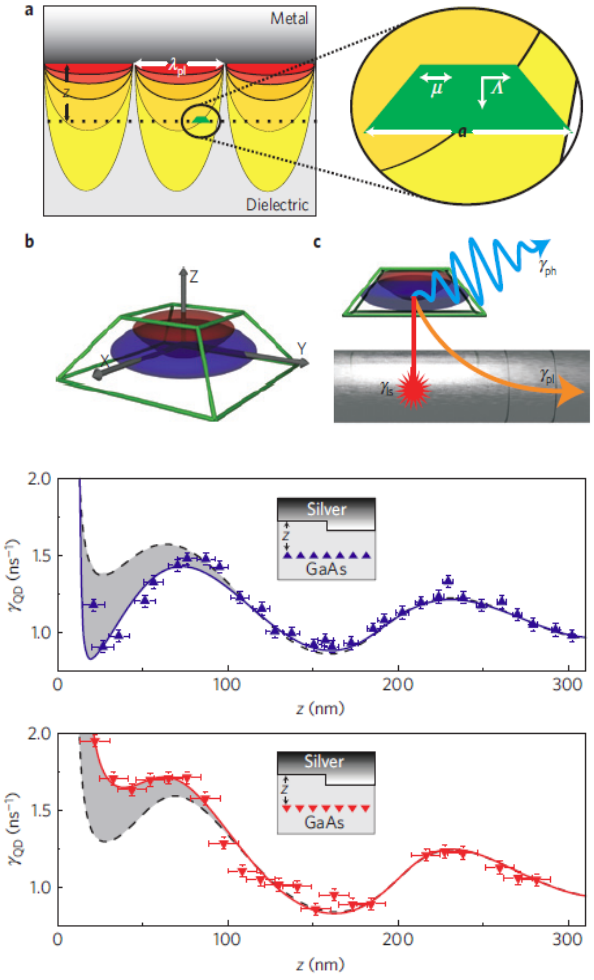

Features of plasmon structures:

1. large Purcell factor 2. anisotropic decay rates

R.R.Chance et al, the journal of cheimical physics, 62,2245 (1975);R. Ruppin, J. Chem.Phys. 76,1681 (1982); Mads Lykke Andersen, et al. nature physics, DOI: 10.1038/NPHYS1870, 2010

Molecular fluorescence near plasmonic strucrures

------Near field excitation of quantum emitters

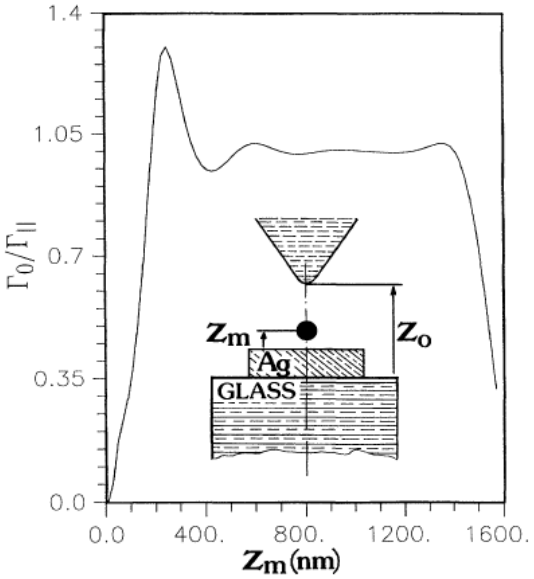

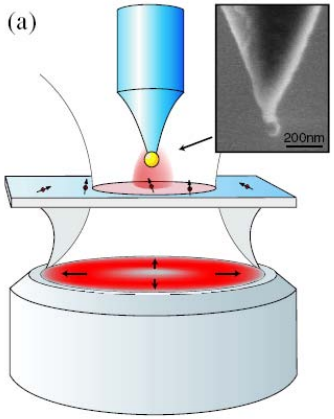

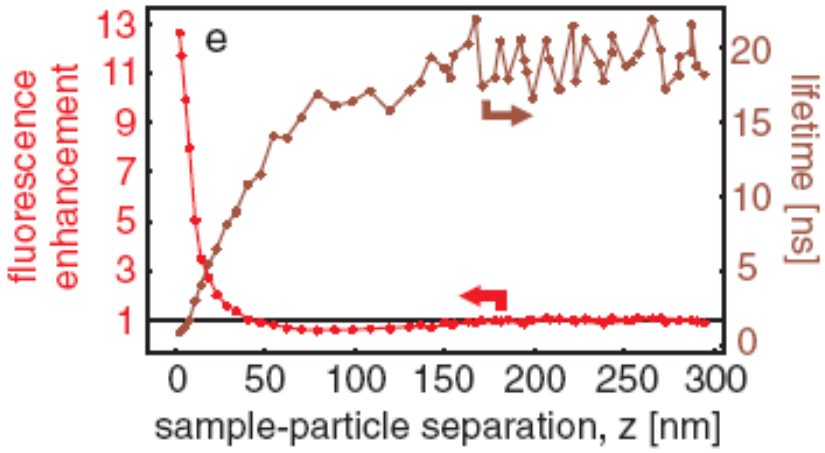

Characteristic:

Reduced life time

Fluorescence: from quenching, via enhancement, to suppressing

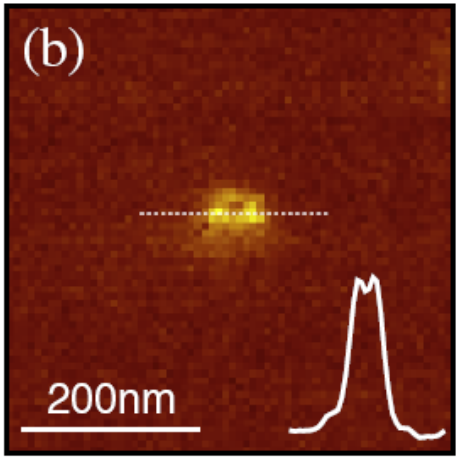

C. Girard et al, PRL, 75,3098(1995); Sergei Kuhn et al, PRL 97, 017402 (2006) ; Pascal Anger et al, PRL 96, 113002 (2006)

Strong coupling between quantum surface plasmons and quantum emitters

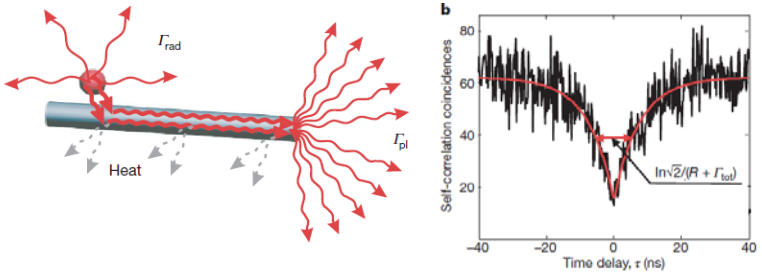

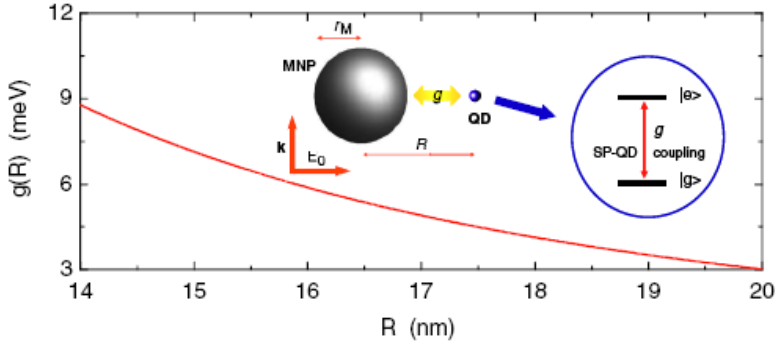

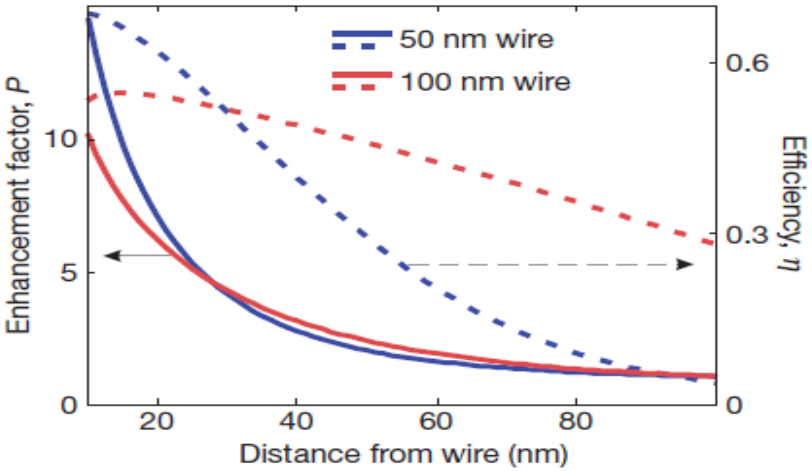

Quantum Plasmonics with Quantum Dot-Metal Nanoparticle ⟺ Cavity QED treatment

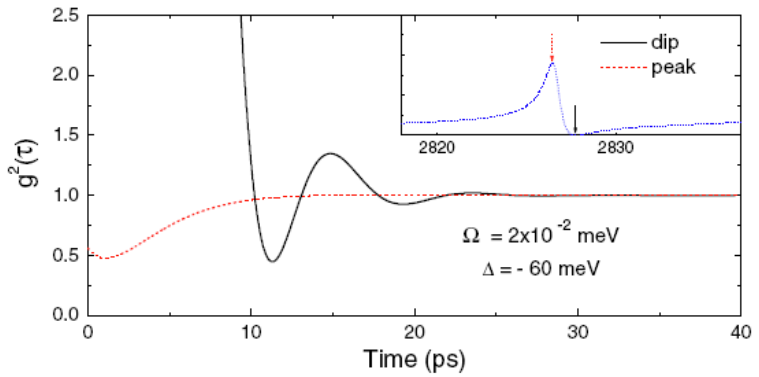

Generation of single surface plasmon source

A. V. Akimov et al, NATURE|Vol 450|402| 2007; A. Ridolfo, PRL 105, 263601 (2010)

hybrid photonic architectures

The assembly of hybrid nanophotonic devices from different fundamental photonic entities—such as single molecules, nanocrystals, semiconductor quantum dots, nanowires and metal nanoparticles—can yield functionalities that exceed those of the individual subunits.

BOX 1

Cavity QED

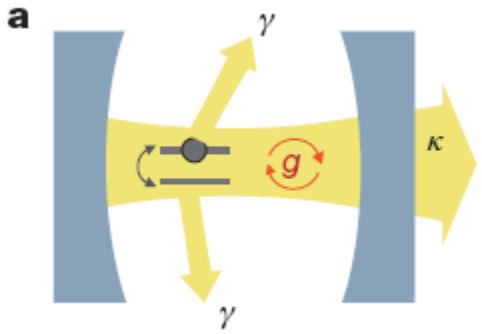

BOX 2

Plasmonic enhancement

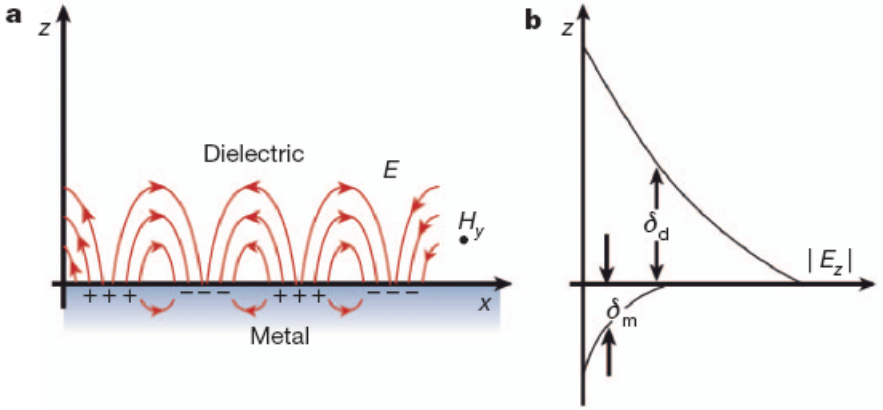

Oliver Benson, nature, 480, 193 (2011)

Functionality on the nanoscale

Light guiding and sorting

Enhanced emission and absorption

Nonlinear elements and switches

Nanophotonic–plasmonic hybrid devices

Plasmonically enhanced single-photon sources

Nanowire photonic elements

Future prospects

plasmons. Also, nonlinear interactions facilitating logical operations are feasible using CQED or plasmonic effects. There is great potential

Oliver Benson, nature, 480, 193 (2011)

Plasmonics Goes Quantum

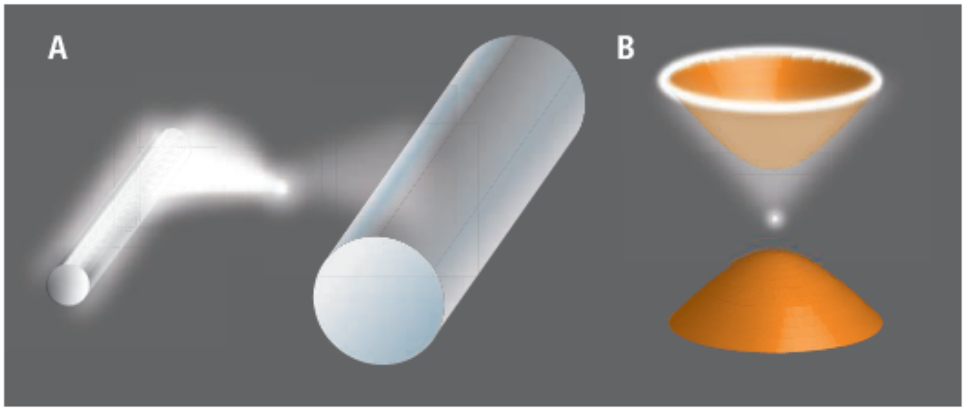

Make it quantum. Building blocks of an integrated nanoscale quantum information system. (**A**) The nanowire supports a single plasmonic oscillation conceptually similar to a single-mode optical fiber. However, the nanoscale mode volumes of the plasmon lead to strong coupling with the quantum emitter. (**B**) An unorthodox approach of enhancing light-matter interaction is by tailoring the dielectric constant of a medium so that it is dielectric in one direction and metallic in another. The resulting hyperboloidal dispersion relation supports infinitely many electromagnetic states for channeling light into a single-photon resonance cone.

A combined plasmonics and metamaterials approach may allow light-matter interaction to be controlled at the single-photon level.

single plasmon →

antibunching statistics

nanoscale-mode volume →

strong coupling

entangling+squeezing →

quantum information

quantum plasmonics →

Spaser

Cavity QED

QI system

Zubin Jacob and Vladimir M. Shalaev, science, 334, 463 (2011)

四、交叉领域相关的几个工作

4.1 基于表面等离激元结构的单分子共振荧光

4.2 原子布居数的本征量子拍频及其在表面等离激元结构中的纳米尺度上的实现

4.3 表面等离激元诱导下的各向异性真空导致的亚波长尺度上的自发辐射谱线的变化

Our work: to pursue intercrossing between quantum optics and plasmonics in weak coupling

1. **Resoanance fluorescence in two-level system:**
   with one transition channel
   anisotropic decay rates and near field excitation

2. **Quantum interferences in four-level system:**
   with two or more transition channel
   anisotropic decay rates and near field excitation
   Crossing damping under anisotropic vacuum

With above considerations, what would happen ?

4.1 Resonance fluorescence of single molecules assisted by a plasmonic structure

Basic idea

Aim to: realize resonance fluorescence of single molecules near the plasmonic structure

4 silver nanostrips, 110*50*40 nm^3

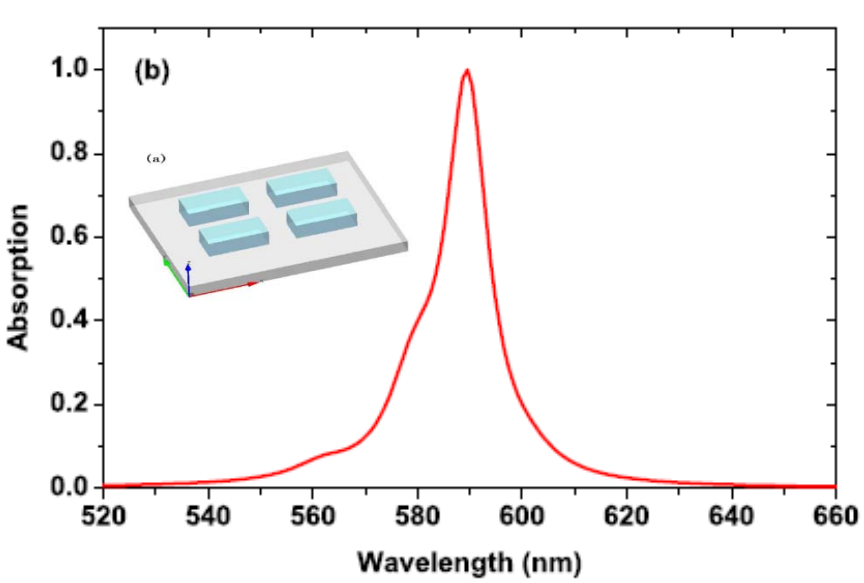

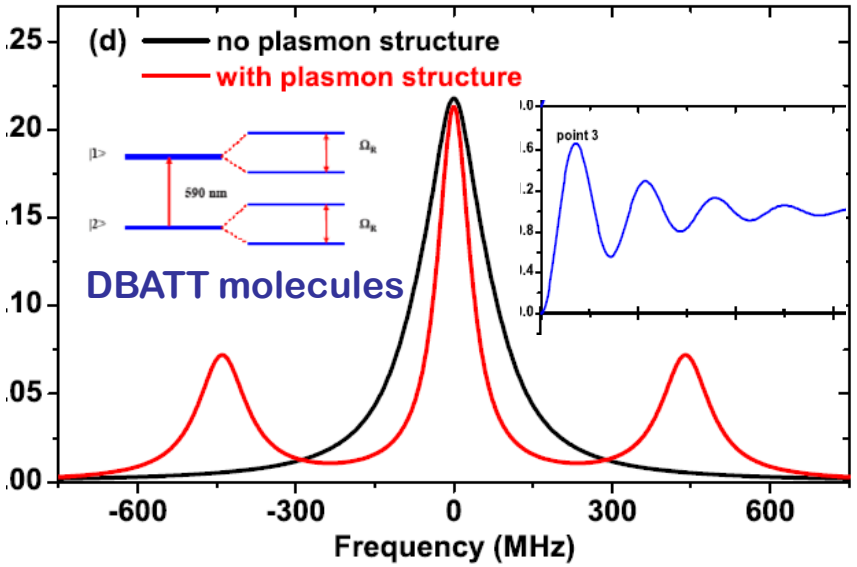

Resonance wavelength matching ($\lambda_{SPR}=\lambda_{RT}=590$ nm)
a balance between near field enhancement and decay rate modification

Mollow triplet and photon antibunching

Resonance Fluorescence of Single Molecules Assisted by a Plasmon Structure
Ying Gu, Lina Huang, Olivier J.F. Martin, and Qihuang Gong, Phys. Rev. B, 81, 193103 (2010).

Plasmonic structure design and optimal area

The Lippmann-Schwinger equation

$$E(\mathbf{r}) = E^0(\mathbf{r}) + k^2 \int_V d\mathbf{r}' G^0(\mathbf{r}, \mathbf{r}', \omega) \epsilon_s(\mathbf{r}, \omega) \cdot E(\mathbf{r}')$$

with Green's tensor

$$G^0(\mathbf{r}, \mathbf{r}', \omega) = (\mathbf{I} - \frac{1 - ik_0R}{k_0^2R^2}\mathbf{I} - \frac{-3 + 3ik_0R + k_0^2R^2}{k_0^2R^4}\mathbf{RR}) \frac{\exp[ik_0R]}{4\pi R}$$

in the arbitrarily shaped nanostructures

Green's tensor method:
solving the optical near field

Green's matrix method:
designing surface plasmon resonance by solving the eigensystems

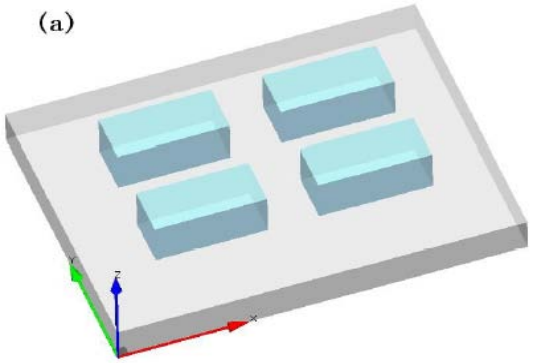

A unique design of silver four-nanostrip system with surface plasmon resonance at λ=590nm

Olivier J. F. Martin et al, Phys. Rev. Lett. 74, 526 (1995); Y.Gu et al, EPL, 83, 27004 (2008).

Optimal coefficient

$$R_\alpha = \frac{E_\alpha / E_0}{\Gamma_{\alpha\alpha}/\Gamma_0}$$

$\Gamma_{\alpha\alpha}/\Gamma_0 = 3\lambda\,\mathrm{Im}(G_{\alpha\alpha})$ where $G_{\alpha\alpha}$ is the Green's tensor

formulas for resonance fluorescence of two-level system:

$$S(\vec{r},\omega) = \frac{I_0(\vec{r})}{8\pi}\left[\frac{3\Gamma/4}{(\omega-\Omega_R-\omega_0)^2+(3\Gamma/4)^2} + \frac{\Gamma}{(\omega-\omega_0)^2+(\Gamma/2)^2} + \frac{3\Gamma/4}{(\omega+\Omega_R-\omega_0)^2+(3\Gamma/4)^2}\right]$$

$$g^{(2)}(\tau) = 1 - \left(\cos\mu\tau + \frac{3\Gamma}{4\mu}\sin\mu\tau\right)e^{-3\Gamma\tau/4} \text{ with } \mu = \left(\Omega_R^2 - (\Gamma/4)^2\right)^{1/2}$$

Using the optimal coefficient, to find specific regions where a large near field enhancement and a small modification of decay rate simultaneously exist.
Mollow triplet and photons antibunching.

B. R. Mollow, Phys. Rev. 188, 1969 (1969); S. M. Barnett et al, J. Phys. B: At. Mol. Opt. Phys. 29, 3763 (1996)

Optimal nanoarea

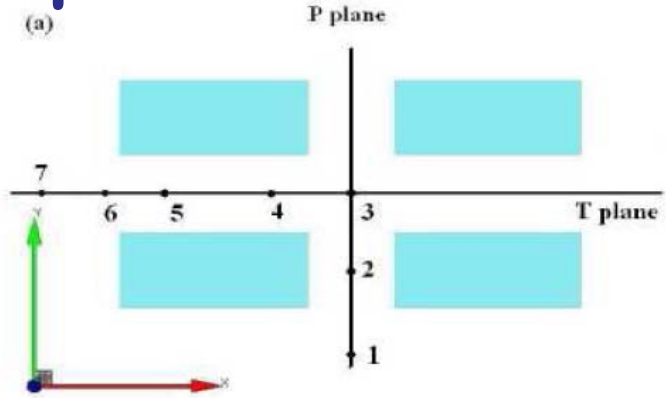

(c)
Optimal coeffient R_x of T plane

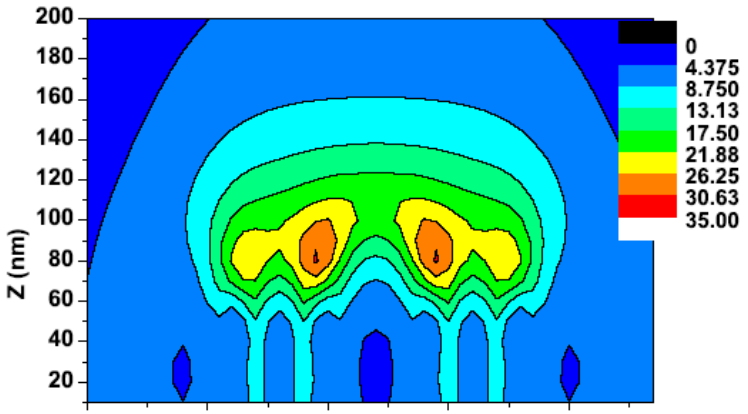

(b) Optimal coeffient R_x of P plane

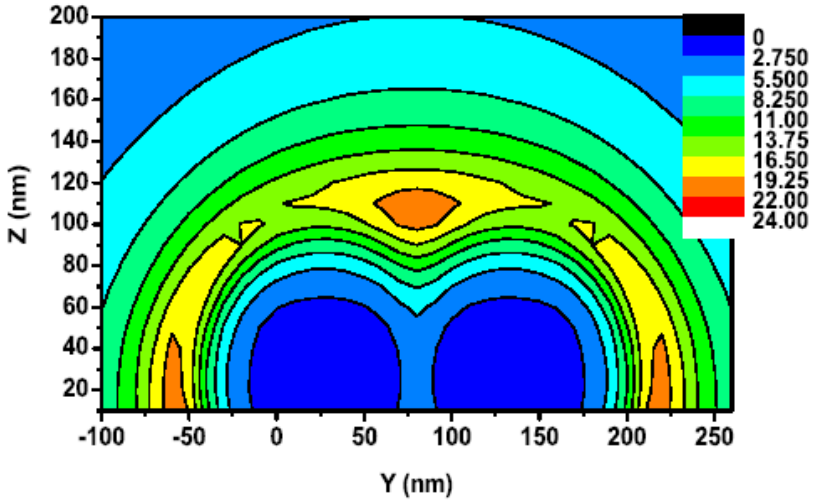

Optimal coeffient R_z of T plane

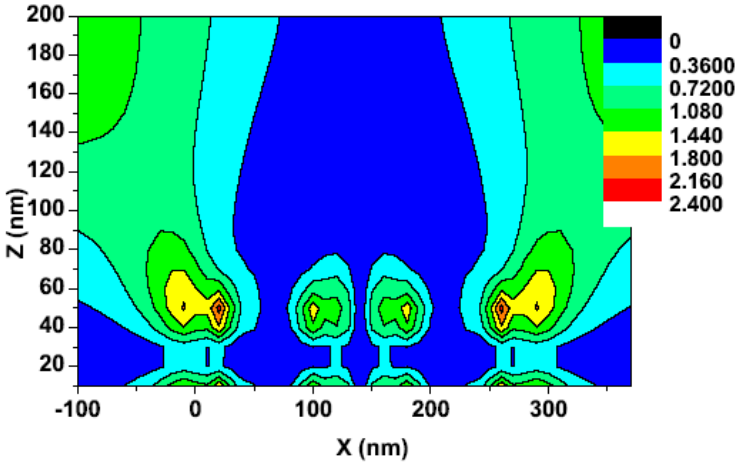

Specific regions 30 to 100 nm away from the metal surface, where Rx reaches 10~30.

Resonance Fluorescence of Single Molecules Assisted by a Plasmon Structure
Ying Gu, Lina Huang, Olivier J.F. Martin, and Qihuang Gong, Phys. Rev. B, 81, 193103 (2010).

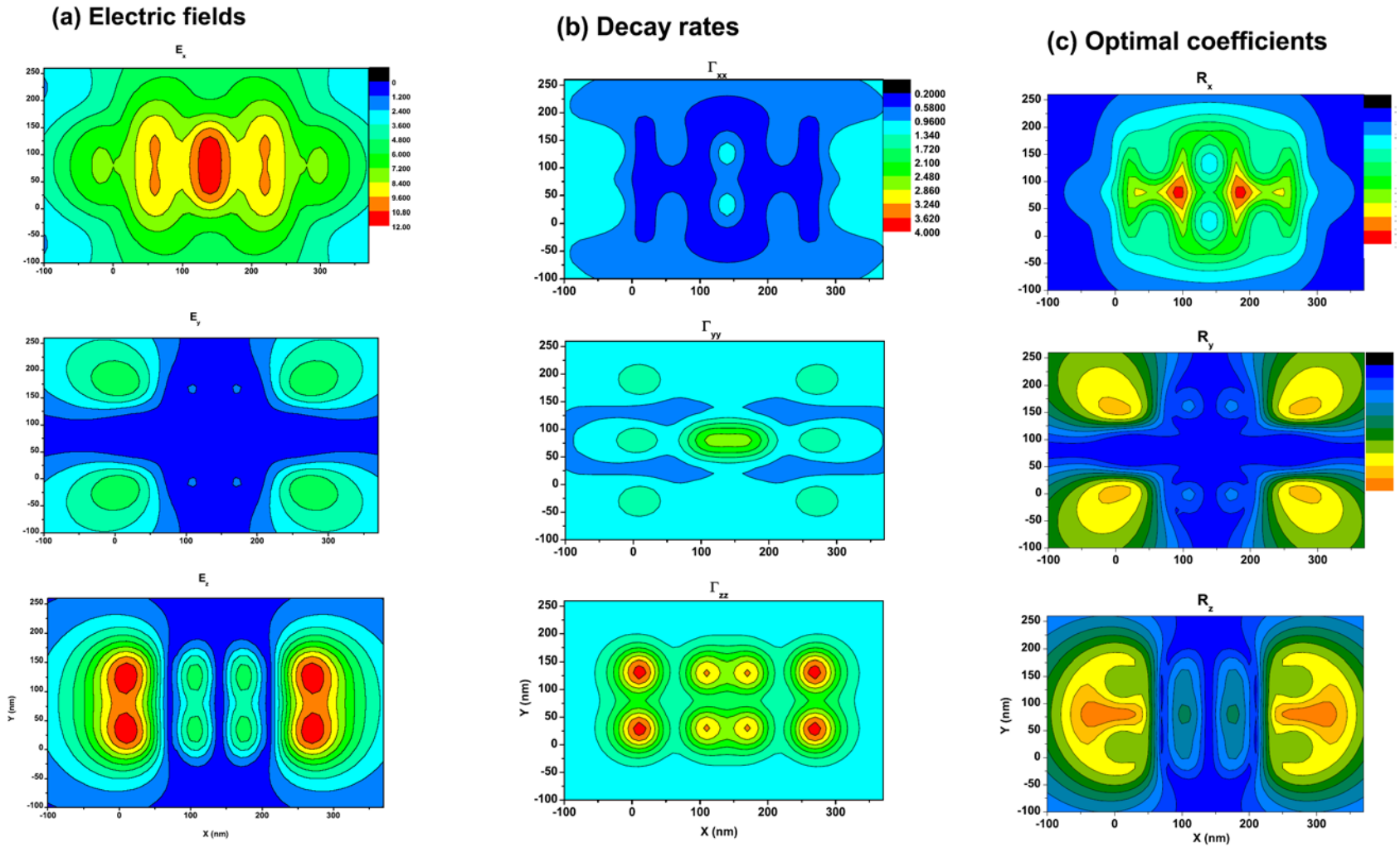

In xy plane 50nm away from metal surface above gaps

We find: Rx =10~30 whereas Ry <5 and Rz<5

A good directivity of emission

Resonance fluorescence

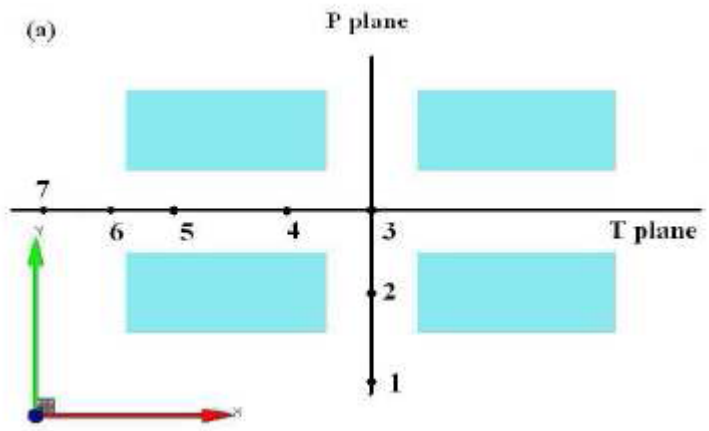

xy plane 50nm away from surface

1. Mollow triplet and photon antibunching in fluorescence.
2. Narrower spectra than natural linewidth due to cavity effects
3. sideband and linewidth of spectra sensitive to the location

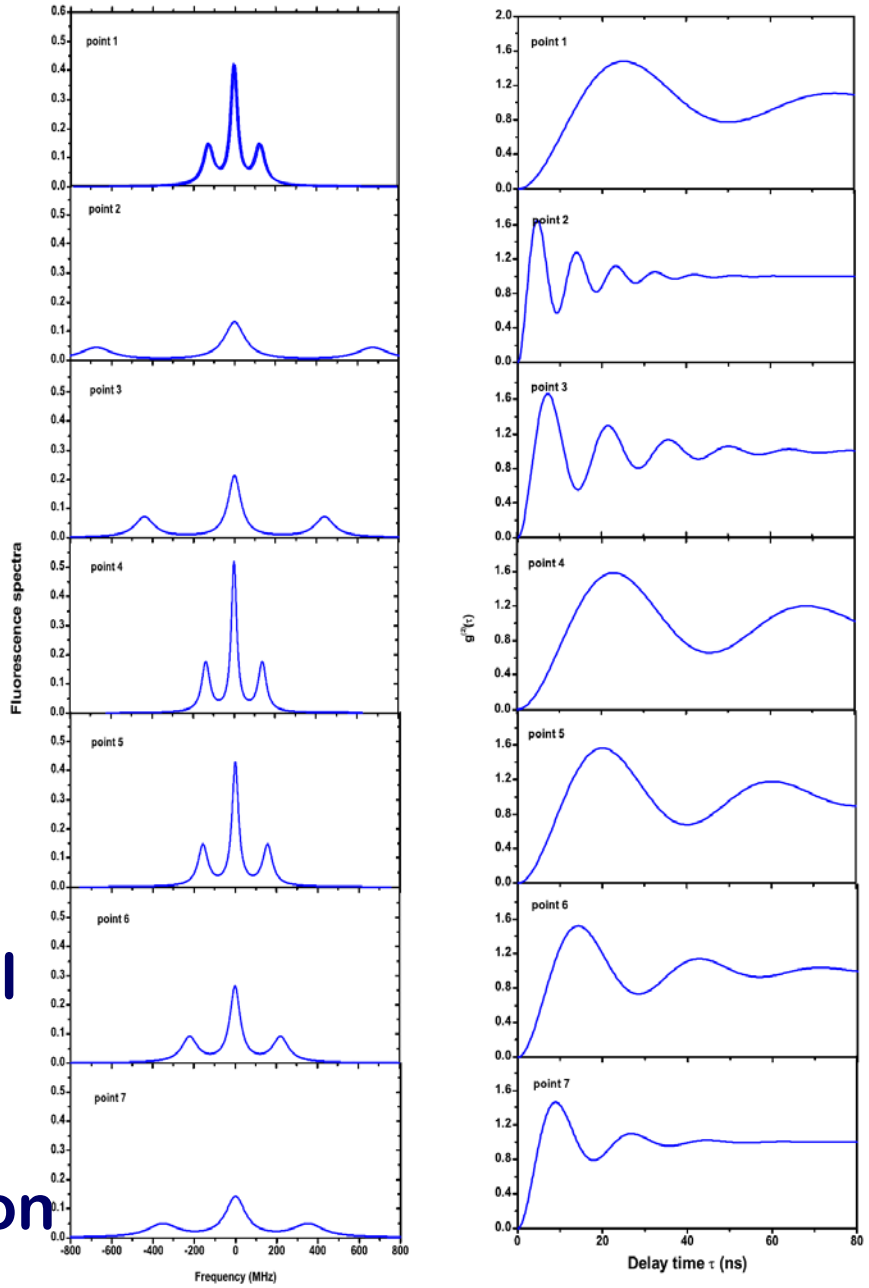

Resonance Fluorescence of Single Molecules Assisted by a Plasmon Structure
Ying Gu, Lina Huang, Olivier J.F. Martin, and Qihuang Gong, Phys. Rev. B, 81, 193103 (2010).

4.2 Intrinsic Quantum Beats of Atomic Populations in Isotropic and Plasmon-induced anisotropic vacuum

Model setup

Schrödinger equation in isotropic vacuum and W-W approximations

with crossing damping terms

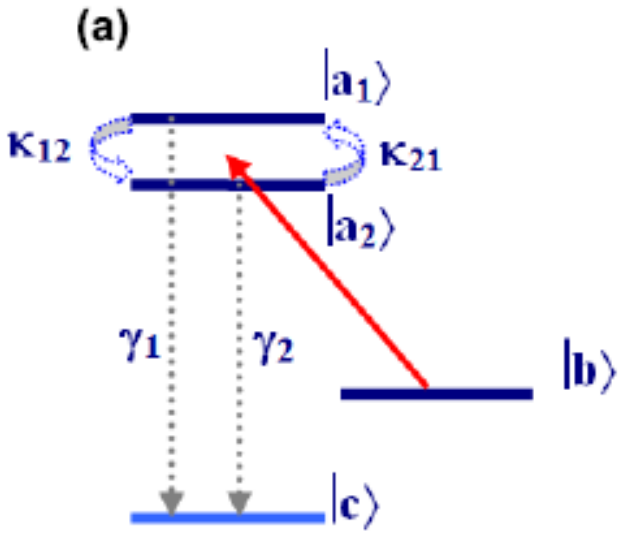

$$\frac{d}{dt}A^{(1)}(t) = -\frac{\gamma_1}{2}A^{(1)}(t) - p\frac{\sqrt{\gamma_1\gamma_2}}{2}A^{(2)}(t)e^{i\omega_{12}t} + \Omega_1 e^{i\Delta_1 t}B(t),$$

$$\frac{d}{dt}A^{(2)}(t) = -\frac{\gamma_2}{2}A^{(2)}(t) - p\frac{\sqrt{\gamma_1\gamma_2}}{2}A^{(1)}(t)e^{-i\omega_{12}t} + \Omega_2 e^{i\Delta_2 t}B(t),$$

$$\frac{d}{dt}B(t) = -\Omega_1^* e^{-i\Delta_1 t}A^{(1)}(t) - \Omega_2^* e^{-i\Delta_2 t}A^{(2)}(t),$$

$$\frac{d}{dt}C_k(t) = -g_1^* A^{(1)}(t)e^{-i(\omega_{a_1c}-\omega_k)t} - g_2^* A^{(2)}(t)e^{-i(\omega_{a_2c}-\omega_k)t}.$$

Population trapping condition

The populations are trapped in upper levels due to quantum interferences.

$$\Delta_1|\Omega_2|^2+\Delta_2|\Omega_1|^2=0,$$

$$p\frac{\Omega_1}{\Omega_2}=\sqrt{\frac{\gamma_1}{\gamma_2}}\quad(p=\pm 1).$$

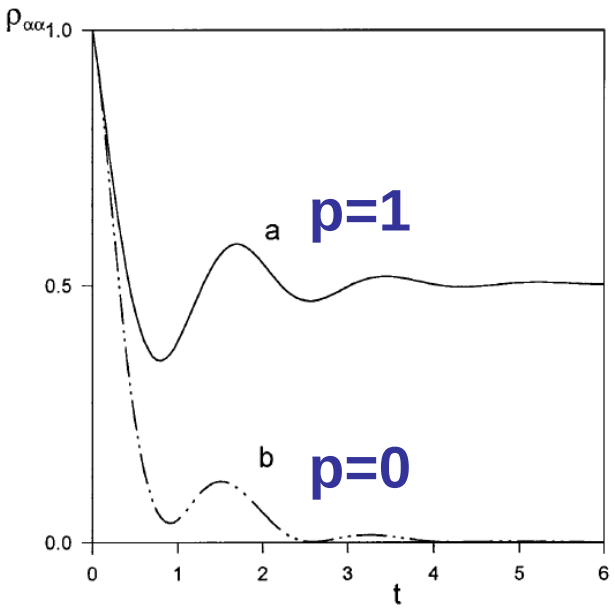

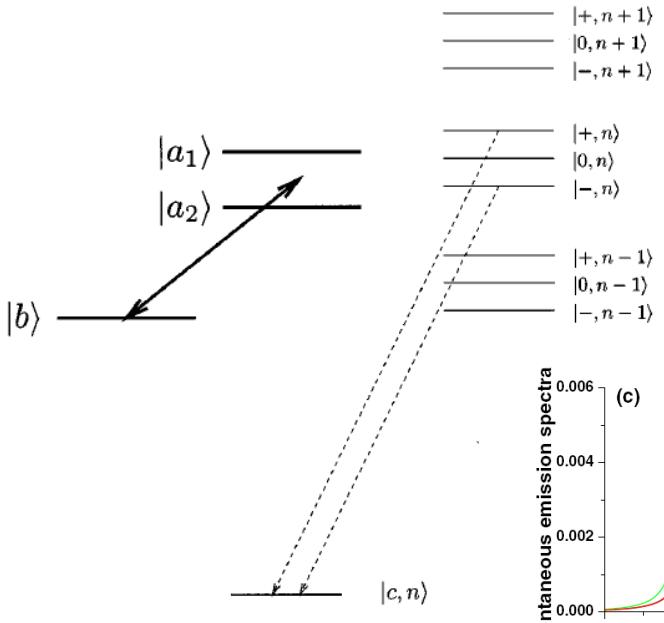

Dressed state analysis

The spontaneous emission from |0,n> to |c> is zero ➡

Spontaneous emission cancellation

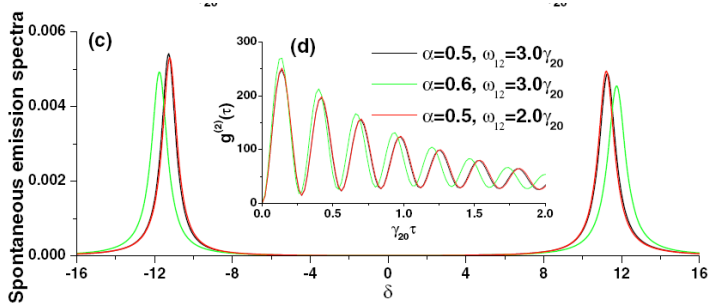

Lee H, Polynkin P, Scully MO, et al., PHYSICAL REVIEW A, 55, 4454-4465 (1997) .

In anisotropic vacuum and W-W approxmations

$$\frac{d}{dt}A^{(1)}(t) = -\frac{\gamma_1}{2}A^{(1)}(t) - \frac{\kappa_2}{2}A^{(2)}(t)e^{i\omega_{12}t} + \Omega_1 e^{i\Delta_1 t}B(t),$$

$$\frac{d}{dt}A^{(2)}(t) = -\frac{\gamma_2}{2}A^{(2)}(t) - \frac{\kappa_1}{2}A^{(1)}(t)e^{-i\omega_{12}t} + \Omega_2 e^{i\Delta_2 t}B(t),$$

$$\frac{d}{dt}B(t) = -\Omega_1^* e^{-i\Delta_1 t}A^{(1)}(t) - \Omega_2^* e^{-i\Delta_2 t}A^{(2)}(t),$$

$$\frac{d}{dt}C_k(t) = -g_1^* A^{(1)}(t)e^{-i(\omega_{a_1c}-\omega_k)t} - g_2^* A^{(2)}(t)e^{-i(\omega_{a_2c}-\omega_k)t}.$$

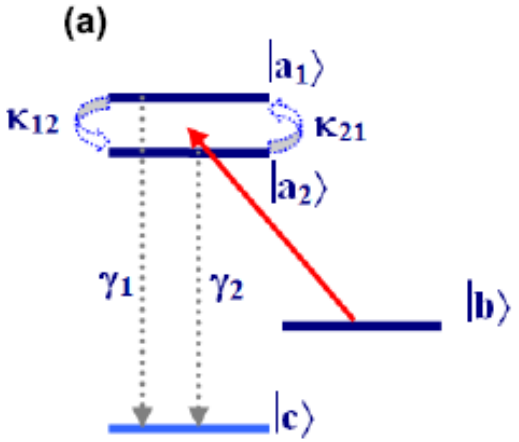

decay rates and crossing damping in terms of Green's tensor.

$$\gamma_{1,2} = \Gamma_{xx}\cos^2\theta_{1,2} + \Gamma_{zz}\sin^2\theta_{1,2} \qquad \Gamma_{zz}/\gamma_0 = 3\lambda_{ac}ImG_{zz}$$

$$\kappa = \Gamma_{xx}\cos\theta_1\cos\theta_2 + \Gamma_{zz}\sin\theta_1\sin\theta_2 \qquad \Gamma_{xx}/\gamma_0 = 3\lambda_{ac}ImG_{xx}$$

new trapping conditions $\gamma_1|\Omega_2|^2 + \gamma_2|\Omega_1|^2 - \kappa(\Omega_1\Omega_2^* + \Omega_2\Omega_1^*) = 0,$

"Two parallel dipoles" can't be broken $\Delta_1|\Omega_2|^2 + \Delta_2|\Omega_1|^2 = 0.$

Ying Gu et al, Plasmonics (2011) DOI 10.1007/s11468-011-9272-x

Quantum beats of population oscillations

Skip the complex formulas

Beat frequency:

$$\omega_e = \frac{1-\alpha^2}{1+\alpha^2}\omega_{12}$$

$$\omega_{a_1} - \omega_{a_2} = \omega_{12}$$

$$|\vec{\mu}_1|/|\vec{\mu}_2| = \alpha$$

Rabi frequency:

$$|\Omega_e|^2 = [\frac{\alpha}{1+\alpha^2}\omega_{12}]^2 + |\Omega_1|^2 + |\Omega_2|^2$$

New quantum interference effect in isotropic and anisotropic vacuum. Beat frequency is determined by spacing and dipole moment ratio.

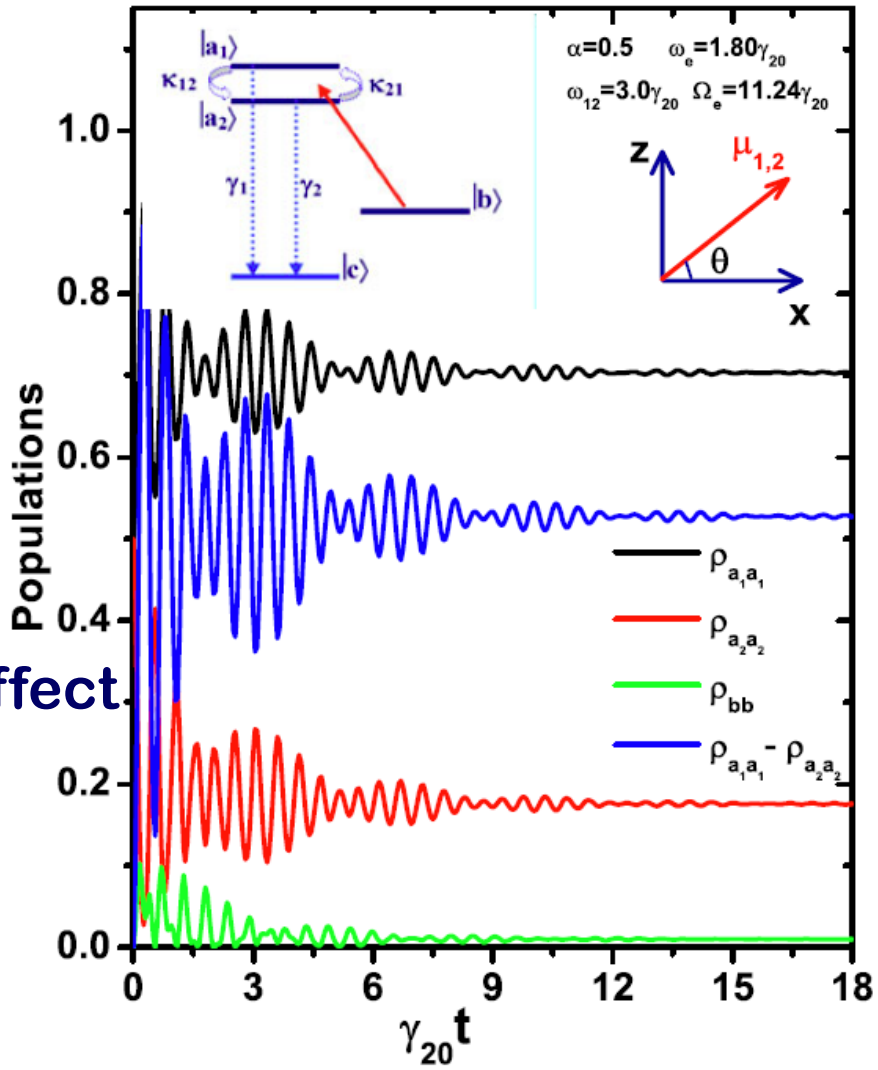

Ying Gu et al, Plasmonics (2011) DOI 10.1007/s11468-011-9272-x

Nanoscale Realization in Plasmon-Induced anisotropic vacuum

Right: absorption, near field distribution, and decay rates of silver nanoantenna at resonant wavelength of 780 nm.

Bottom: quantum beats of atomic populations in near field region

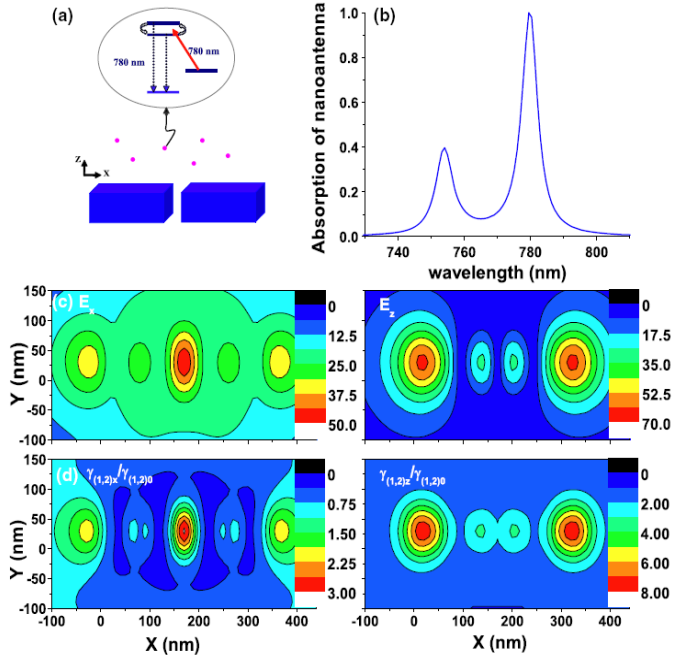

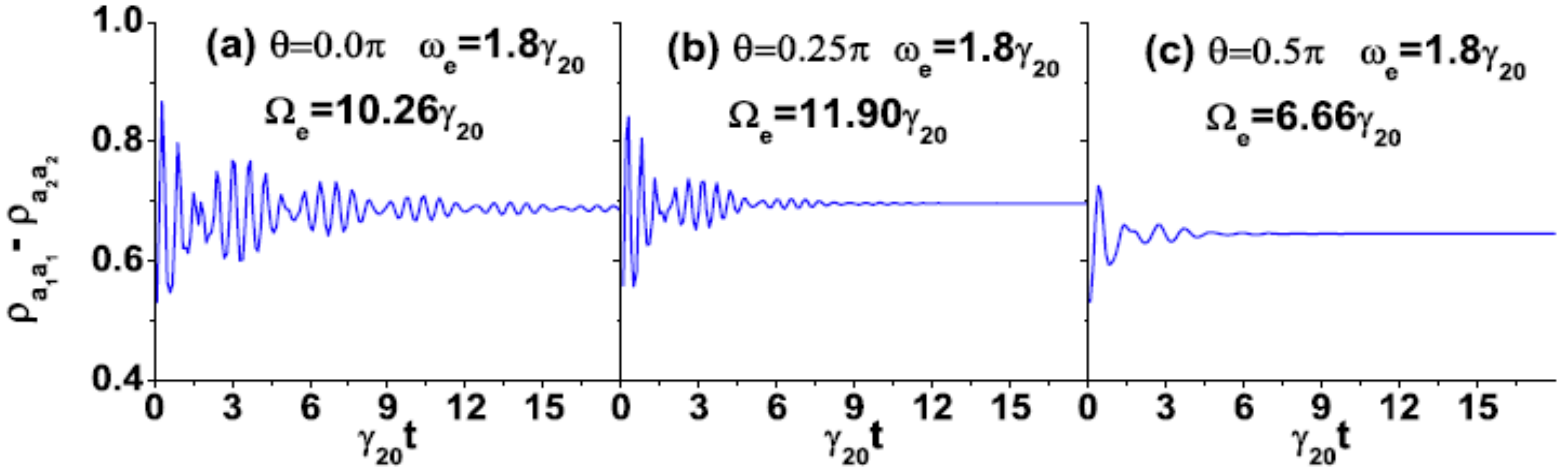

Ying Gu et al, Plasmonics (2011) DOI 10.1007/s11468-011-9272-x

4.3 Surface-Plasmon-Induced Modification on the Spontaneous Emission Spectrum via Subwavelength-Confined Anisotropic Vacuum

Quantum interferences In isotropic vacuum

crossing damping between two closely lying upper states

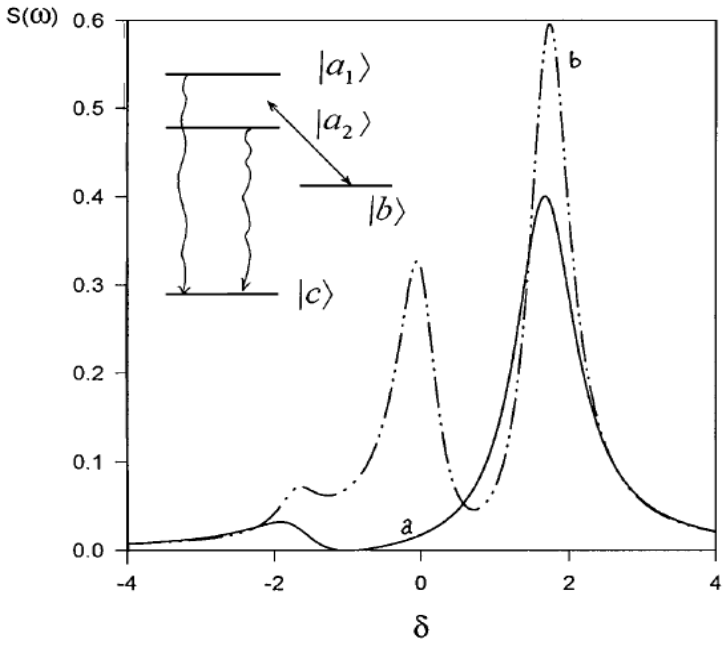

a: parallal dipole moments
spontaneous emission cancellation

b: orthogonal dipole moments
three emission peaks

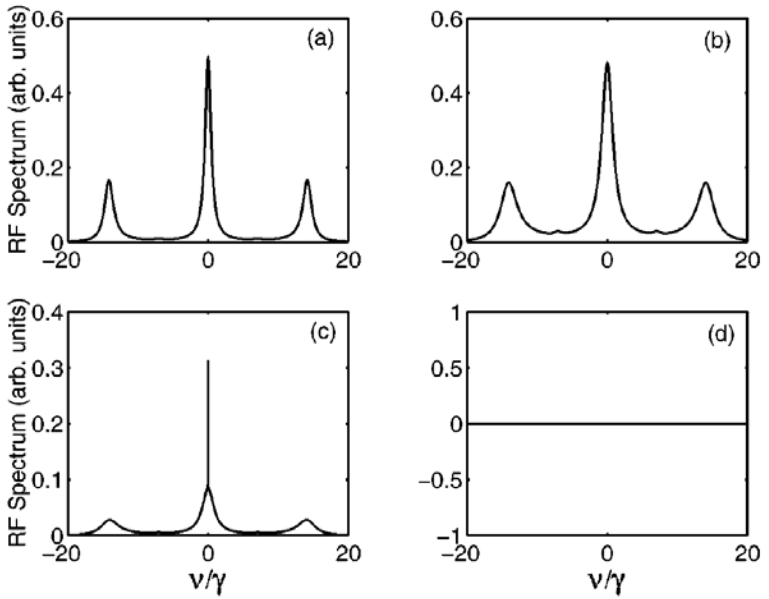

For nearly parallel dipoles,
ultranarrow spectral lines as
crossing damping increases

S. Y. Zhu, et al., Phys. Rev. Lett. 76, 338 (1996); P. Zhou and S. Swain, Phys. Rev. Lett. 77, 3995 (1996).

Theory

Green's tensor coefficients

$$\Gamma_{zz}/\gamma_0 = 3\lambda_{ac} ImG_{zz}, \quad \Gamma_{xx}/\gamma_0 = 3\lambda_{ac} ImG_{xx}$$

decay rates and crossing damping in anisotropic vacuum

$$\gamma_{1,2} = \Gamma_{xx}\cos^2\theta_{1,2} + \Gamma_{zz}\sin^2\theta_{1,2}$$

$$\kappa = \Gamma_{xx}\cos\theta_1\cos\theta_2 + \Gamma_{zz}\sin\theta_1\sin\theta_2$$

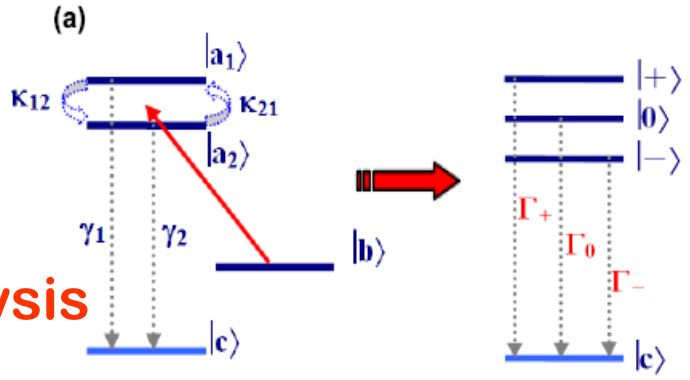

Master equation, dressed state analysis

quantum regression thereom

linewidths of the central peak and sidebands

$$\Gamma_0 = (\gamma_1 + \gamma_2 - 2\kappa)4\eta^2,$$

$$\Gamma_\pm = (\gamma_1 + \gamma_2)\frac{1+\epsilon^2}{4} \pm (\gamma_1 - \gamma_2)\frac{\epsilon}{2} + \kappa\frac{1-\epsilon^2}{2}$$

$$\epsilon = \omega_{12}/\Omega_R, \eta = \Omega/\Omega_R$$

$$\Gamma_0 \doteq (\gamma_1 + \gamma_2)/2 - \kappa$$

$$\Gamma_\pm \doteq (\gamma_1 + \gamma_2)/4 + \kappa/2$$

Ying Gu, et al., submitted, 2011.

Mechanism of linewidth control

If the polarization angle bisector of two dipole moments lies along the major/minor axis of the effective decay rate ellipse, destructive/constructive interference narrows/widens the center spectral lines associated with fluorescence.

Enlarging the anisotropy increases the variation.

$$\Gamma_0/\Gamma_\pm = 0.0528$$

$$\Gamma_0/\Gamma_\pm = 0.2112$$

$$\Gamma_0/\Gamma_\pm = 0.8446$$

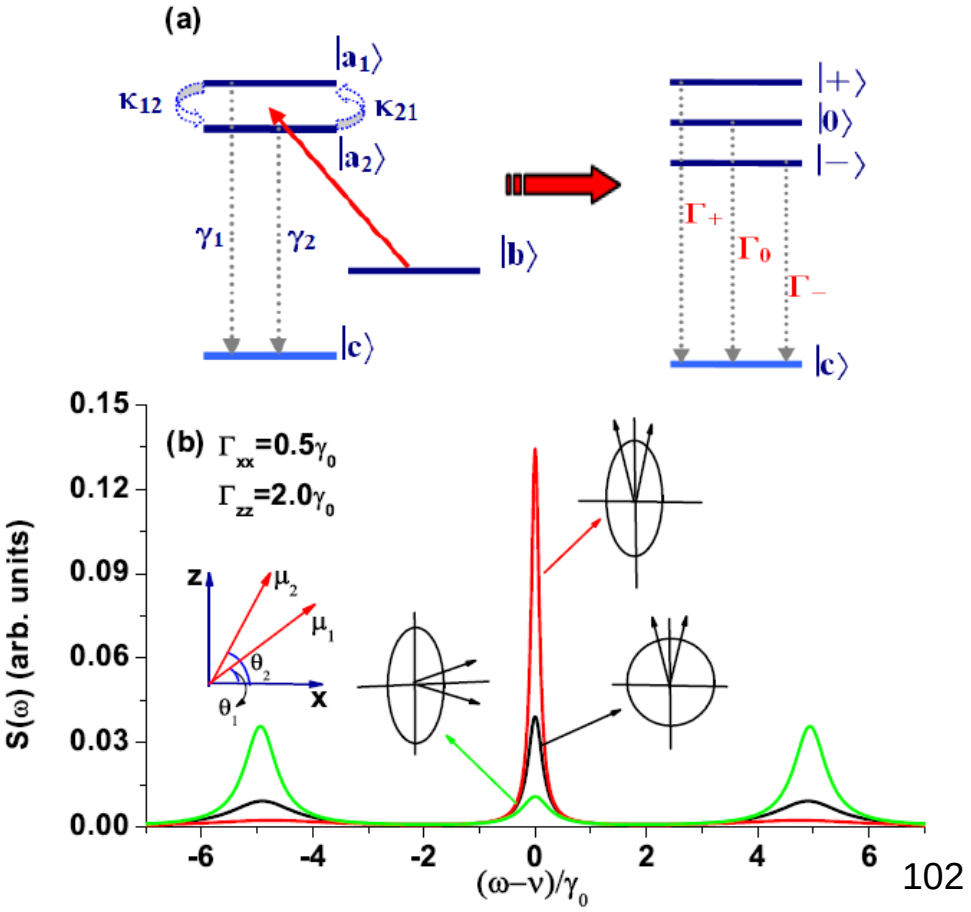

Ying Gu, et al., submitted, 2011.

In Surface-Plasmon-Induced Subwavelength-Confined Anisotropic Vacuum

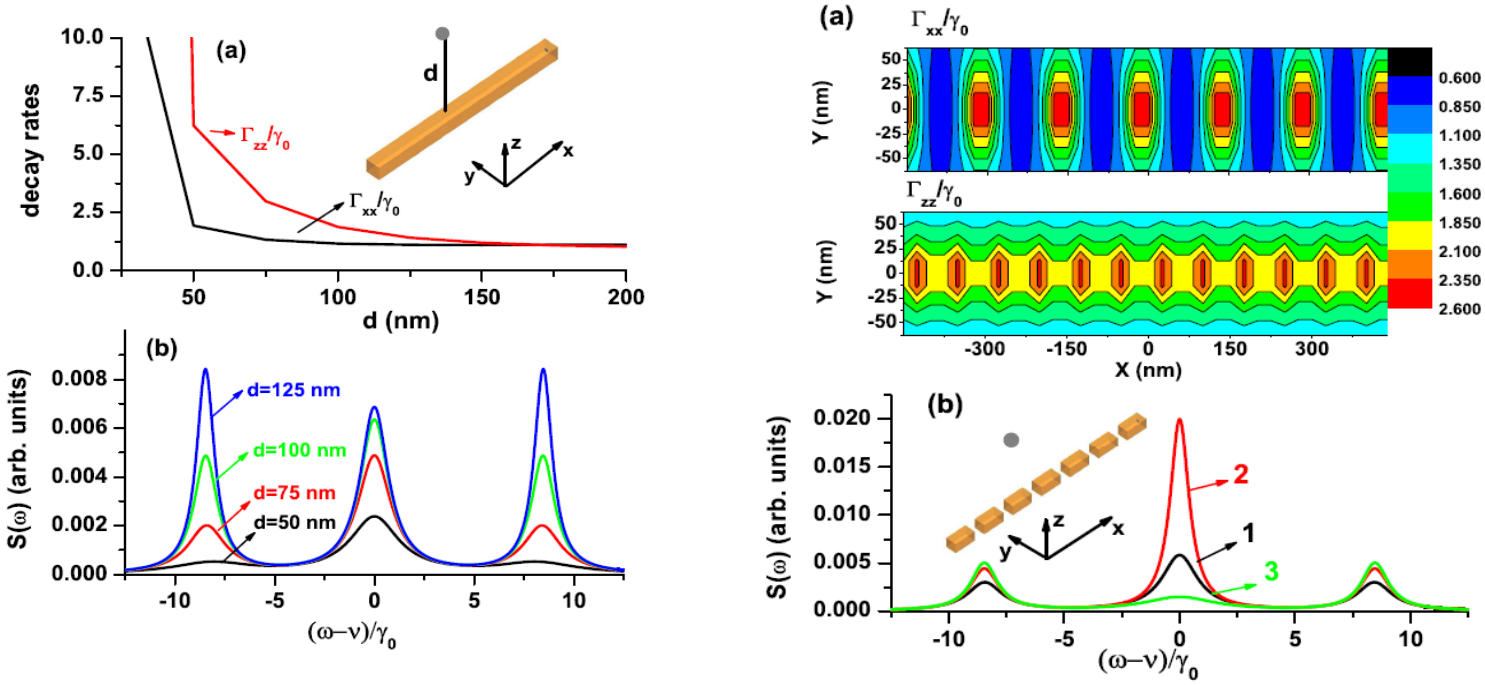

Left: Rapid spectral line narrowing of atom approaching a metallic nanowire

Right: the linewidth "pulsing" following periodically-varying decay rates near a periodic metallic nanostructure

Ying Gu, et al., submitted, 2011.

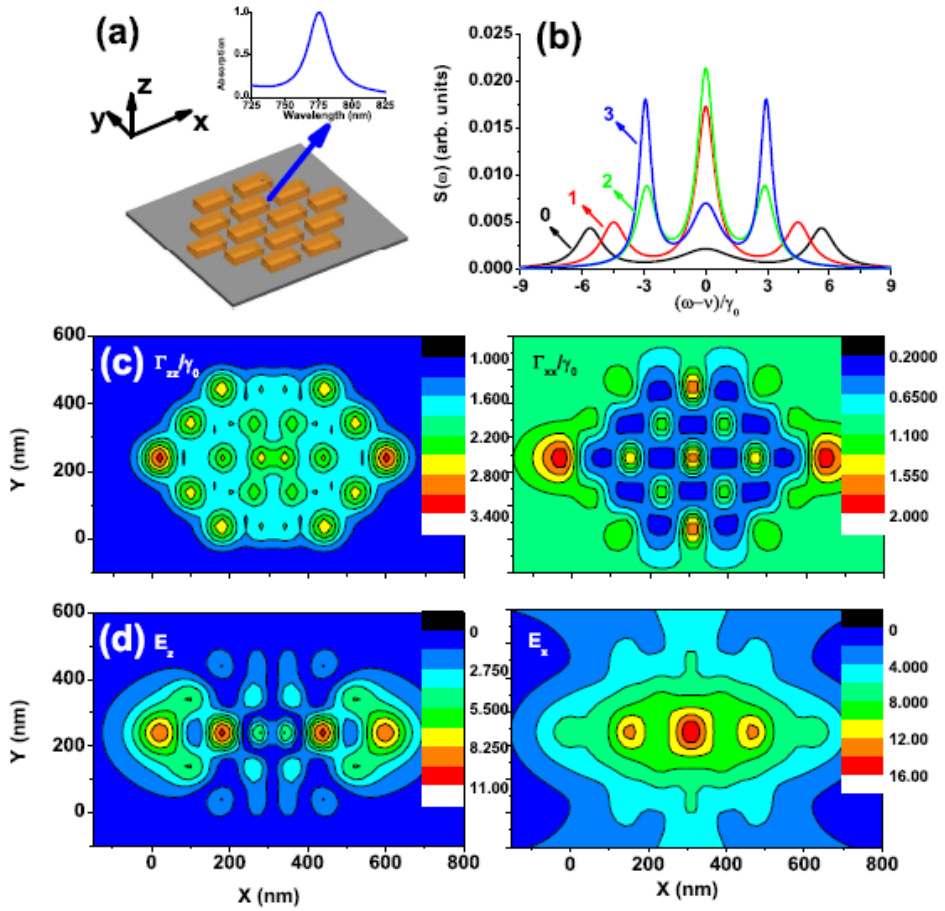

Top: dramatic modification on the spontaneous emission spectrum near a custom-designed resonant plasmon nanostructure, even subnatural linewidth

Ying Gu, et al., submitted, 2011.

4.4 Summary

1. Mollow triplet and photon antibunching of molecular fluorescence assisted by plasmonic structure

2. Quantum beats of atomic populations in isotropic vacuum, its nanoscale realization in plasmon-induced anisotropic vacuum

3. Mechanism of spontaneous emission spectrum control, its proof and demonstration in subwavelength-confined anisotropic vacuum

Next, strong coupling ……

Significance:

1. bridges the fields of quantum optics and plasmonics
2. low-level light nonlinear optical properties
3. efficient coupling of single photons into the single plasmons.
4. Superior to the cavity QED, anisotropic vacuum and plasmon excitation cover a broad frequency region and require no sophisticated experimental setups to achieve the resonances.
5. for applications in ultracompact active quantum devices.

Experiments!

五、结束语

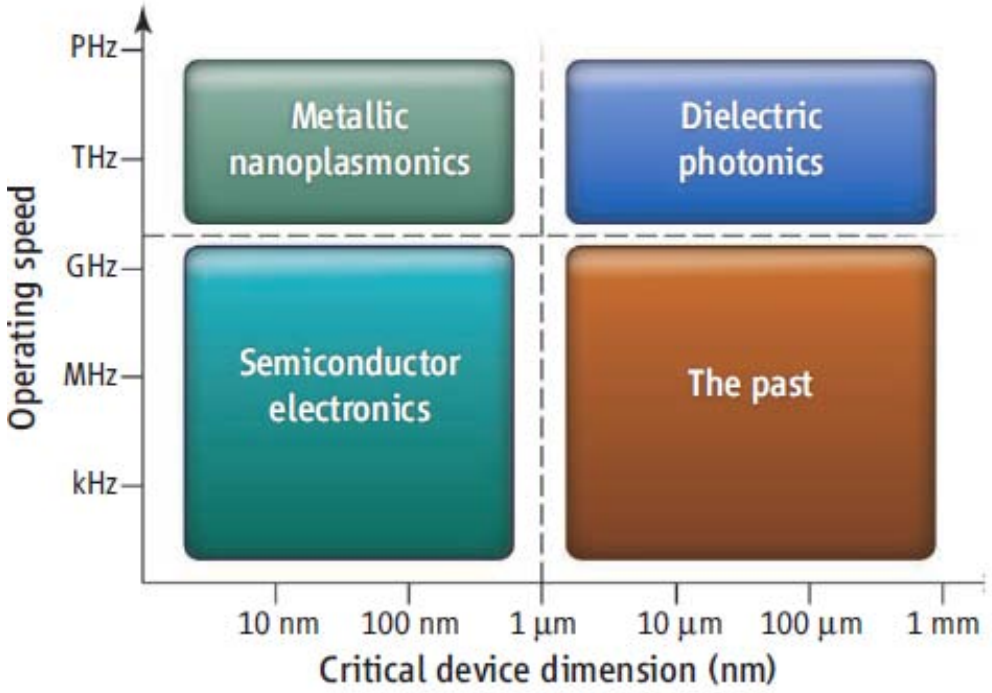

表面等离激元光学是纳米尺度上光子学和电子学的结合，在光子回路，数据存储，光谱学，生物光子学，太阳能，非线性光学，量子光学和量子信息方面都有应用，能够实现纳米尺度上控制光的超小器件，如滤波器，波导，偏振器和纳米光源等。

The Case for Plasmonics，Mark L. Brongersma, et al,science, VOL 328,440 (2010).

未来发展方向

come. Important new directions for this field include the following: (1) merging plasmonics with quantum systems,[74,79] providing challenges for both theory and experiment; (2) coherent phenomena in plasmonics, where Fano resonances, superradiance, and plasmon-induced transparency result in novel new lineshapes and plasmonic properties;[107,21] (3) active plasmonic devices and media; new types of devices and media combining plasmonics with other functional materials for active and nonlinear responses;[100] (4) improved sensors and detectors; from ultrasmall detectors to LSPR sensors with single molecule sensitivity and specificity,[51] there are many possibilities for advancing the ability to increase detection sensitivities and responsivities; (5) the role of plasmons in modifying chemical reactions; and (6) biomedical applications, where new types of nanoscale devices can be developed for diagnosis[11] and treatment of diseases, to improve treatment efficacy, and to develop prevention strategies for global health challenges. We predict the fu-

Plasmonics: An Emerging Field Fostered by Nano Letters， Naomi J. Halas, Nano Letters, 10,3816 (2010).

我们小组的工作

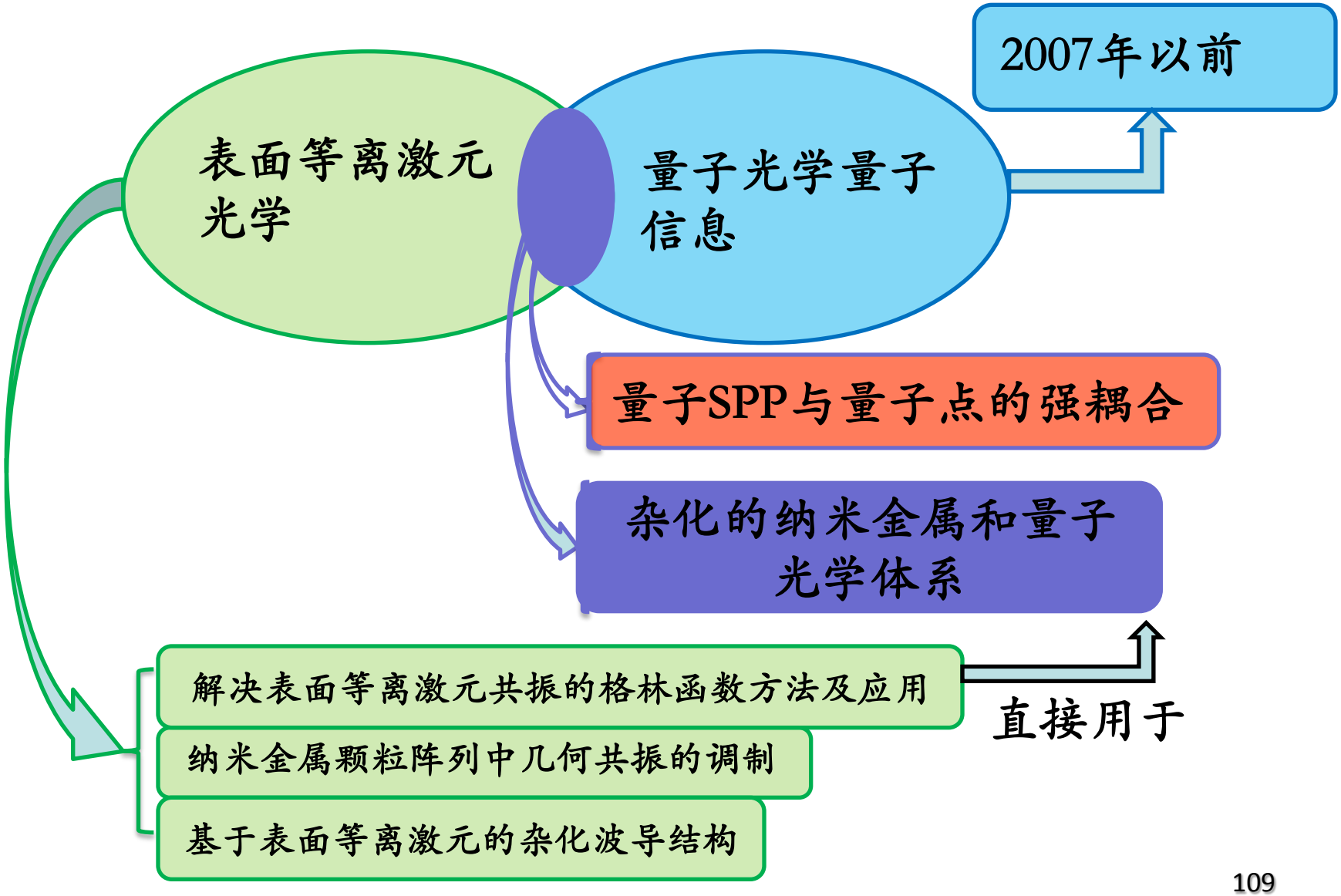
表面等离激元光学
量子光学量子信息
2007年以前
量子SPP与量子点的强耦合
杂化的纳米金属和量子光学体系
解决表面等离激元共振的格林函数方法及应用
纳米金属颗粒阵列中几何共振的调制
基于表面等离激元的杂化波导结构
直接用于

Contributors:

陈亮亮、王立金、张海汐、杨鹏飞、李蓬勃、胡雪元、
李佳、任攀、王岩、孙宝清、王珞珈等

Collaborators:

龚旗煌、胡小永（北京大学）

童利民（浙江大学）

Olivier J. F. Martin (EPFL)

张俊香、张天才（山西大学）

Iam-Choon Khoo（Pennsylvania State Univ.）

许静平（同济大学）

朱诗尧（计算科学中心）

致谢：

国家基金委面上基金、重点基金、创新群体基金和科技部973项目、学校985及重点实验室开放基金。


谢谢大家！